Second-Order Nonlinearity in Poled-Polymer Systems

Donald M. Burland,* Robert D. Miller, and Cecilia A. Walsh

IBM Research Division, Almaden Research Center, 650 Harry Road, San Jose, California 95120-6099

Contents

I. Introduction

It has been more than 10 years since the first electric field poled second-order nonlinear polymers were reported.[1,2] During this period a wide variety of polymeric systems have been formulated and investigated. Several reviews have been written concentrating primarily on the polymer systems and the development and decay of the electric field induced ordering.[3-11] Other reviews have focused on the relationship between the physical and chemical properties of second-order nonlinear polymers and their potential applications in electrooptic and frequency-doubling devices.[12-17] The field in general has been summarized in the two-volume series edited by Chemla and Zyss[18] and in the book by Prasad and Williams.[19] A good overview of current work in the field can also be found in the annual volumes published by the Society of Photo-Optical Instrumentation Engineers (SPIE) entitled "Nonlinear Optical Properties of Organic Materials".

This review concentrates on the macroscopic second-order nonlinearity, the development and decay of the electric field poled order responsible for the nonlinearity, methods of measuring this nonlinearity and the chemical nature of the polymeric systems identified as promising second-order materials. Less attention is paid to the application of these polymers in frequency-doubling and electrooptic devices. These applications are mentioned only briefly to indicate the desired chemical and physical properties that one requires in a useful polymer. Much of the current work in this field is in fact motivated by an attempt to find practical polymeric materials for these applications.

II. Origins of Second-Order Nonlinearity

A. Microscopic to Macroscopic Nonlinearity

Nonlinear optical (NLO) materials owe their bulk nonlinearity to the optical nonlinearity of their constituents. A polymeric system is nonlinear because of the presence of suitably oriented nonlinear guest molecules dissolved in a host polymer or because the monomer subunit itself contains suitably oriented chromophores. Estimates of the macroscopic nonlinearity can be obtained by considering the microscopic ordering of noninteracting nonlinear chromophores. This approximation, which treats the individual chromophores as independent units, is known as the oriented gas model.[1,20-22] It has been widely used in describing the optical properties of mixed molecular crystals, for example.[23] Its validity rests on the fact that in molecular systems intermolecular interactions are much weaker than intramolecular ones. Bulk properties can thus be thought of as being built up from the corresponding properties of individual molecules.

The component in the i-th molecule fixed-coordinate direction of the electric field induced dipole moment (the dipole polarization) for an isolated molecule can be written:[24]

$$p_i(\omega) = \alpha_{ij}(\omega)E_j(\omega) + \beta_{ijk}(-\omega;\omega_1,\omega_2)E_j(\omega_1)E_k(\omega_2) + \gamma_{ijkl}(-\omega;\omega'_1,\omega'_2,\omega'_3)E_j(\omega'_1)E_k(\omega'_2)E_l(\omega'_3) + \ldots \quad (1)$$

where $\alpha_{ij}(\omega)$ is the linear molecular polarizability and $\beta_{ijk}(-\omega;\omega_1,\omega_2)$ and $\gamma_{ijkl}(-\omega;\omega'_1,\omega'_2,\omega'_3)$ are the frequency-dependent first and second hyperpolarizabilities, respectively. The subscripts i, j, and k refer to a molecule-based coordinate system. Energy conservation requires that $\omega = \omega_1 + \omega_2$ and $\omega = \omega'_1 + \omega'_2 + \omega'_3$. Symmetry requires that all terms of even order in the electric field vanish when the molecule possesses an inversion center. Equation 1 is written for the specific case where the fields along the various molecular axes are monochromatic as is the induced dipole polarization. In general,

Donald M. Burland was born in 1943 in La Jolla, CA. He received an A.B. in Chemistry from Dartmouth College in 1965 and a Ph.D. in Chemistry and Physics from the California Institute of Technology in 1970 working with Professor G. Wilse Robinson. He then spent two years at the University of Leiden with Professor J. H. van der Waals working on applications of microwave-induced delayed emission and the Zeeman effect to problems in molecular crystals. In 1971 Dr. Burland joined the IBM Research Division as a Research Staff Member. Since that time he has held a variety of technical management positions in the areas of optical and electrooptical materials, magnetic recording, and electrophotographic and ink jet printing technologies. He is currently manager of the Electrooptic Materials and Devices Department. He is a member of the Optical Society and the American Chemical Society and a fellow of the American Physical Society. Dr. Burland's current research interests include polymeric electrooptic materials, photorefractive polymers, investigation of slow structural relaxation processes in polymers and subpicosecond spectroscopic investigations of energy and charge transport processes in amorphous solids.

Robert D. Miller was born in Philadelphia, PA, in 1941. He received a B.Sc. in Chemistry from Lafayette College in 1963 and a Ph.D. in Organic Chemistry from Cornell University in 1968 working with Professor A. T. Blomquist. After postdoctoral work at Union Carbide Research Institute in Tarrytown, NY, where he worked on the generation and characterization of reactive intermediates by flash vacuum pyrolysis, he joined the Research Division of IBM in 1969. His current interests include basic photochemical processes, radiation-sensitive polymers, the spectroscopy and chemistry of reactive intermediates, reactions and rearrangements of strained ring compounds, new synthetic methods, and nonlinear optical materials.

the external electric field along any given polarization direction is a sum of dc and frequency-dependent parts. The Einstein summation convention has been used and is important to the correct expansion of eq 1.

It is instructive to write out the second-order dipole polarization $p_i^{(2)}(\omega)$ for some specific examples. For the case of second-harmonic generation, when the molecule is exposed to an external field of a single frequency $E_j(\omega) = e_j(\omega) \cos \omega t$, one obtains

Cecilia A. Walsh received her B.S. in Chemistry from the University of Notre Dame in 1982 and her Ph.D. in Physical Chemistry from Stanford University in 1987 working with Professor M. D. Fayer. She was a member of the technical staff at Sandia National Laboratories in Albuquerque, NM, from 1987 to 1989. She has been a visiting scientist at the IBM Almaden Research Center since 1989 as a member of the organic optoelectronics materials group. Her research interests include polymeric materials for optoelectronics and photorefractive materials, dynamics in polymers and glasses, and time-resolved spectroscopy.

Table 1. Numerical Values of K for Various Second-Order Processes

ω	ω_1	ω_2	K	process
$\omega_1 + \omega_2$	ω_1	ω_2	1	up-conversion
$\omega_1 - \omega_2$	ω_1	$-\omega_2$	1	down-conversion
0	ω	$-\omega$	$1/2$	optical rectification
2ω	ω	ω	$1/2$	frequency doubling
ω	0	ω	2	dc-Pockels effect

$$p_i^{(2)}(2\omega) = (1/2)\beta_{ijj}(-2\omega;\omega,\omega)e_j(\omega)^2 \cos 2\omega t \quad (2)$$

For frequency up-conversion processes two frequency-dependent fields are present, for example $E_j(\omega_1)$ and $E_k(\omega_2)$. In this case one obtains

$$p_i^{(2)}(\omega_1 + \omega_2) =$$
$$\beta_{ijk}(-\omega_1-\omega_2;\omega_1,\omega_2)e_j(\omega_1)e_k(\omega_2) \cos \omega_1 t \cos \omega_2 t \quad (3)$$

Note the factor of $1/2$ associated with second-harmonic generation but not with the up-conversion process. For a general second-order process one can write

$$p_i(\omega) =$$
$$K\beta_{ijk}(-\omega;\omega_1,\omega_2)e_j(\omega_1)e_k(\omega_2) \cos(\omega = \omega_1 + \omega_2)t \quad (4)$$

The factor K in this expression takes into account these numerical coefficients.[25] Values of K for various second-order nonlinear processes are listed in Table 1. Equation 4 may be considered as a convention defining the first hyperpolarizability β. The use of other conventions has been discussed.[26] In particular, the factor of K is sometimes incorporated into the definition of β so that it does not appear explicitly in the expression analogous to eq 4 relating the polarization to the exciting electric fields.[27] This convention avoids the troublesome factors K and is consistent with definitions of the second-harmonic coefficient d_{ijk} discussed below.[24] The convention defined by eq 4 and used throughout this paper results in values of β for the various second-order processes that approach the same value as all involved frequencies go to zero. This is satisfying from an algebraic point of view and it permits one to compare directly values of β measured by different experimental techniques.

In moving from the microscopic second-order polarization defined in eq 1 to a macroscopic polarization $P_I(\omega)$ one needs to take three things into account: the concentration of the chromophores given by the number density N, the value of the hyperpolarizability averaged over all orientations of the individual chromophores $\langle\beta_{ijk}\rangle_{IJK}$, and the effect of the dielectric properties of the bulk medium in modifying the externally applied electric field, so-called local field effects. Here IJK is the coordinate system of the bulk material. One defines a set of linear and nonlinear susceptibilities by direct analogy to eq 1:

$$P_I(\omega) = \chi_{IJ}^{(1)}(\omega)E_J(\omega) + \chi_{IJK}^{(2)}(-\omega;\omega_1,\omega_2)E_J(\omega_1)E_K(\omega_2) +$$

$$\chi_{IJKL}^{(3)}(-\omega;\omega'_1,\omega'_2,\omega'_3)E_J(\omega'_1)E_K(\omega'_2)E_L(\omega'_3) + ... \quad (5)$$

As in the molecular case, the bulk material must not have a center of symmetry for the even-order susceptibilities to be nonzero.

B. Local Field Factors

Equation 5 is written in terms of the externally applied electric field. In a dielectric medium consisting of a polarizable species, the local field at a given molecule differs from this external field due to the sum of the dipole fields from all of the polarizable particles. Its exact description is still an area of active research.[28,29] The local field $F_I(\omega)$, using the Lorentz prescription, is taken to be a function of the externally applied field $E_I(\omega)$ and the polarization $P_I(\omega)$[30-32]

$$F_I(\omega) = E_I(\omega) + 4\pi L_{IJ}P_J(\omega) \quad (6)$$

The chromophore is assumed to be imbedded within a cavity inside a uniformly polarized medium. The dimensionless second-rank tensor L_{IJ} connecting local field and polarization accounts for the shape of the cavity. This factor is often called the depolarization factor and is identical in functional form to the demagnetization factor responsible for shape anisotropy in magnetic particles.[33] For a crystalline system the determination of the local field tensor can be quite complicated.[34,35] In polymeric systems, where the center of symmetry is destroyed by electric field poling of the nonlinear chromophore, the symmetry is high enough so that the depolarization factors are diagonal along principal axes of the spheroidal cavity given by a, b, and c. These factors for prolate and oblate spheroids have been tabulated.[36,37] For a spherical cavity the tensor L_{IJ} becomes $L_a = L_b = L_c = \frac{1}{3}$.

For a linear dielectric, the polarization is assumed to be linearly proportional to the polarizability, i.e. the higher order terms in eq 5 are neglected:

$$P_I(\omega) = N\alpha_{IJ}(\omega)F_J(\omega) = \chi_{IJ}^{(1)}(\omega)E_J(\omega) \quad (7)$$

In this case it is convenient to write eq 6 in a principal-axis system as

$$F_I(\omega) = (1 + 4\pi L_I\chi_{II}(\omega))E_I(\omega) =$$

$$[1 + (\epsilon_I(\omega) - 1)L_I]E_I(\omega) \quad (8)$$

$\epsilon_I(\omega)$ is the dielectric constant at the frequency ω, the relationship $\epsilon_I = 1 + 4\pi\chi_{II}$ between dielectric constant and linear susceptibility is used and $L_I \equiv L_{II}$. It is useful to define a local field factor

LOCAL FIELD FACTORS

$$f_\infty^E = L_0\,(\varepsilon_\infty - 1) + 1$$

$$\Uparrow\ \varepsilon = \varepsilon_\infty$$

$$f_0^E = \varepsilon\,(L_0\,\varepsilon_\infty + 1 - L_0)/[\varepsilon(1 - L_0) + L_0\varepsilon_\infty]$$

$$\Downarrow\ L_0 = 1/3$$

$$f_0^S = \varepsilon\,(\varepsilon_\infty + 2)/(2\varepsilon + \varepsilon_\infty)$$

$$\Downarrow\ \varepsilon = \varepsilon_\infty$$

$$f_\infty^S = (\varepsilon_\infty + 2)/3$$

Figure 1. Various limits for the Onsager local field function. The superscript S refers to evaluation of the function using a spherical cavity and E using an elliptical one. The subscripts 0 and ∞ refer to evaluation of the dielectric constants at low frequencies and optical frequencies respectively.

$$f_I(\omega) = 1 + (\epsilon_I(\omega) - 1)L_I \quad (9)$$

such that the internal local field is given in terms of the externally applied field as

$$F_I(\omega) = f_I(\omega)E_I(\omega) \quad (10)$$

Assuming that the tensors α, f and L commute, one obtains the following relationship between microscopic and macroscopic nonlinear properties:

$$\chi_{IJK}^{(2)}(-\omega;\omega_1,\omega_2) =$$

$$Nf_I(\omega)f_J(\omega_1)f_K(\omega_2)\langle\beta_{ijk}(-\omega;\omega_1,\omega_2)\rangle_{IJK} \quad (11)$$

where the term in brackets is a weighted sum of values of the various β_{ijk}'s, an average over all orientations of the chromophore in the polymer.[27,38-40] *This equation relates microscopic to macroscopic nonlinear properties provided both $\chi_{IJK}^{(2)}$ and β_{ijk} have been defined using consistent conventions.*[26]

For a spherical cavity one obtains for the local field factor

$$f_\infty^S = \frac{(\epsilon_\infty + 2)}{3} \quad (12)$$

This is the Lorentz–Lorenz local field correction. The subscript ∞ is meant to indicate that this factor is valid at optical frequencies. For dc and low-frequency fields, one needs to include the orientation of permanent dipoles in the system due to fields associated with both external fields and neighboring dipoles. In this case, the Onsager local field is appropriate.[41] It is shown in its general form in Figure 1. For a spherical cavity, the Onsager local field correction is

$$f_0^S = \frac{\epsilon(\epsilon_\infty + 2)}{2\epsilon + \epsilon_\infty} \quad (13)$$

In eqs 12 and 13, ϵ is the low-frequency dielectric constant and $\epsilon_\infty = n^2$ is the optical frequency dielectric constant (n is the index of refraction). The superscript S indicates that the factors are appropriate for a spherical cavity.

Figure 1 shows the relationship among some of the forms that the local field factor may take. It has been shown that for measurements in solution the use of the Onsager local field for dc fields and the Lorentz–Lorenz field for optical frequencies yields consistent values for the molecular hyperpolarizabilities.[42,43] This is perhaps not surprising since the dielectric properties of the

Table 2. Local Field Factors Using Various Models (See Figure 1)[a]

b/a	L_a	f_0^E	f_∞^E	f_0^S	f_∞^S
1.0	0.333	1.75	1.63	1.75	1.63
0.8	0.276	1.61	1.52		
0.6	0.210	1.46	1.40		
0.4	0.135	1.29	1.26		
0.2	0.056	1.12	1.11		

[a] Using values of ϵ = 3.6 and ϵ_∞ = 2.9.

medium surrounding a nonlinear chromophore are, to a good approximation, statistically isotropic. It is much less clear for the fixed environment of a chromophore embedded in a polymer. Table 2 presents values for the various local fields factors including ones for a prolate ellipsoidal cavity in which a is the major axis and $b = c$ are the minor axes. The values of ϵ and ϵ_∞ are values appropriate for the polymer poly(p-nitroaniline) (PPNA) (see section VI.B).[44] For comparison, a molecule like p-nitroaniline (PNA 1) has a b/a ratio of ~0.4 based on van der Waals' radii and the more extended molecule 4,4'-nitroaminotolan (NAT 2) a value of 0.2. It is not clear that the molecular aspect

NO$_2$

NH$_2$

PNA

1

NH$_2$—◯—≡—◯—NO$_2$

NAT

2
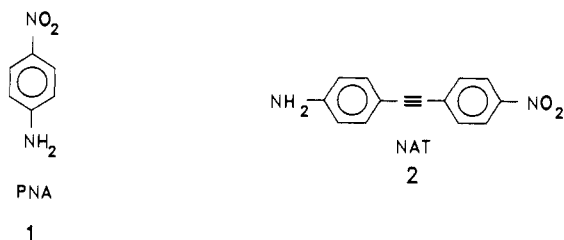
ratio is the correct quantity to use in defining the shape of the ellipsoidal cavity. It is clear, however, that the shape of the Lorentz cavity can make a difference if one wishes to compare microscopic and macroscopic values using eq 11.

The local field factors do not include all of the effects of the dielectric medium surrounding the nonlinear chromophore. Chromophores that have high values of β are also highly electrochromic and solvatochromic, i.e. their lowest energy absorption maxima shift as a function of electric field and solvent polarity. Solvatochromism is in fact a technique for obtaining an estimate of the magnitude of β.[45,46] A greater solvatochromic shift usually indicates a larger β. The shift of molecular energy levels as a function of solvent polarity results in the measurement of differing values of β for the same molecule in different solvents, even when local field factors are taken into account.[47] The dielectric environment for a chromophore in a polymer will in general be different from that of the same chromophore in solution. Therefore, hyperpolarizabilities measured in solution may not be appropriate for describing the chromophore in a polymer.

C. Second-Harmonic Generation and Electrooptic Coefficients

The second-order susceptibility $\chi_{IJK}^{(2)}(-\omega;\omega_1,\omega_2)$ is defined by eq 5. For second-harmonic generation (SHG) and optical rectification processes, a coefficient d_{IJK} is defined such that in the case of SHG processes, by analogy to eq 2:

$$P_I(2\omega) = (^1/_2)\chi_{IJK}^{(2)}(-2\omega;\omega,\omega)e_J(\omega)e_K(\omega) =$$
$$d_{I,JK}(-2\omega;\omega,\omega)e_J(\omega)e_K(\omega) \quad (14)$$

The d tensor is frequently written in contracted form (Voigt notation) with $d_{I,JK} \rightarrow d_{I\mu}$ using the convention (11) $\rightarrow$ 1, (22) $\rightarrow$ 2, (33) $\rightarrow$ 3, (23,32) $\rightarrow$ 4, (13,31) $\rightarrow$ 5, (12,21) $\rightarrow$ 6. This contraction can be performed because the value of $d_{I,JK}$ is independent of the order in which the external electric fields appear in the equation and is a consequence of the fact that the frequencies of the two fields are equal. In an electric field poled polymer, if the 3-axis is taken to be the direction of the poling field, then the chromophores are preferentially aligned with their dipoles pointing in this direction. The system is isotropic in the 1,2-plane. In this symmetry system (∞mm or $C_{\infty v}$), only three of the tensor elements are nonzero, d_{33}, d_{31}, and d_{15}.[48] Another set of symmetry conditions can be used if all three frequencies in $\chi_{IJK}^{(2)}(-\omega_1;\omega_2,\omega_3)$ are in a region far away from lattice or electronic resonances of the system. In this case Kleinman symmetry holds and all three subscripts IJK may be permuted without permuting the frequencies.[49] For this case $d_{15} = d_{31}$ and there are only two independent tensor elements for the poled polymer system.

For the electrooptic or Pockels effect another tensor $r_{IJ,K}$ is defined related to the susceptibility $\chi_{IJK}^{(2)}(-\omega;\omega,0)$.[27,50,51] The Pockels effect is a linear change in the index of refraction of a system in the presence of an external electric field and was originally treated as an electric field induced rotation of the index of refraction ellipsoid. The IJ-th component of the change in the dielectric constant is written as

$$\Delta\left(\frac{1}{\epsilon}\right)_{IJ} \equiv \frac{1}{\epsilon_{IJ}} - \frac{1}{\epsilon_{IJ}(0)} \simeq -\frac{\Delta\epsilon_{IJ}}{\epsilon_{IJ}^2} = r_{IJ,K}E_K \quad (15)$$

where $\epsilon_{IJ}(0)$ is the IJ-th component of the dielectric constant in the absence of the external dc field and the approximation is valid in the limit where field-induced changes in the dielectric constant are small. The electrooptic coefficient can be related to the corresponding susceptibility tensor element (in mks units)[27]

$$\chi_{IJK}^{(2)}(-\omega;\omega,0) = -(^1/_2)\epsilon_{II}(\omega)\epsilon_{JJ}(\omega)r_{IJ,K}(-\omega;\omega,0) \quad (16)$$

When all quantites in eq 16 are in esu units, the factor of $^1/_2$ is replaced by $1/(8\pi)$. Units in nonlinear optics can often be confusing. Skinner and Garth[52] have discussed esu and mks units for these processes. The electrooptic coefficient is frequently contracted on the first two subscripts in a manner analogous to the contraction of the second-harmonic generation tensor. Since the input and output frequencies involved in the electrooptic effect are equal ($\omega = \omega_1$), this contraction can be done with complete generality. For the symmetry ∞mm the nonzero elements are r_{13}, r_{33}, and r_{51}. When Kleinman symmetry is appropriate, $r_{13} = r_{51}$.

In general there is no simple relationship between $r_{\mu K}$ and $d_{I\mu}$, since the second-order susceptibilities involved (eqs 14 and 16) depend on different combinations of electric field frequencies. It has been shown[27,53] that if one uses eq 11 to relate macroscopic to microscopic properties and one assumes that only one component of the molecular hyperpolarizability β_{zzz} is important, where the z-direction is along the direction of the molecule's permanent dipole moment,

one can obtain an approximate relationship between these two quantities using the "two-level" model[54] to describe the dispersion of the hyperpolarizability:

$$r_{1J,K}(-\omega;\omega,0) = -\frac{4d_{K,IJ}}{n_I{}^2(\omega)n_J{}^2(\omega)}\frac{f_{II}^\omega f_{JJ}^\omega f_{KK}^0}{f_{KK}^{2\omega'}f_{II}^{\omega'}f_{JJ}^{\omega'}} \times$$

$$\frac{(3\omega_0{}^2 - \omega^2)(\omega_0{}^2 - \omega'^2)(\omega_0{}^2 - 4\omega'^2)}{3\omega_0{}^2(\omega_0{}^2 - \omega^2)^2} \quad (17)$$

Here ω_0 is the angular frequency of the first strongly absorbing electronic transition in the molecule, ω' is the frequency of the fundamental field used in the second-harmonic generation measurement, and ω is the frequency used for the electrooptic coefficient measurement. The two-level model assumes that second-order hyperpolarizabilities can be described solely in terms of the molecular ground state and a single excited state. In deriving this equation it has been assumed that for optical frequencies the relationship $\epsilon_{LL} = n_L{}^2$ holds. Note that the indices for the second-harmonic tensor element have been permuted so that both SHG and electrooptic experiments have I- and J-th optical frequencies equal. The two-level model has been shown to describe adequately the shape of the dispersion curve for substituted benzene molecules.[55] Its application to more complex molecular systems is less clear. For example, Clays and Schildkraut[56] have measured the value of r_{33} for two side-chain polymer systems as a function of wavelength. They find that the dispersion of r_{33} can be explained quite well by the two-level model but the wavelength of the absorption maximum obtained from the model as a fitting parameter does not seem to agree with its measured value. Given the uncertainties in the reliability of the two-level model along with uncertainties in local field correction factors, it is probably wise to consider eq 17 as a means of obtaining only a rough estimate of $r_{\mu K}$ from a measured value of $d_{K\mu}$.

D. Electric Field Poling Methods

In order to have a finite second-order susceptibility, a polymer system must consist of chromophores oriented in such a way that the total system does not possess a center of symmetry. This is most easily accomplished by applying a dc electric field to the polymer at a temperature where the chromophores' dipoles can be readily oriented. Several approaches have been used to induce this polar order. Interdigitated[1] and coplanar[57,58] electrodes can be used where one desires the polar axis to lie in the plane of the thin film being poled. The thin polymer film can be formed as a "sandwich" between two parallel conducting plates in which case the polar axis is perpendicular to the film's plane.[21] One, of course, wants to use the largest possible electric field for poling in order to obtain the highest degree of polar order. Interdigitated and coplanar electrodes are limited by charge injection processes at regions of high electric field near the sharp electrode edge.[58,59] Charge injection can also occur when parallel plate electrodes are used, and pinholes can substantially reduce the magnitude of the field that can be applied. High field strengths can be obtained using electrode poling provided careful attention is given to material purity, dust-free thin-film processing, and electrode design. The electric field strength across the
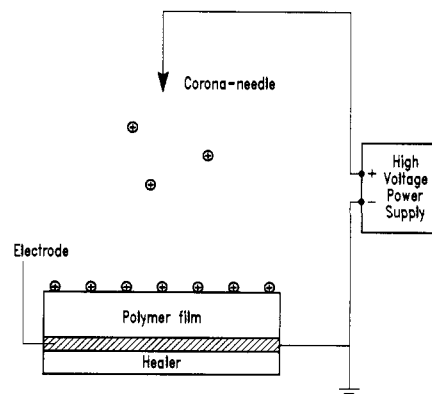

Figure 2. A typical setup for corona poling (from ref 44).

optically nonlinear polymer film depends on the nature of the substrate[60] and the buffer layers used.[61] Electrode poling is compatible with electrooptic and second-harmonic device processing requirements.

Perhaps the most commonly used electric field poling technique for polymeric systems is corona poling.[62-64] Corona poling has been used in other applications to charge the photoconductor in electrophotographic printers and copiers[65] and to pole electrets.[66] The technique has been used for poling second-order nonlinear polymeric systems both at room temperature[67] and at elevated temperatures.[21,44,68] A typical corona-poling setup is illustrated in Figure 2. A sharp needle, wire, or grid is charged to several kilovolts until electric breakdown of the surrounding atmosphere occurs. Depending on the polarity of the corona needle either positive or negative ions can be deposited on the surface of the polymer film. Fields across the polymer film exceeding 4 MV/cm can be obtained in this way.[64] Such high fields are very difficult to achieve using electrode poling. A constant voltage grid can be interposed between the corona needle and the polymer film to control more accurately the voltage across the film. Because of the extremely high electric field in the vicinity of the thin corona wire, electrons present naturally in the surrounding gas are accelerated to energies high enough to ionize molecules and atoms in the gas. Depending on the polarity of the corona wire, either positive or negative ions are swept out of the ionizing region onto the insulating surface of the nonlinear polymer.[69,70] Although negative and positive coronas appear superficially similar, they are really quite different. In a positive corona, electrons are accelerated in the high-field region close to the wire, colliding with and ionizing molecules or atoms in the surrounding atmosphere. This process takes place entirely in the gas phase and does not involve the wire electrode in an active way. For negative coronas, similar processes occur, but the corona wire is intimately involved in sustaining the discharge avalanche, providing a source of feedback electrons by secondary emission, ion impact, and the photoelectric effect. As a result the negative coronas tends to be less stable and very dependent on the chemical composition of the gas in which discharge occurs.

Hampsch et al.[63] have investigated corona-poling processes in polymer films using both negative and positive coronas and in He, N_2, and air atmospheres. The results of the normalized growth and decay of the second harmonic intensity, related to the degree of corona-induced poled order, is shown in Figure 3 for a
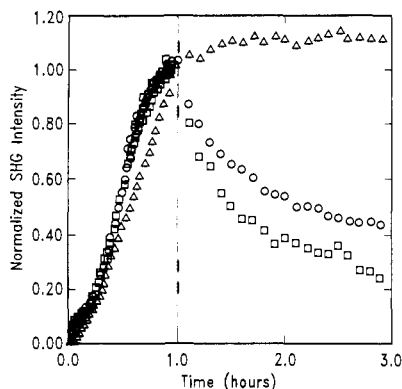
Figure 3. The effect of atmosphere on corona poling and decay of poled order in a polymer film, monitored by SHG intensity (from ref 63). The sample is poled using a positive corona in He (△), N_2 (○), and air (□) atmospheres. After 1 h, the corona is turned off, and the poled order decays due to dissipation of surface charge and rotational relaxation of the chromophores.

positive corona. Growth of the poled order for a period of 1 h is shown (although not specified, the temperature is assumed to be near T_g). Decay of the poled order after turning off the corona is dependent on the nature of the surrounding atmosphere. Two mechanisms contribute to this decay. First, the electric field decays due to neutralization of the charge on the surface of the polymer film and second as the field is reduced, the poled order within the polymer relaxes due to rotational relaxation of the chromophores. These effects can be seen clearly in Figure 3 where the apparent enhanced stability of the second harmonic signal from films poled in a He atmosphere is simply due to the slower neutralization of surface charges in this environment.

In most cases electric field poling is done at a temperature near T_g. If the polymer has a high T_g, this temperature may be above the decomposition temperature of the chromophore or the chromophore may sublime out of the polymer if it is not covalently attached. Barry and Soane[71] have described a way of poling a polymer below its glass transition temperature by using a high pressure of carbon dioxide to plasticize the polymer. For the dye Disperse Red 1 (DR1, **3**) dissolved in poly(methyl methacrylate) (PMMA), a pressure of 500 psi reduces T_g to room temperature. This experiment is discussed further in section VI.A. When the pressure is removed the CO_2 leaves the polymer film and the glass transition returns to its original value.

DR1

3
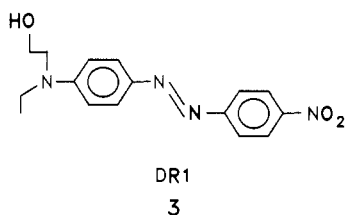
E. Electric Field Poling Dynamics

The degree of poling achieved for a particular polymeric system with a particular poling geometry is critical to an assessment of both the polymer and the poling method for producing second-order optically nonlinear polymers. This can be seen clearly from eq 11 where the quantity $\langle \beta_{ijk} \rangle_{IJK}$ depends on the precise orientation of the chromophores in the polymer. Linear

optical properties, absorption and index of refraction changes can be measured to determine the degree of order.[72] In fact electric field orientation of chromophores incorporated in polymer hosts was used as a method of measuring excited-state dipole moments even before its use in producing second-order nonlinear polymers.[73]

The effect of poling on linear optical properties can be seen by examining the linear term in eq 1:

$$p_i(\omega) = \alpha_{ij}(\omega) F_j(\omega) \tag{18}$$

where the local field $F_j(\omega)$ has been used since here we are ultimately interested in the polarizable chromophore in the dielectric environment of a polymer. Considering the 3-direction as the direction of the externally applied electric field, the macroscopic moment in this direction is simply:

$$P_3(\omega) = \int [p_z(\omega) \cos(z,3) + p_x(\omega) \cos(x,3) +$$
$$p_y(\omega) \cos(y,3)] G(\Omega) \, d\Omega = \chi_{33}^{(1)}(\omega) E_3(\omega) \tag{19}$$

where for example $\cos(z,3)$ is the direction cosine between the molecule fixed z-direction and the macroscopic 3-direction. The quantity $G(\Omega)$ is a normalized distribution function for the chromophores over the solid angle Ω. For an isotropic distribution its value is $1/(8\pi^2)$.[74]

If, as is often the case, the chromophore is an axially symmetric polar molecule one can write the molecular linear polarizability tensor in a principal axis system as

$$\alpha_\perp(\omega) \equiv \alpha_{xx}(\omega) = \alpha_{yy}(\omega) \tag{20}$$

$$\alpha_\parallel(\omega) \equiv \alpha_{zz}(\omega)$$

Using the relationship between $\chi^{(1)}$ and the index of refraction, in the limit where the index of refraction change in the I-th direction given by $\Delta n_I(\omega)$ is small compared to the value of the index itself, it can be shown that[75]

$$\Delta n_3(\omega) \simeq \frac{2\pi N}{n}(\alpha_\parallel - \alpha_\perp)[\langle \cos^2\theta \rangle - {}^1/_3] \tag{21}$$

and

$$\Delta n_1(\omega) = \Delta n_2(\omega) = -({}^1/_2)\Delta n_3(\omega) \tag{22}$$

where N is the number density of chromophores. The induced birefringence according to eqs 21 and 22 depends on the quantity $\langle \cos^2\theta \rangle$. For an isotropic system $\langle \cos^2\theta \rangle = {}^1/_3$ and there is, as expected, no birefringence. Polarizability and hyperpolarizabilities depend on averaged quantities of the form $\langle \cos^n\theta \rangle$. In general, the function $G(\Omega)$ is quite difficult to evaluate.[74] For the important case where both microscopic and macroscopic systems have uniaxial symmetry, $G(\Omega)$ becomes a function only of the polar angle θ between molecular z axis and macroscopic 3 axis. This, to a good approximation, is the situation in poled polymers. One then can write

$$\langle \cos^n\theta \rangle = \int_0^\pi G(\theta) \cos^n \theta \sin \theta \, d\theta \tag{23}$$

The distribution function for a system at thermal equilibrium is related to the Helmholtz free energy $A(\theta)$, via the Boltzmann equation:

$$G(\theta) = \frac{\exp[-A(\theta)/kT]}{\int_0^\pi \exp[-A(\theta)/kT]\sin\theta\, d\theta} \qquad (24)$$

where $A = U - TS$. In eq 24 integration over the other two Euler angles have been canceled out in numerator and denominator. S is the entropy of the system and is usually neglected. The uniaxial symmetry of the system is implicit in the assumption that the free energy is a function of θ only. The energy of an individual molecule in the polymer environment and in an external electric field is given in the mean field approximation by

$$U(\theta) = U_c(\theta) - \mu\cdot\mathbf{F} - (^1/_2)\mathbf{p}\cdot\mathbf{F}\cdot\mathbf{F} \qquad (25)$$

where $U_c(\theta)$ is the intermolecular interaction and $\mathbf{p}$ is the polarizability. (Vector and tensor quantities are indicated in this expression in bold type.) Recall that $\mathbf{F}$ refers to the magnitude of the internal electric field. The term involving the polarizability is generally neglected in systems with large dipole moments μ. For an isotropic system the intermolecular interaction term U_c is not a function of θ. For other systems such as liquid crystals, this term does depend on θ and the dependence is critical to the determination of the order.[5,76] For poled polymer systems the mean field describing intermolecular interactions is assumed to be isotropic. The only term influencing polar order is thus the one involving the dipole moment μ. The average value of $\cos^n\theta$ becomes in this approximation:

$$L_n(\mu F/kT) \equiv \langle\cos^n\theta\rangle =$$

$$\frac{\int_0^\pi \exp[(-\mu F\cos\theta)/kT]\cos^n\theta\sin\theta\, d\theta}{\int_0^\pi \exp[-\mu F\cos\theta/kT]\sin\theta\, d\theta} \qquad (26)$$

The set of functions $L_n(u)$ are known as Langevin functions. They appear in a variety of contexts.[72,73,77] The first three Langevin functions and their relationship to the thermally averaged values of the Legendre polynomials $\langle P_n(\cos\theta)\rangle$ are given below:

$$L_1(u) = \coth u - \frac{1}{u} = \langle P_1(\cos\theta)\rangle \qquad (27)$$

$$L_2(u) = 1 + \frac{2}{u^2} - \frac{2}{u}\coth u = \frac{1}{3}(2\langle P_2(\cos\theta)\rangle + 1) \qquad (28)$$

$$L_3(u) = \left(1 + \frac{6}{u^2}\right)\coth u - \frac{3}{u}\left(1 + \frac{2}{u^2}\right) =$$

$$\frac{1}{5}(2\langle P_3(\cos\theta)\rangle + 3\langle P_1(\cos\theta)\rangle) \qquad (29)$$

where $u = \mu F/kT$. The averaged value of the second-order Legendre polynomial is frequently referred to as an order parameter $\Phi = \langle P_2(\cos\theta)\rangle$. Its value is zero in a completely disordered system and unity in a system in which all chromophores have their dipole axes along the same direction. Note that this order parameter does not distinguish between the case when all dipoles are pointing in the same direction and the one in which the dipoles have two orientations along and opposite to the uniaxial direction. The functions $L_2(u)$, $L_3(u)$, and $\Phi(u)$ are plotted in Figure 4. More extensive discussion of these functions, including the case where the polarizability cannot be neglected in the energy expression eq 25, has been given by Kielich.[38]
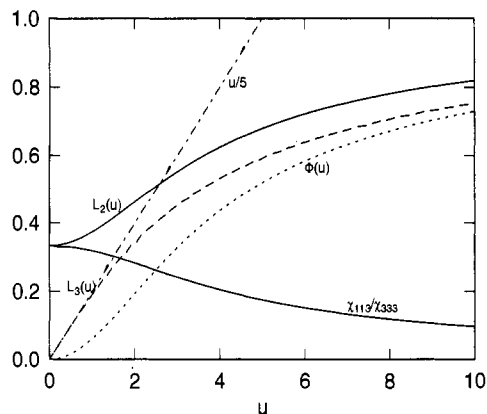
Figure 4. The second and third Legendre polynomials ($L_2(u)$ and $L_3(u)$) as a function of u, where $u = \mu F/kT$. Also shown are $u/5 = \mu F/5kT$, the order parameter $\Phi(u)$ and the ratio $\chi_{113}(u)/\chi_{333}(u)$.
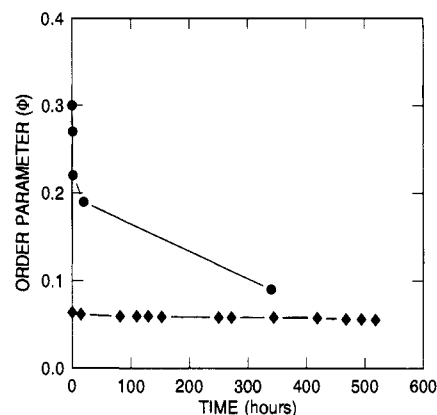
Figure 5. The decay in order parameter Φ for two poled-polymer systems at room temperature, one in which the chromophore is dissolved in the polymer matrix as a guest (●) and one in which the chromophore is covalently attached as a side chain to the polymer backbone (♦). The data are from ref 72.

The order parameter Φ can be determined from measurements of the index of refraction parallel, $n_\parallel = n_0 + \Delta n_3(\omega)$, and perpendicular, $n_\perp = n_0 + \Delta n_1(\omega)$, to the direction of the poling field by noting that

$$\Phi = \frac{n_\parallel - n_\perp}{n_\parallel + 2n_\perp - 3n_0} \qquad (30)$$

n_0 is the isotropic dielectric constant before poling. Page et al.[72] have measured the indices of refraction in a waveguide for a system in which the chromophore is incorporated in the polymer as a guest and one in which the chromophore is covalently attached to the polymer backbone as a side chain. Figure 5 shows their experimental data as a function of time after poling indicating the enhanced stability of the side chain system. Differences in the magnitude of Φ are due to differences in thickness and consequently the poling electric field.

The absorption spectrum of a system also changes with electric field poling.[73,78] For a film of the dye DR1 3 in PMMA this effect can be quite striking. The initially reddish-orange film becomes purple after poling and slowly returns to reddish-orange as the chromophores relax. The absorption changes are directly related to the orientation of the chromophores and can be used as a means of evaluating the degree of orientation. If one assumes that the molecular elec-
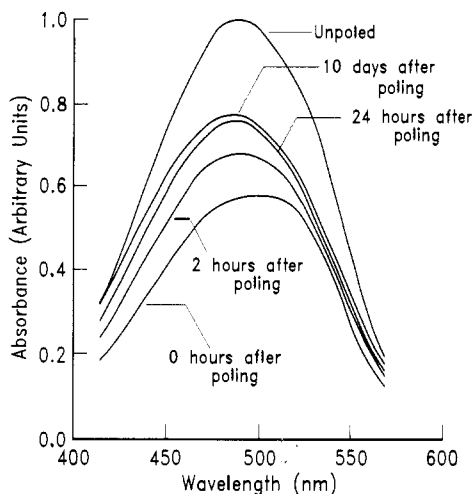
Figure 6. The change in absorption spectrum after poling due to orientation of the chromophores for a film of DR1 3 in PMMA (from ref 62). The spectra are measured with light polarized perpendicular to the poling field.

tronic transition moment is parallel to the permanent ground-state dipole moment, one can obtain the order parameter Φ by measuring the absorbance of an unpoled system A_0 and of a poled sample with light polarized perpendicular to the poling direction $A_\perp$:[62,72]

$$\Phi = 1 - (A_\perp / A_0) \tag{31}$$

Figure 6 shows measurements of the absorption spectrum of a polymer system unpoled and at various times after electric field poling. The spectrum is measured with light polarized perpendicular to the poling direction. As poling proceeds the chromophores reorient in the polymer so that their permanent dipole moment is along the field direction. Since the transition moment is assumed to be parallel to the permanent moment, absorption in the polymer film perpendicular to the poling direction decreases. Effects other than chromophore orientation can cause changes in the absorption spectrum during poling and complicate the analysis. Sublimation of the chromophore out of the polymeric host,[79] in those cases where it is not chemically bound, or thermal decomposition of the chromophore at the poling temperature[57] can lead to reductions in the absorption not related to poling order. In addition the electric field applied during the poling process can lead to irreversible absorption changes.[80]

By using either index of refraction or absorbance measurements to determine the degree of polar orientation in corona-poled polymers, values of Φ of 0.2–0.3 have been obtained shortly after poling in the guest-host systems DR1/PMMA.[62,72] This implies a value of $u \approx 2$, which in turn indicates that the internal electric field responsible for orientation of the chromophores is on the order of 3–5 MV/cm. The external field actually applied across the thin polymer film will be somewhat reduced from this value by local field factors. The order parameter after corona poling has been measured for a variety of other systems[81,82] and found to be in the above range. For parallel plate poling Φ is found to be smaller, on the order of 0.08.[21] By using interdigitated electrodes for poling, a value of $\Phi = 0.3$ has been found for a thermotropic nematic liquid crystalline copolymer doped with a nonlinear chromophore.[1] The large order parameter for this system is attributed to enhanced ordering of the chromophore due to the liquid crystalline nature of the host.

The second-order nonlinear properties of a poled polymer system are related to the susceptibility $\chi_{IJK}^{(2)}$ ($- \omega;\omega_1,\omega_2$) given by eq 11. In general the average $\langle \beta_{ijk} \rangle_{IJK}$ can be quite complicated even when the macroscopic system possesses uniaxial symmetry.[27,38-40,83] Considerable simplification results if one assumes that only one component of the molecular hyperpolarizability β_{zzz} needs to be considered. In most cases of practical interest this approximation can be made. The susceptibility tensor in the direction of the poling electric field then becomes

$$\chi_{333}^{(2)}(-\omega;\omega_1,\omega_2) = Nf_\omega f_{\omega_1} f_{\omega_2} \int \cos^3(z,3) G(\Omega) \, d\Omega$$

$$= N\beta_{zzz}^\times \langle \cos^3 \theta \rangle \tag{32}$$

$$= N\beta_{zzz}^\times \frac{1}{5}[3\langle P_1(\cos\theta) \rangle + 2\langle P_3(\cos\theta) \rangle]$$

where $\beta_{zzz}^\times$ incorporates the local field factors into the hyperpolarizability for notational simplicity. Similarly one may write

$$\chi_{113}^{(2)}(-\omega;\omega_1,\omega_2) = Nf_\omega f_{\omega_1} f_{\omega_2} \int \cos^2(x,3) \cos(z,3) G(\Omega) \, d\Omega$$

$$= N\beta_{zzz}^\times \frac{1}{2}[\langle \cos\theta \rangle - \langle \cos^3\theta \rangle] \tag{33}$$

$$= N\beta_{zzz}^\times \frac{1}{5}[\langle P_1(\cos\theta) \rangle - \langle P_3(\cos\theta) \rangle]$$

The averages $\langle \cos^n\theta \rangle$ are described by eq 26 in the limit where only the contribution μF to the free energy needs to be considered. In this case eqs 32 and 33 can be written in terms of the Langevin functions as

$$\chi_{333}^{(2)}(-\omega;\omega_1,\omega_2) = N\beta_{zzz}^\times L_3(u) \tag{34}$$

$$\chi_{113}^{(2)}(-\omega;\omega_1,\omega_2) = N\beta_{zzz}^\times \frac{1}{2}[L_1(u) - L_3(u)] \tag{35}$$

Equations 34 and 35 may be simplified by utilizing the expansions of the Langevin functions for small values of the argument u.

$$L_1(u) \approx u/3$$
$$\tag{36}$$
$$L_3(u) \approx u/5$$

These expansions work quite well even for values of the argument $u \approx 1$.[72,77] This can be seen in Figure 4 for L_3 where the function deviates significantly from its approximation only for $u > 1$. In the region where these expansions are valid, it is easy to show that

$$\frac{\chi_{113}}{\chi_{333}} \approx \frac{1}{3} \tag{37}$$

Figure 4 shows this ratio as a function of the argument u. Equation 37 implies that d_{13}/d_{33} and r_{31}/r_{33} also are approximately equal to $1/3$. In many cases this approximation is simply assumed to be the case in the analysis of the data. In those cases where both tensor components are independently measured it is frequently found to be a good approximation.[27,68,84-89] In other cases substantial deviations from the $1/3$ ratio have been measured.[44,90-93]

Deviations from $1/3$ can have a variety of origins. At very high fields, all of the Legendre polynomials in eqs 32 and 33 approach unity and the ratio χ_{113}/χ_{333} goes to zero. Meyrueix et al.[86] have assumed that the small
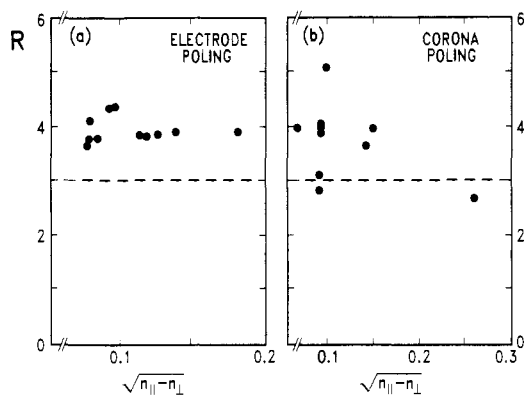
Figure 7. The ratio $R = n_{\parallel}^4 r_{33}/n_{\perp}^4 r_{13}$ for the linear epoxy polymer poly(bisphenol A–aminonitrotolan) (BisA-ANT) as a function of the square root of the birefringence Δn for corona- and electrode-poled samples (from ref 95). The expected value of $R = 3$ is indicated by a dashed line.

deviation from $1/3$ that they observe is due to this effect and used it to obtain the decays of $\langle P_1 \rangle$ and $\langle P_3 \rangle$ separately. In situations where liquid crystalline phases influence the chromophore orientations the ratio can deviate from $1/3$ even at low fields.[1,85,90] If any of the optical frequencies are near a chromophore resonance, the approximations leading to eqs 34 and 35 may not be valid.[91] Kuzyk et al.[94] have measured this ratio in polymer systems under uniaxial stress and found values for the ratio ranging from 0.33 for a film under no stress to 0.7 for one under moderate stress. They have used the technique to obtain estimates of the parameters $\langle P_1 \rangle$, $\langle P_2 \rangle$, $\langle P_3 \rangle$, and $\langle P_4 \rangle$.

Herminghaus et al.[95] have shown that, even in the case where none of the complicating features described above are present, substantial deviations may be obtained for the ratio

$$R = n_{\parallel}^4 r_{33}/n_{\perp}^4 r_{13} \qquad (38)$$

from the expected value of 3 for the linear epoxy polymer poly(bisphenol A–aminonitrotolan) (see section VI.C), assuming $n_{\parallel} \approx n_{\perp}$. Their results are shown in Figure 7. In the low-field limit the square root of the birefringence $(n_{\parallel} - n_{\perp})^{1/2}$ is proportional to u. Even for small values of the poling field, significant deviation from $R = 3$ is observed. One explanation for this deviation is that chromophore–chromophore interactions need to be included in the orientational averaging. These interactions are explicitly ignored in the oriented gas model. Typical chromophores have dipole moments in the range 4–8 D.[96] The dipole–dipole interaction energy for dipoles of this strength and separated by 10 Å can be equal to or greater than the energy μF due to the poling electric field. However, in the absence of symmetry-breaking effects, such as liquid crystalline ordering, the net effect of the dipole–dipole interactions cannot induce polar ordering even though individual pairwise interactions are large.[95] There is currently no clear evidence of chromophore–chromophore correlations in these chromophore–polymer systems in the absence of liquid crystalline ordering.[97]

Herminghaus et al. have explained the results shown in Figure 7 by assuming that not all chromophores are equally easy to orient. A threshold torque is required before a dipole can be oriented and this threshold is different for different chromophores. This model would predict that, if the poling were performed at high enough
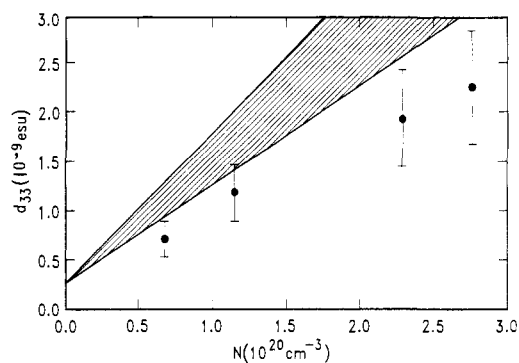

Figure 8. d_{33} as a function of number density N for the guest–host polymer system DR1 3 in PMMA (from ref 21). The hatched region indicates d_{33} values expected from eq 40.

temperature or long enough times at lower temperatures for the restrictions on rotation to disappear, the value of R would approach the expected value of 3. Wu[75] has attempted to model the dynamics of the poling process by considering rotational diffusion in the presence of an external electric field. All chromophores are assumed to possess the same rotational diffusion constant. Considerations of the value of R actually observed would seem to indicate that in many cases this is a considerable over-simplification and that one must, at the very least, consider a system possessing an ensemble of rotational diffusion constants.

Boyd et al.[88] have attempted to measure constrained rotation in guest–host polymers, not by measuring R but by measuring a quantity $\bar{\rho}(T)$ they call the average rotational mobility parameter. This quantity is defined as

$$\bar{\rho}(T) \equiv \frac{\langle \cos^3\theta \rangle_T}{\langle \cos^3\theta \rangle_{\text{free}}} \qquad (39)$$

The denominator is the average value of $\cos^3\theta$ when the dipolar chromophores are completely free to rotate and is given by $L_3(u)$, and the numerator is its value at a temperature T. The value of $\bar{\rho}(T)$ may vary from 0 for dipoles that are unable to rotate in the electric field to 1 for completely unconstrained dipoles. The denominator of eq 39 is determined from a measurement of the SHG signal from a guest–host system in an orienting electric field above T_g where it is assumed that the chromophores are completely free to rotate. The numerator is determined by measuring the orientation that occurs in the same electric field at the temperature T. As might be expected the mobility parameter at a given temperature is related to the chromophore size.

It is possible, for modest degrees of poling, to write eq 11 as

$$\chi_{333}^{(2)}(-\omega;\omega_1,\omega_2) = N\beta_{zzz}^{\times}(-\omega;\omega_1,\omega_2)\frac{\mu F}{5kT} \qquad (40)$$

From this equation one would expect the second-order susceptibility to be linearly proportional to chromophore concentration. This linear relationship is shown in Figure 8[21] for the guest–host system DR1 3 in PMMA and has been observed for a variety of other nonlinear polymer systems as well.[82,98,99] The shaded area in Figure 8 represents the range of values that would be expected using eq 40 and independent measurements of the chromophore dipole moment, indices of refraction, and hyperpolarizability. Figure 9[85] shows the deviations from linearity that can occur
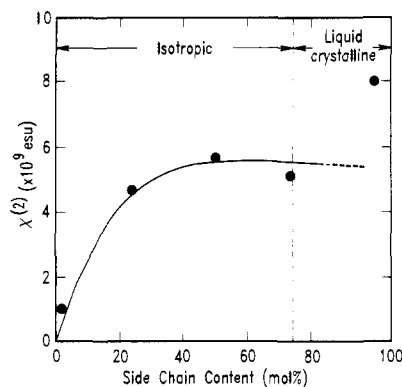
Figure 9. The dependence of $\chi^{(2)}$ on functionalization level for a side-chain polymer that becomes liquid crystalline at 75% mol fraction functionalization (from ref 85).
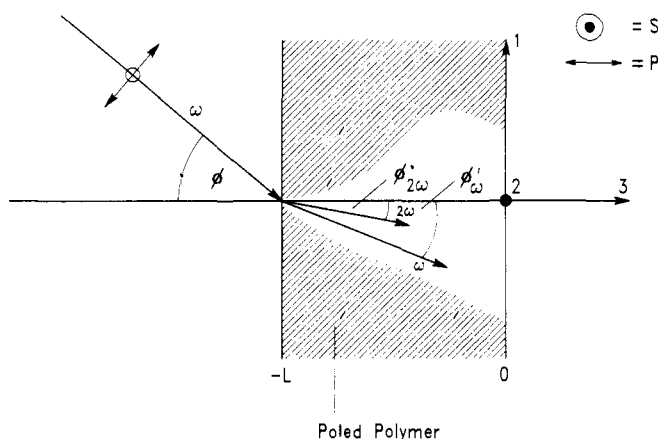

Poled Polymer

Figure 10. Maker fringe technique for poled polymers (from ref 9). The fundamental light beam at frequency ω is incident at an angle ϕ on the polymer film of thickness L (poled along axis 3). The angles of the fundamental- and second-harmonic beams inside the polymer are given by ϕ'_ω and $\phi'_{2\omega}$, respectively.

when liquid crystalline ordering is present. A similar linear dependence on the externally applied electric field is expected from eq 40 and observed.[21,98,100] In solution the electric field dependence has been shown to obey the functional form $L_3(u)$ implied by eq 34.[101]

III. Measurement Techniques

A. Second-Harmonic Generation

A variety of experimental techniques have been used to obtain both absolute and relative values of the second-order susceptibility $\chi^{(2)}(-\omega;\omega_1,\omega_2)$. These have been reviewed by Kurtz.[102] For poled polymer systems the Maker fringe second-harmonic generation technique is frequently used to obtain this quantity.[102,103] This technique is illustrated in Figure 10. Polarized light is incident at an external angle ϕ to the surface normal of a poled polymer film. As previously mentioned, the poled polymer has ∞mm symmetry with the 3-direction as the poling direction. Using the contracted SHG coefficients defined in eq 14, it can be shown that in this symmetry group[44,91,103]

$$I^S_{2\omega} \propto d_{31}{}^2 \sin^2 \phi'_{2\omega} I_\omega{}^2 \sin^2[\pi(l/2l_c)] \quad (41)$$

and

$$I^P_{2\omega} \propto d_{\mathrm{eff}}{}^2 I_\omega{}^2 \sin^2\left(\pi \frac{l}{2l_c}\right) \quad (42)$$

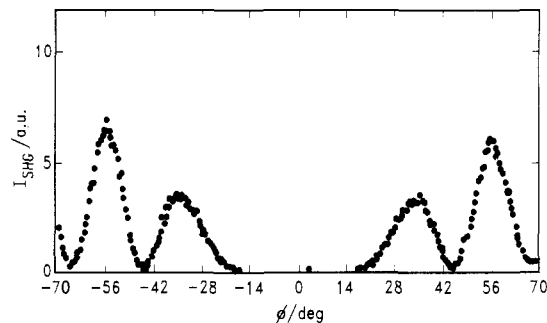where the effective SHG coefficient is given by

Figure 11. Typical Maker fringe curve showing SHG intensity vs ϕ (defined in Figure 10) for a polymer film of thickness 94 μm (from ref 9).

$$d_{\mathrm{eff}} = d_{33} \sin^2 \phi'_\omega \sin \phi'_{2\omega} + d_{31} \cos^2 \phi'_\omega \sin \phi'_{2\omega} +$$
$$2d_{15} \sin \phi'_\omega \cos \phi'_\omega \cos \phi'_{2\omega} \quad (43)$$

The angles above are defined in Figure 10 with the prime indicating internal angles. $I^S_{2\omega}$ refers to the second-harmonic intensity measured with intensity I_ω of the fundamental beam polarized perpendicular to the plane formed by the direction of the incident fundamental beam and the polymer film surface normal (s-polarized). $I^P_{2\omega}$ is the second-harmonic intensity with the fundamental beam polarized in this plane (p-polarized). l_c is the coherence length. The second-harmonic light generated at a point x in the polymer is 180° out of phase with second-harmonic light generated at the point $x + 2l_c$ and thus can destructively interfere with it. This constructive and destructive interference is expressed in the coherence length which is given in terms of the indices of refraction n_ω at ω and $n_{2\omega}$ at 2ω and the wavelength λ of the fundamental:

$$l_c = \frac{\lambda}{4|n_\omega \cos \phi'_\omega - n_{2\omega} \cos \phi'_{2\omega}|} \quad (44)$$

As a result of this spatially modulated interference, the measured second-harmonic intensity will depend as shown on the polymer film thickness. The coherence length is on the order of a few micrometers for poled polymers.

From eqs 41–43, it can been seen that light incident parallel to the poling direction cannot generate second harmonic light. Furthermore one cannot obtain all three nonzero components of the d tensor from measurements of $I^S_{2\omega}$ and $I^P_{2\omega}$ alone. An additional assumption or measurement must be made. Away from resonance Kleinman symmetry can be assumed yielding the identity $d_{31} = d_{15}$. This assumption is almost always made. By making a third measurement Hayden et al.[91] have been able to measure d_{15} and d_{31} separately. They find that the ratio d_{15}/d_{31} is as high as 1.25 in some systems. It is also often assumed that $d_{31} = {}^1/_3 d_{33}$. This last assumption along with Kleinman symmetry means that only a single measurement, for example of $I^S_{2\omega}$, needs to be made. As we have previously discussed, this assumption quite frequently is not correct.

In the Maker fringe experiment, the angle ϕ is varied by rotating the sample, changing the coherence length l_c and the path length of the light through the sample. This results in an oscillating variation of the SHG intensity according to either eq 41 or eq 42. A typical Maker fringe pattern for a poled-polymer system is shown in Figure 11. In this example, the polymer film is fairly thick and several periods of oscillation are
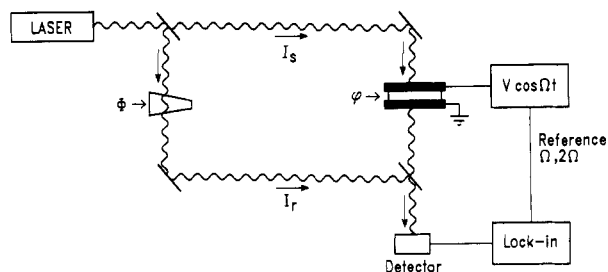
Figure 12. Typical Mach–Zehnder interferometer for measuring r. Wavy lines indicate the light path and solid lines the electrical connections.

observed. For very thin samples with thicknesses less than l_c, only the envelope function of the Fresnel factors is seen.

In these experiments the SHG intensity from the poled-polymer film is measured relative to the intensity of a reference material, often quartz. The most frequently used value of d_{11} for quartz is 1.2×10^{-9} esu (0.49 pm/V) measured at 1.064 μm.[104] This reference value is itself obtained by ultimately reference to the d_{31} coefficient of LiIO$_3$, measured by parametric fluorescence.[105] The value for d_{11} of quartz has recently been called into question as a result of SHG experiments by Eckardt et al.[106] These authors find a much smaller value for d_{31} of LiIO$_3$ (−4.1 pm/V ± 10% instead of −7.1 pm/V ± 8%). If this more recently measured value for LiIO$_3$ is accepted, then the quartz and the polymer film values for d must be reduced by 42%. Recently Roberts[107] has assessed the SHG coefficients for a number of nonlinear optical crystals and has concluded that the smaller value ($d_{11} = 0.30$ pm/V) is more consistent with other measurements. In the words of Eckhardt et al., "It is remarkable that after more than 25 years of study in nonlinear optics, there should exist such uncertainty in the scale of the nonlinear parameters." Fortunately the microscopic hyperpolarizabilities β are also frequently measured with respect to the same quartz reference value.[108] Provided both β and $\chi^{(2)}$ measurements are made using the same value for the quartz reference, comparisons between macroscopic and microscopic quantities using eq 39 can still be made. On the other hand, calculations of r from d using eq 17 cannot be made unless a correct absolute value of d of the reference is known.

B. Electrooptic Effect

The electrooptic coefficient can be determined by measuring the change of the dielectric constant or index of refraction when a field is applied across the sample of interest. The basic relationship used is eq 15 which is rewritten below in terms of the index of refraction and to include a term second order in the applied electric field:

$$\Delta n = -(n^3/2)(r_{\mu,k} + s_{\mu,\nu}E_l)E_k \quad (45)$$

In this equation $s_{\mu,\nu}$ is a fourth-order tensor responsible for the quadratic electrooptic or Kerr effect.[109] It is written in contracted notation for both subscripts. A Mach–Zehnder interferometric technique for measuring r is shown in Figure 12.[27,53] (Hayden et al.[91] have recently described a waveguide embodiment of this technique.) Coherent light from a laser source is split into two paths, one through the sample and one through

a wedge-shaped reference material. The two beams are recombined at the detector. The intensity of the signal at the detector $S(\Phi)$ can be written

$$S(\Phi) = (^1/_2)(I_r + I_s) + (I_rI_s)^{1/2} \cos(\Phi - \phi) \quad (46)$$

where I_r is the intensity in the reference arm and I_s is the intensity in the sample arm of the interferometer. Φ is the reference-controlled phase and the phase in the sample arm is

$$\phi = 2\pi(n - 1)h/\lambda \quad (47)$$

where h is the sample thickness and λ is the laser wavelength. If a modulated voltage (with modulation frequencies small compared to optical frequencies) is applied across the sample, the phase ϕ will change as a result of changes in the index of refraction given by eq 45. It is also clear that any changes in thickness due to piezoelectricity will also affect the phase ϕ. Piezoelectric thickness changes are controlled by the coefficient d^P where

$$\Delta h = hd^PE \quad (48)$$

By applying a modulated voltage to the sample at a frequency Ω and measuring the index of refraction change only at this frequency one measures the following signal:

$$S_\Omega(\Phi) =$$
$$\frac{2\pi}{\lambda}V(I_rI_s)^{1/2}\left[-\frac{1}{2}n^3r_{13} + (n-1)d^P\right]\sin(\Phi - \phi) \quad (49)$$

where V is the amplitude of the modulated voltage. By measuring the modulated signal as a function of the variable reference phase Φ and comparing the amplitude of this signal to the signal when $V = 0$, one can obtain a value for the quantity in brackets in eq 49. It is not possible by this experiment alone to distinguish between piezoelectric and electrooptic contributions. If the poling plane is parallel to the sample laser beam direction, it is only possible to obtain the r_{13} component of the electrooptic tensor and then only if one assumes the piezoelectric contribution to be negligible.

If a substantial dc voltage exists across the sample, perhaps as a result of trapped charges injected during poling, the quadratic electrooptic effect can make a contribution as given by eq 45. Many mechanisms contribute to this higher order effect: electronic and orientational effects, electrode attraction, electrostriction, motion of the trapped charges themselves, and heating. These contributions have recently been analyzed in detail by Kuzyk et al.[110] In most cases, unless the dc voltage is quite large, these higher order effects will be negligible. Internal charges can, however, significantly affect the measured value of r_{13} by setting up an internal field opposing the applied electric field and thus reducing the effective electrooptic coefficient measured.

Other techniques have been used to measure r. Uchiki and Kobayashi have described a Fabry–Perot interferometric technique.[111] In this approach the light beam is perpendicular to the film thickness. Interference patterns related to the film's thickness and index of refraction are generated by scanning the wavelength. Since the beam contains no polarization component perpendicular to the plane of the film, only r_{13} can be measured in this way. Meyrueix et al.[86] have recently described a variation of this approach that permits both

Table 3. Experimental Values of Electrooptic and Piezoelectric Coefficients

polymer[a]	r_{13}	r_{33}	d^P	$-(^{1}/_2)nr_{13}$	$(n-1)d^P$
FSCL240	−0.4	−2.2	−0.43	0.82	0.26
FSCL251	−1.9	−5.8	−2.5	4.17	1.59

[a] Reference 93, the polymers measured are side-chain systems from Thomson-CSF. All numerical values are in pm/V.

r_{13} and r_{33} to be obtained. This is accomplished by having the light beam incident at an angle to the film surface. Both s- and p-polarized output waves are measured. Instead of scanning the wavelength, the sample is wedge shaped and translation of it effectively scans the thickness.

An ellipsometric technique has been used by Teng and Man.[100] A thin film sample is prepared with one surface coated with a reflective layer of gold. The opposite surface is illuminated by a laser beam incident at an angle of 45° to the surface. The phase difference between s- and p-polarized reflected light is measured with a Soleil–Babinet compensator. Variations of this difference at the frequency of an applied electric field are then measured. Teng and Man did not obtain r_{13} and r_{33} separately using this technique. Clays and Schildkraut[56] have recently used a variation of this technique to demonstrate the importance of electrochromic effects in the ellipsometric determination of r.

An attenuated total reflection (ATR) technique has been described that, while more involved in terms of sample preparation, can yield both components of the electrooptic coefficient as well as the piezoelectric contribution.[93,112] In this approach both sides of a polymer film are coated with a thin Ag layer. The angle of incidence of the light beam is varied and reflectivity minima are observed when the incident light is at the correct angle to couple into one of the guided modes of the polymeric film. Since this angle depends on the index of refraction of the polymer film, it can be modulated via the electrooptic effect by an externally applied field. In a sense, this experiment is a Fabry–Perot measurement where, instead of scanning wavelength or film thickness, one scans the incidence angle.

Measured values of electrooptic and piezoelectric coefficients for two polymers with the chromophores attached as a side chain are presented in Table 3. In addition the material-related quantities in eq 49 are given. One can see that for this particular sample configuration, the piezoelectric effect makes a significant contribution at the modulation frequency used. The magnitude of this contribution will depend on the nature of the sample surfaces, whether they are free or clamped, and on the frequency of the measurements. One way of eliminating the piezoelectric contribution is to perform experiments as a function of increasing modulating frequency to the point where the frequency dependence vanishes. The electrooptic effect will not be frequency dependent at rf frequencies.

IV. Poled-Order Relaxation

A. Rotational Diffusion

The axially ordered state induced in a polymer by electric field poling will slowly decay to its equilibrium isotropic state when the poling electric field (including

any fields from residual trapped charges) is removed. Understanding the nature of this poled-order relaxation is important from two points of view. First, the ultimate use of second-order nonlinear polymers in devices (see section V) requires that the poled order be stable. It is thus important to understand how to design polymer systems to enhance this stability. Second, the study of slow orientational relaxation processes in polymers below T_g can be used as an important tool for investigating polymer dynamics over these very long time scales. This is a particularly difficult time regime to investigate, yet it is precisely the time scale that is relevant to the long-term aging of polymers. Singlet and triplet transient grating experiments can probe relaxations up to at most a few milliseconds.[113–115] Dielectric relaxation measurements can be made, with a great deal of difficulty, at frequencies as low as 10^{-6} Hz.[116] Recently, very slow chromophore orientational relaxation processes have been measured by monitoring the recovery of the absorption signal after photobleaching using polarized light.[117,118] Measurement of poled-order decay by following either the SHG, electrooptic, or birefringence decay can easily follow decays over months or even years.

The description of relaxation of poled-order frequently begins with the Smoluchowski equation for rotational diffusion,[119] with the additonal assumption that one only need consider relaxation of the average value of the angle θ between the poling direction and the direction of the chromophore dipole moment:[57,120]

$$\frac{1}{D_r}\frac{\partial G(\theta,t)}{\partial t} = \nabla^2 G(\theta,t) \qquad (50)$$

where $G(\theta,t)$ is the distribution function, now time dependent. It need not be equal to eq 24 even at $t = 0$. The rotational diffusion coefficient D_r can be written in terms of the mean square deviations of the time-dependent angle $\theta(t)$ as[121]

$$\langle(\theta(t)-\theta(0))^2\rangle = 4D_r t \qquad (51)$$

Equation 50 is simply Fick's law for diffusion. In the absence of diffusion, that is, when the left-hand side of eq 50 is identically zero, the Legendere polynomials are solutions of the differential equation. Since these functions form a complete set, one can expand the time-dependent distribution function as

$$G(\theta,t) = \sum_{n=0}\frac{2n+1}{2}C_n a_n(t)P_n(\cos\theta) \qquad (52)$$

The set of coefficients C_n describe the initial orientation at $t = 0$. Each coefficient is, in fact, the ensemble average of the corresponding Legendre polynomial at this time:[27,57]

$$C_n = \langle P_n(\cos\theta)\rangle_0 \qquad (53)$$

In the case where the poling can be described by eq 24 with $A(\theta) = -\mu\cdot\mathbf{F}$, Wu[57] has shown that C_n can be represented as a ratio of Bessel functions with argument u. By substituting eq 52 back into eq 50 and solving the resulting differential equation, the following expression for $a_n(t)$ can be obtained:

$$a_n(t) = \exp[-n(n+1)D_r t] \qquad (54)$$

Solutions to the rotational diffusion equation in more complex situations where diffusion is geometrically
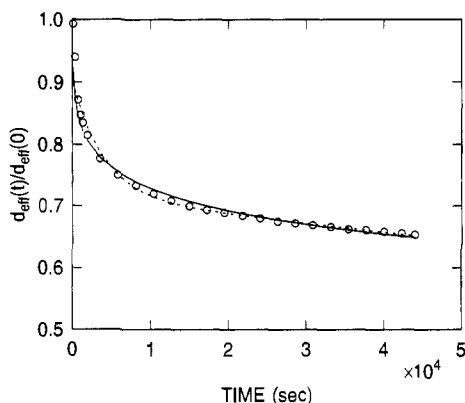
Figure 13. A typical decay of the normalized effective second harmonic coefficient (eq 43) of a poled polymer (from ref 59). The experimental data (O) can be fit with either a Kohlrausch–Williams–Watts (KWW) stretched exponential (solid line) (eq 58) or with a biexponential decay (dashed line).

restricted have been described by Wang and Pecora.[122] From eqs 52 and 54 one obtains the time dependence of the average value of the Legendre polynomials:

$$\langle P_n(\cos\theta)\rangle_t = C_n a_n(t) = C_n \exp(-D_n t) \qquad (55)$$

where $D_n \equiv n(n+1)D_r$. Using eqs 21 and 32 one can write the decay of the birefringence and the second-order nonlinearity as

$$\Delta n_3(\omega|t) = \frac{2\pi N}{n}(\alpha_\parallel - \alpha_\perp)(^2/_3)C_2 \exp(-D_2 t) \quad (56)$$

$$\chi^{(2)}_{333}(-\omega;\omega_1,\omega_2|t) =$$
$$N\beta^x_{zzz}(^1/_5)[3C_1 \exp(-D_1 t) + 2C_3(-D_3 t)] \quad (57)$$

In the case where the C_n can be represented by the Langevin functions, the second term in eq 57 is an order of magnitude smaller than the first and $\chi^{(2)}_{333}$ exhibits single exponential decay. These equations indicate that birefringence decay will be a factor of 3 faster than decay of second-order nonlinear effects such as second-harmonic generation. This difference in decay times has been observed in several polymer systems.[92,123]

The use of eq 50 to describe relaxation implies that all chromophores have the same rotational diffusion coefficient. In amorphous polymers, this is very frequently not the case. As a result, one does not necessarily expect to observe the single exponential decays shown in eqs 55 and 56. Instead one expects a continuous range of decay times expressing the variations in D_r. A variety of functional decay forms have been used to describe time-dependent processes in disordered systems.[124,125] The Kohlrausch–Williams–Watts (KWW) stretched exponential function[126,127] has often been used to fit the orientational decay of chromophores in polymers:[92,117,118,123,128,129]

$$\Phi(t) = \exp(-t/\tau)^\beta \qquad (58)$$

where $\Phi(t)$ may be the normalized birefringence or second harmonic signal decay for example. The KWW function corresponds to a continuous distribution of single exponential decays, with the width of the distribution characterized by β. β has values between 0 and 1. (β here is not related to the β defined in eq 1.) The average relaxation time is given by
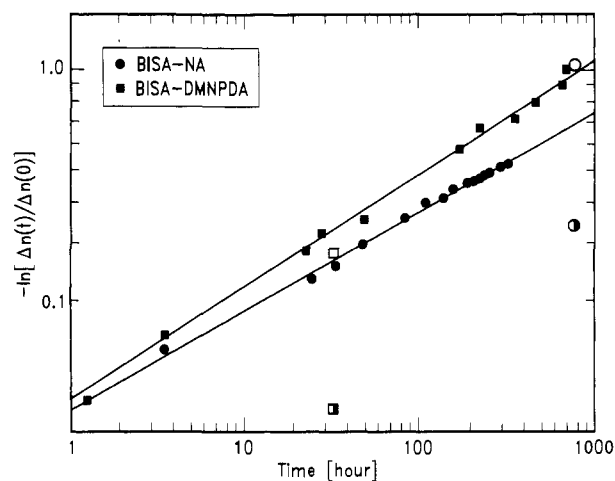

Figure 14. Log–log plot of $-\ln[\Delta n(t)/\Delta n(0)]$ as a function of time at room temperature for two polymers in which the chromophores are incorporated into the polymer backbone (see section VI.C). The data are from ref 92. The solid lines represent fits to the KWW stretched exponential (eq 58). The half-filled and open circles and squares represent the decay of the second-order nonlinear optical coefficient for the two polymers. The fully open circle and square are these SHG decay times multiplied by 3.

$$\langle\tau\rangle = (\tau/\beta)\Gamma(1/\beta) \qquad (59)$$

where the Γ function is a well-known numerically tabulated integral.[130] The KWW function can be related to the fractal properties of the underlying disordered system.[131] It has also been proposed that nonexponential decay may arise from an underlying nonexponential molecular relaxation resulting from cooperative motions.[132,133] In general, however, it is best not to over-interpret the significance of eq 58. It should perhaps simply be viewed as a means of characterizing nonexponential decay with only two adjustable parameters.

Decays have also been described by a sum of two exponentials with, of course, the addition of a third fitting parameter.[134,135] Figure 13 shows that in many cases it is difficult to distinguish between these two functional forms from the experimental decays alone. Figure 14 is a log–log plot of $-\ln[\Delta n(t)/\Delta n(0)]$ vs time for two polymers in which the chromophore is chemically bound to the polymer backbone. The straight line indicates that eq 58 adequately, but not necessarily uniquely, describes the data. The half-filled circles and squares are values of the decay time for second harmonic decay. If these values are multiplied by 3, as would be indicated by eqs 56 and 57, the points fall nicely on the birefringence decay line.

B. Measurements of Poled-Order Decay

It is of interest to attempt to relate the poled-order relaxation process to relaxation processes measured in polymers using other experimental techniques such as dielectric relaxation.[136] Resonances in the dielectric relaxation spectrum of polymers are indicated by the designations α, β, γ, ..., with the α relaxation process being the one occurring at the highest temperature. (These designations should not be confused with similar tensor designations of the linear polarizability and hyperpolarizabilities.) α-Relaxations are usually identified with the glass transition and involve relative motions of polymer chains. β-Relaxations are frequently associated with local motions of side groups on the polymer chain.
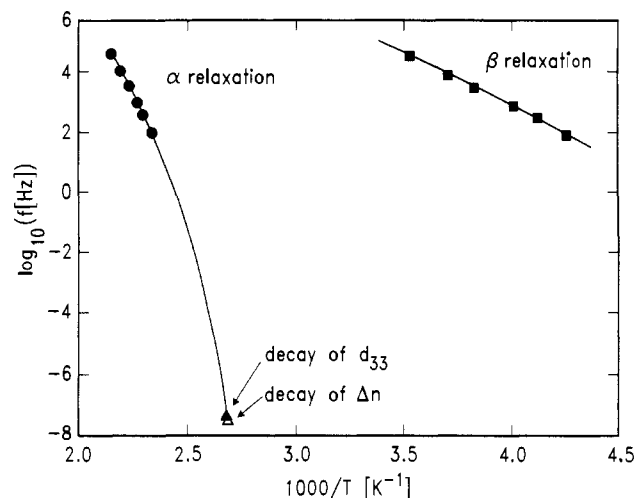
Figure 15. A plot of the $\log_{10}$ of the dielectric relaxation frequencies of the α (●) and β (■) relaxation modes vs $1/T$ for the epoxy-based polymer bisA-NAT (see section VI.C) (from ref 123). Also shown are the decay of d_{33} (▲) and the decay of the birefringence Δn (△).

For the guest–host system DR1 3 in PMMA, the location of the α-transition (associated with T_g) shifts to lower temperatures as a result of plasticization of the polymer by the guest.[137] A weak β-relaxation has also been noted in this system. The dielectric strength of the β-transition decreases with increasing chromophore concentration and the decrease has been tentatively ascribed to the interaction between the hydroxyl group of the dye molecules and the ester moiety of PMMA. This interaction is assumed to suppress the normal β-motion of PMMA. Köhler et al.[138] have investigated dielectric relaxation of polymers in which the nonlinear chromophore is attached either as a side chain or in the main chain itself. A β-transition is observed only in the methyl methacrylate (MMA) based polymer. In this case the relaxation is presumably due to the ester units of MMA and not to motion of the NLO chromophore. Dielectric measurements on main-chain[92,123] nonlinear polymers in which one end of the chromophore is incorporated into a bisphenol A epoxy backbone exhibit weak and broad β-transitions. Figure 15 is a plot of the log of the relaxation frequency as a function of $1/T$ for both α- and β-relaxation modes for one of the polymers, BisA-ANT, which is described in detail in section VI.C. Also shown are points indicating the frequency associated with the stretched exponential decay time τ for $\chi^{(2)}_{333}$ and Δn_3. A straight line would imply Arrhenius behavior. Clearly the relaxation of the poled order is correlated with the α-relaxation process. Similar results are obtained for the other main-chain polymers as well.

Additional evidence for the correlation between poled-order relaxation and the α-transition has been presented by Köhler et al.[97] These authors compare the decay of the SHG intensity from a poled polymer with the thermally stimulated discharge (TSD) current measured while the system is warmed from room temperature. The TSD experiments measure the thermally stimulated release of polarization that has been frozen in during the electric field poling process. The current is due to rotational motion of dipolar components of the polymer and to motion of mobile charges in the system. Figure 16 shows both the SHG and TSD signals as a function of temperature. The
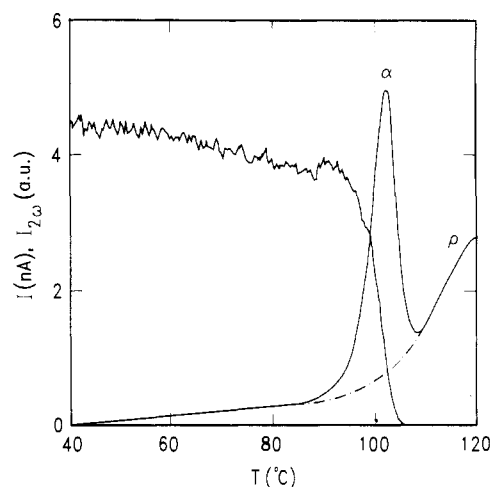

Figure 16. Simultaneous measurements of the decay of second-harmonic signal (SHG) and the release of polarization monitored by the thermally stimulated discharge current (TSD), as a poled side-chain polymer is slowly heated (from ref 97). The SHG signal is in arbitrary units and the TSD signal in nanoamperes. The loss of SHG is clearly associated with the α relaxation for this polymer, and no β relaxation is observed between room temperature and T_g. The feature indicated by ρ is due to motion of trapped charges.

poled-order relaxation is seen to be associated with α-relaxation in this system.

Dielectric and TSD experiments have indicated that the rotational motion of the chromophore responsible for decay of poled order is related to the α-relaxation process, which is in turn related to the glass transition temperature. The Williams–Landel–Ferry (WLF)[139] or the equivalent Vogel–Tamann–Fulcher (VTF)[140] equation has proven useful in relating viscoelastic properties of polymers to the glass transition temperature at temperatures above T_g. Below T_g, it is generally assumed that the functional form of the time–temperature relationship becomes Arrhenius-like.[116] Figure 15 also indicates that β-relaxation does in fact exhibit Arrhenius thermally activated behavior over the temperature range investigated.

For temperatures above T_g, the VTF equation has been used very successfully to describe the temperature dependence of viscoelastic properties. The relationship for the viscosity $\eta(T)$ can be written:

$$\eta(T) = A \exp\left(-\frac{B}{T - T_0}\right) \qquad (60)$$

where A and B are constants and T_0 is a reference temperature. If A, B, and T_0 are chosen to obtain the best universal function for a wide variety of polymers, then T_0 is found to be about 50 °C below T_g.

It has recently been shown that the longer time portion of the SHG decay can be fit to a stretched exponential of the form of eq 58 for a variety of chromophores in a number of host polymers and for a range of concentrations.[59,141] The temperature dependence of the relaxation time τ is shown to follow the functional relationship:

$$\tau(T) = A' \exp\left[\frac{-B'}{(T_0' - T)}\right] \qquad (61)$$

where A' and B' are positive constants independent of polymer host and the guest molecule. T_0' is empirically
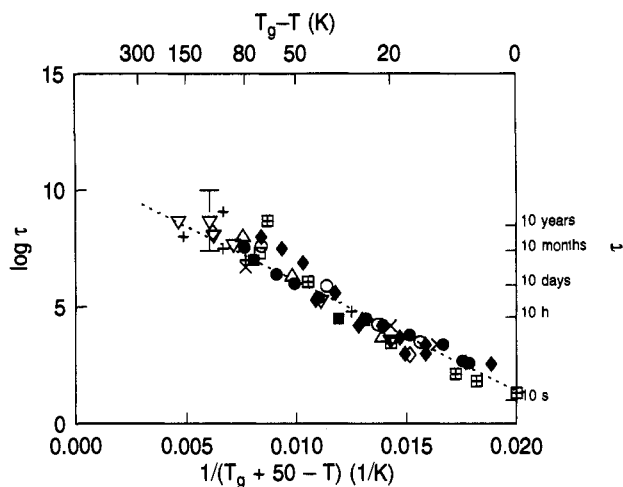
Figure 17. Log τ (τ in seconds) versus $1/(T_0' - T)$ (eq 61) for a wide variety of guest–host polymer systems, where $T_0' = T_g + 50$ °C (eq 62), from ref 143. τ is determined by fitting the decay of the square root of the second harmonic intensity to a KWW stretched exponential (eq 58). A typical error bar is indicated for one of the samples. The dashed line is a linear fit to the data points.
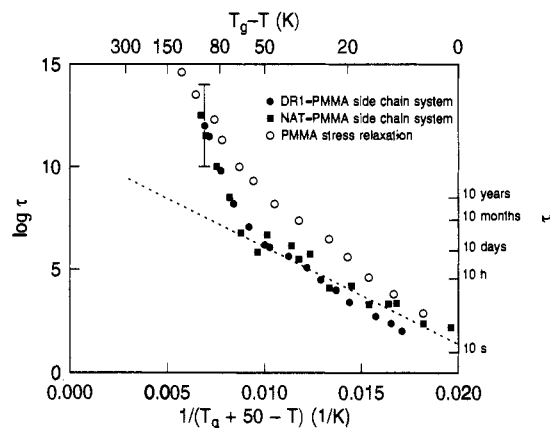

Figure 18. Log τ (τ in seconds) versus $1/(T_g + 50 - T)$ for two PMMA-based polymers in which the chromophores are attached to side chains (from ref 143). Plotted for comparison are mechanical stress relaxation data for neat PMMA (O), taken from ref 142. The dashed line indicates the best fit of eq 61 to the guest–host data shown in Figure 17. The error bar shows the large error in obtaining τ for very long relaxation times.

shown to be related to the glass transition temperature by

$$T_0' = T_g + (50 \pm 10 \text{ °C}) \tag{62}$$

This relationship is illustrated in Figure 17. Equation 61 describes the poled-order relaxation only for "large" chromophores such as substituted stilbenes and tolans and larger. The relaxation of smaller chromophores such as substituted benzenes and styrenes is much faster than would be expected from eqs 61 and 62. The stretched exponential relaxation time τ as a function of temperature for two PMMA-based side-chain polymers is shown in Figure 18. These systems fall on or near the line for guest–host temperatures above about $T_g - 50$ °C, but deviate strongly from it below these temperatures.[143] Further studies are necessary to determine whether this behavior is specific to the PMMA-based side-chain systems studied.

The VTF equation is often explained using a free volume model.[144,145] In fact the glass transition itself
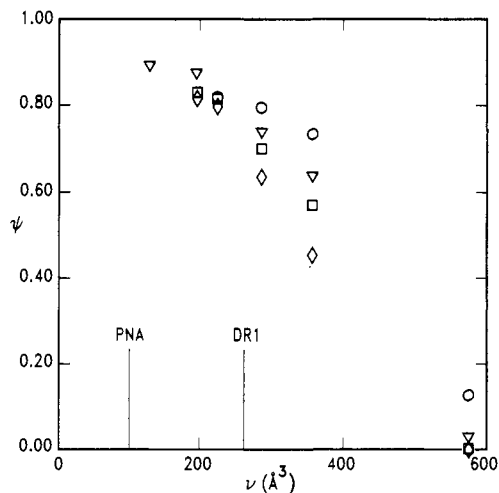
Figure 19. Fraction of "free volume" greater than size ν, $\psi(\nu)$, for PMMA and polystyrene (PS) films at room temperature before and after aging at 50 °C below the glass transition (from ref 148): (O) PMMA, before aging; ($\triangledown$) PMMA, after aging; ($\square$) PS, before aging; ($\diamond$) PS, after aging. Also shown for comparison are the approximate molecular volumes of the chromophore PNA 1 and DR1 3.

has been considered as a percolation threshold in the distribution of free volume.[146] Free volume can be described reasonably precisely from a theoretical point of view as that portion of the total unoccupied volume in an amorphous system that can be redistributed without a change in the free energy.[145] It is much more difficult to measure experimentally. Torkelson and co-workers[147-149] have tried to estimate the free-volume distribution in PMMA, bisphenol A polycarbonate, poly(vinyl acetate), and polystyrene by measuring the rate of photoisomerization of chromophores of varying size doped into these polymers and comparing the rate with the volume necessary for isomerization. The free volume distribution measured in these experiments is shown in Figure 19. Also shown is the approximate molecular volume for PNA 1 and DR1 3.[88] The Figure shows the fraction of free volume ψ greater than an amount ν. As mentioned, eq 61 describes relaxation for chromophores of roughly the size of DR1 and larger, but not for PNA.

Another way of measuring the free volume in a polymer is by measuring positron annihilation.[150] The sensitivity of the positron annihilation lifetime method as a probe of free volume arises from the fact that the positronium atom (a positron–electron bound state) is preferentially trapped in free-volume holes. The observed positron annihilation signals are assumed to originate directly from unoccupied regions. Accordingly, this technique measures, not free volume in the sense of the theoretical definition given above, but unoccupied volume. Figure 20 shows the free volume or unoccupied volume distribution measured at several pressures using this technique for an epoxy polymer. The analysis of the positron annihilation results assumes that the free-volume cells are spherical. Figures 19 and 20 do not necessarily measure the same quantity, although in both cases what is measured is referred to as "free volume". Qualitatively, however, one can infer that the faster poled-order relaxation times measured for the smaller chromophores are due to the fact that these chromophores can fit into at least some of the free-volume voids in the polymer host. The larger molecules that appear to obey eq 61 are bigger than a
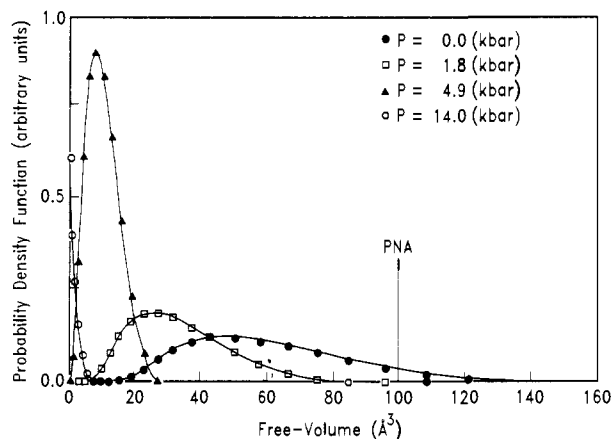
Figure 20. Hole volume distribution functions as measured by positron annihilation experiments on an epoxy polymer at various pressures (from ref 150). For comparison, the estimated molecular volume of PNA 1 is shown.

large fraction of the free-volume voids and thus must displace the host polymer in order to relax.

Within the free volume model, polymer relaxation processes are assumed to be related to the amount of free volume greater than some critical size v^x. This probability is given by[144]

$$\psi \propto \exp[-v^x/v_f(T)] \tag{63}$$

where $v_f(T)$ is the total free volume at a given temperature T. For polymers above T_g, $v_f(T)$ is assumed to be linearly proportional to temperature and to approach a constant, temperature independent value at T_0, often described as the glass transition temperature that would be measured if the polymer could be cooled infinitely slowly so that equilibrium was maintained throughout the process. Relaxation times are then related to ψ in this model:

$$\tau \propto 1/\psi \tag{64}$$

Clearly relaxation times become temperature independent at the temperature T_0.

Rusch[142,151] has suggested modifying the VTF equation for use at temperatures below T_0 by including an additional nonequilibrium contribution to the free volume $w_f(T)$ that does not become constant at T_0. The total free volume thus becomes $v_f(T) + w_f(T)$. This model has been applied to stress relaxation in PMMA and polystyrene[142,151] and recently to the relaxation of poled order in side-chain polymers.[152] Its application to poled-order decay of side-chain polymers can be seen by referring again to Figure 18. As the temperature is lowered, relaxation times increase at one rate above $T \approx T_g - 50\ °C$ and at a different, much slower rate below this temperature. The high-temperature relaxation is dominated by changes in the equilibrium free volume and the low-temperature relaxation by the nonequilibrium free volume. It is difficult, however, to use this modified VTF equation in a quantitative manner since it requires a knowledge of the thermal expansion coefficient of the polymer material above and below T_g, as well as the thermal expansion coefficient of the equilibrium glassy polymer, a quantity that cannot be measured directly and becomes an adjustable parameter. The relaxation of guest–host polymers, shown in Figure 17, does not exhibit the change in slope observed for the PMMA-based side-chain systems within the temperature range measured. The modified free-

volume model would thus seem to describe poled-order relaxation processes in a very general way, but cannot explain many of the details, such as the origin of eq 61 and why for guest–host systems the value of τ seems to depend only on T_g, and not on the chemical nature of the polymer or chromophore.

Recently Lindsay et al.[135] have fit the poled-order decay of methacrylate-based polymers with coumarin side chains to a biexponential decay (see section VI.B). They discuss this functional form of the decay in terms of a bimodal distribution of free volume hole sizes arising from a grainy structure of the polymer. Decays within and outside of the grains, in this model, occur at different rates.

Several features complicate the analysis of poled-order decay in polymers. First the poling process can inject charges into the polymer and a portion of the observed SHG decay may be due to movement of these charges out of the system.[134] This is a particular problem for corona-poled polymers since the poling process deposits a layer of charge on the surface. The data in Figures 17 and 18 were taken after attempting to wipe off the surface charge before beginning each decay measurements.[59] Physical aging of the polymer has also been shown to change the poled-order decay.[88,153,154]

V. Applications

A. Frequency Doubling

To date no commercial devices using optically nonlinear polymers exist, although prototypes have been described. There are at least two reasons for this. First, and probably foremost, second-order nonlinear optical devices (inorganic or organic, polymeric or crystalline) have simply not been needed for current applications. This situation appears about to change with the rapid increase in the rate of information transmission via high-speed optical fibers and the need for increased storage density in optical storage devices. Second, nonlinear optical polymers still need to be shown to be inexpensively processible into practical devices that can operate under real conditions inside a system.

In order to be useful for frequency doubling applications, the active nonlinear optical material must have a sufficiently large second-order susceptibility $\chi^{(2)}(-2\omega;\omega,\omega)$. To estimate the required magnitude of $\chi^{(2)}$ it is helpful to consider a specific application, an optical storage device. To move into the Gbit/cm^2 storage density regime, the effective operating wavelength of the laser system in such a device must be shorter than 500 nm. This can be achieved in several ways, such as by development of blue diode laser,[155] frequency up-conversion of diode lasers,[156] or frequency doubling of infrared lasers using a second-order non-linear material.

In designing an optical storage device, it is desirable to have on the order of 5–10 mW of blue light incident on the surface of the optical disk.[157] Making allowances for losses in the optical system between light source and disk, this would require 2–3 times more power from the blue source. A typical GaAlAs laser can generate on the order of 100 mW in a single spatial mode at 800 nm. Assuming that the blue source must produce at least 10 mW of light, one requires a frequency doubling device with at least a 10% output conversion efficiency when pumped with 100 mW. The specific requirements
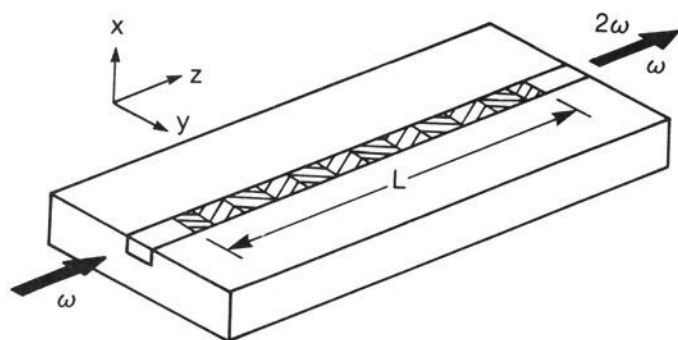
Figure 21. A typical frequency doubling waveguide configuration. The nonlinear optical material forms a channel waveguide. The two different hatching patterns indicate that the material has been periodically poled (the regions are alternately poled along the $+x$ and $-x$ directions) to achieve quasi-phase matching (from ref 158).

Figure 22. A waveguide Mach–Zehnder modulator (from ref 168).

that this places on the polymeric nonlinear optical material have been discussed by Burland et al.[157]

A typical frequency-doubling waveguide configuration is shown in Figure 21.[158] The optically nonlinear material forms a channel waveguide. The electric field poling direction is the z-direction. The poled-polymer system cannot be phase matched, that is, $n_\omega \neq n_{2\omega}$ and, according to an equation like eq 41, the second harmonic power will oscillate along the length of the waveguide. In a crystalline material one tries to find a direction along which the two indices of refraction will be equal. In this phase-matched condition, the second-harmonic light intensity will build up as the square of the crystal length. One way of overcoming this problem is to quasiphase match the system by periodically poling the system in the positive z-direction in some regions and the negative z-direction in others.[159,160] These periodically arranged regions of poling are shown in Figure 21. Using reasonable waveguide parameters, it has been shown[157] that the value of $\chi^{(2)}$ required in a periodically poled device to achieve the necessary 10% doubling efficiency is on the order of 60 pm/V. In addition the chromophore must exhibit neglible absorption at either the fundamental or the second harmonic wavelengths over the length of the active device. Unfortunately, there is a rough relationship between the magnitude of a chromophore's hyperpolarizability β and the wavelength of its lowest energy absorption peak.[96] The larger the value of β is, the redder the absorption. No systems have yet been identified that have a hyperpolarizability large enough to yield the required value of $\chi^{(2)}$ and simultaneously to have negligible absorption in the blue. Quasiphase matching has been demonstrated in a polymeric system with an active layer of a copolymer of methyl methacrylate and a monomer derived from a 4-oxo-4′-nitrostilbene.[160] Over a length of 5 mm a frequency-doubling efficiency of 0.01% per watt at a fundamental wavelength of 1.34 μm was measured. In this case $\chi^{(2)}$ was 4 pm/V.

Other approaches to the phase matching problem have been suggested and investigated. Anomalous dispersion phase matching,[161,162] in which the chromophore absorption is positioned between the fundamental and second-harmonic wavelengths, is one way of producing a system in which the index of refraction at the two wavelengths can be equal. Systems of this type have the advantage that the value of β can also be significantly resonantly enhanced due to the proximity of the chromophore absorption maximum to either the fundamental or harmonic wavelength. Systems of this
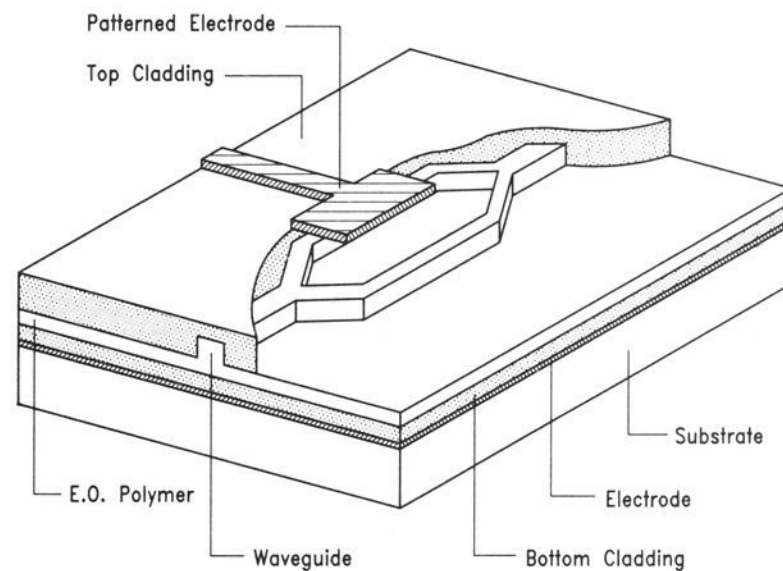
type would, in general, seem to be even more sensitive to absorption, since the second-harmonic wavelength falls in the middle of the region of chromophore absorption. SHG efficiencies on the order of 1% have been estimated for power densities of 100 mW/4 μm² using this approach taking into account absorption.[162] Launching the fundamental and harmonic signals into different waveguide modes such that their indices of refraction are matched has also been considered as a means of phase matching.[163,164]

Cerenkov SHG provides an alternative approach to frequency doubling that is free from severe phase-matching and absorption constraints.[165] In this approach a fundamental guided mode is converted into a radiating second-harmonic wave. The radiated wave leaves the active part of the waveguide and is thus not as strongly absorbed. To date this approach has yielded only relatively low SHG efficiencies (0.21% with a fundamental power of 195 kW).

It has recently been suggested that the large values of $\chi^{(2)}$ and the ease with which thin films can be fabricated make poled polymers ideal for doubling femtosecond pulses.[166,167] For very short pulses, the index of refraction dispersion in the frequency-doubling medium results in a lengthening of the pulse produced at the second harmonic. Thin films, while desirable, are difficult to prepare for conventional frequency-doubling crystals. It is quite simple to prepare thin polymer films of a few micrometers or less. A 2.5-μm-thick corona-poled polymer film has been used to double a 13-fs pulse.[167]

B. Electrooptic Devices

The linear electrooptic effect has been used to produce a variety of guided wave optical devices including waveguide switches, modulators, filters, and polarization-transforming devices. One such device, a Mach–Zehnder modulator, is shown in Figure 22. This device is simply the waveguide analog of the Mach–Zehnder interferometer shown in Figure 12. An electrode over one or both arms of the interferometer allows one to apply a voltage across the nonlinear polymer and thus vary the index of refraction via $\chi^{(2)}(-\omega;\omega,0)$. This variation of the index can be used to modulate the light intensity exiting the device via constructive or destructive interference that occurs when the light from both arms of the interferometer is recombined. The bulk of the modulator work to date has been done with Ti-diffused LiNbO₃ and GaAs.

Table 4. Figure-of-Merit Comparison

material	n	ϵ	r	n^3r/ϵ
LiNbO$_3$[a]	2.24	85	31	4.2
GaAs[a]	3.6	13	1.6	5.9
PPNA[b]	1.7	3.7	$\approx$15	20.
3RDCVXY[c]			40	$\approx$50.
MONS–side-chain polymer[d]			18	$\approx$20.

[a] Reference 24. [b] Reference 44. [c] Shuto, Y.; Amano, M.; Kaino, T. *IEEE Trans. Photonics Tech. Lett.* **1991**, *3*, 1003; n^3r/ϵ calculated using n, ϵ for PPNA. Measured at 633 nm. [d] Möhlmann, G. R. *Proc. SPIE* **1989**, *1147*, 245, n^3r/ϵ calculated using n, ϵ for PPNA. Measured at 633 nm.

From eq 15 it can been shown that the electric field induced change in the index of refraction is proportional to n^3r. For efficient modulation of the optical signal the low-frequency dielectric constant must be small. These two criteria result in a figure of merit F_m given by

$$F_m = \frac{n^3r}{\epsilon} \qquad (65)$$

Other figures of merit can also be defined.[169-172] The figures of merit F_m for LiNbO$_3$ and GaAs are compared, in Table 4, with several polymeric systems. From the table it can be readily seen that polymeric systems have significantly higher values of F_m due mainly to the reduced polymer dielectric constants. High-frequency modulation of polymer-based electrooptic devices have been demonstrated at 20 GHz[173] and at 40 GHz.[174] In addition, the underlying electrooptic response of a polymer film has been demonstrated up to 460 GHz.[175]

In order to be considered for most practical applications, electrooptic polymers must be compatible with the processing technologies and operating environments already established for microelectronic chips and modules. Key among these requirements is thermal stability. Typical chip-bonding processes use solders that melt at high temperatures.[176] Flip chip bonding, used to assemble thermal conduction modules, requires temperature in excess of 300 °C. Laser fabrication processes require temperatures over 280 °C. Solders for surface-mounted components melt at temperatures above 125 °C and require temperature excursions of several minutes above 200 °C. In addition to these short-term temperature excursions, an electrooptic device must function for years at use temperatures up to 80 °C and storage temperatures that may reach 120 °C. Unlike LiNbO$_3$ and GaAs in which the nonlinear optical properties are thermally stable, poled polymers tend to lose their polar order over time and the orientational decay process is substantially increased at elevated temperatures, as has been shown in section IV. As indicated by eqs 61 and 62, the decay time is intimately connected with the glass transition. For a practical electrooptic device, one requires a nonlinear polymer with a coefficient r measured in a device configuration substantially greater than 10 pm/V and a glass transition temperature in excess of 250 °C. No such polymeric system has currently been identified.

Optical losses in the materials can also be a serious problem. Recently, Skumanich et al.[178] have identified a weak but significant absorption feature around 830 nm in a side-chain nonlinear polymer using photothermal deflection spectroscopy. This absorption is strong enough to make the systems in which it appears useless for waveguide devices in the wavelength region of the absorption.

VI. Polymer Systems

A. Guest–Host Systems

The earliest electric field poled polymer systems to be investigated were those in which the nonlinear chromophore was incorporated as a dissolved guest in a polymer host. One of the first such systems was the nonlinear chromophore DANS [4-(dimethylamino)-4'-nitrostilbene] (4) dissolved ($\sim$2 wt %) in a thermotropic nematic liquid crystalline polymer.[1] In this system the

DANS

4
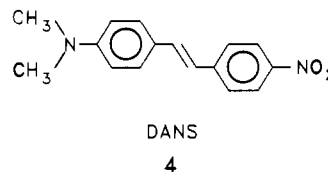
chromophore orientation decayed quite rapidly. The susceptibility χ_{333} was also small, about 1 pm/V at 1.06 μm. Subsequent investigations have focused on increasing both the susceptibility and the thermal stability of the poled order. A wide variety of chromophores have been investigated as guests in a number of polymer hosts.[179] One of the most thoroughly studied guest–host polymer systems is PMMA doped with the azo dye DR1 3. The early poling experiments used sandwich electrode poling and a variety of doping levels up to $\sim$15 wt %.[21] A maximum d_{33} = 2.5 pm/V at 1.58 μm was obtained. Subsequent measurements of the electrooptic coefficient yielded a resonantly enhanced value of r_{33} = 2.5 pm/V at 633 nm.[27] Corona poling of DR1/PMMA polymer films was shown to increase d_{33} to 6.7 pm/V at 1.58 μm.[62,180]

A variety of other guest–host systems have been formulated by incorporating a chromophore into PMMA. Singer et al.[181] have doped 4-(dicyanovinyl)-4-(dialkylamino)azobenzene into PMMA with a chromophore density N = 2.3 × 10^{20} cm^{-3} and obtained d_{33} = 74 pm/V at 1.58 μm. Unfortunately, this high d value decayed to 19 pm/V within several days at room temperature. Hayden et al.[91] have corona-poled DR1 3, Disperse Orange 3 (DO3) 5, and a variety of dicyanosubstituted dyes in PMMA. At 1.064 μm, they have

DO3

5
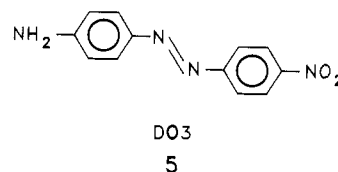
obtained d_{33} = 9 pm/V for DR1 (N = 2.3 × 10^{20} cm^{-3}), d_{33} = 5.8 pm/V for DO3 (N = 3 × 10^{20} cm^{-3}), and d_{33} = 16 pm/V for 4-(tricyanovinyl)-N,N'-dimethylaniline (N = 3.2 × 10^{20} cm^{-3}).[182] None of these values was corrected for absorption of the second harmonic. In addition, they are expected to be resonantly enhanced. It is thus difficult to predict what the values of d_{33} might be at other wavelengths. Gadret et al.[183] have studied three chromophores with dicyanomethylene acceptor groups as guests in PMMA: 2-[[4-[4-(dimethylamino)styryl]phenyl]methylene]propanedinitrile, 3-(dicyanomethylene)-5,5-dimethyl-1-[p-(di-

methylamino)styryl]cyclohexene, and 3-(dicyano-methylene)-5,5-dimethyl-1-[[5-(dimethylamino)-2-thienyl]vinyl]cyclohexene. They have measured d_{33} values of 27, 26, and 38 pm/V at 1.3 μm, respectively.

Although guest–host systems are relatively simple to formulate, their usefulness, as discussed in section V, will be limited unless the thermal stability of the electric field poled order is sufficient. To address this issue, several authors have investigated the effect of guest chromophore size on poling dynamics and relaxation.[88,184-186] Boyd et al.[88] have investigated the rotational mobility of a set of chromophores in both PMMA and bisphenol A polycarbonate hosts. The chromophores investigated include PNA 1, 4-amino-4'-nitrostilbene, DR1 3, and 1-(4-nitrophenyl)-4-[4-(dimethylamino)phenyl]-1,3-butadiene with approximate molecular volumes of 103, 194, 261, and 250 Å^3, respectively. As observed in other studies,[185,186] it was found that chromophores with small molecular volumes (e.g. PNA) have much higher rotational mobilities than the other chromophores in either polymeric host. This is consistent with the discussion of free volume in section IV.B. DR1 is shown to have a more restricted rotational mobility in polycarbonate than one might expect from its molecular volume. Boyd et al. suggest that hydrogen bonding between the hydroxyl group on the DR1 and the backbone of the polycarbonate is responsible.

Levenson et al.[184] have compared both the d and r values and poling stabilities for two thiophene derivatives doped into PMMA. The first and larger chromophore consists of three conjugated rings separated by two azo linkages, while the second contains only two conjugated rings separated by a single azo group. A poled film containing 10 wt % of the larger dye (r_{33} = 2.4 pm/V at 830 nm) is shown to be more stable at room temperature than one containing 15 wt % of the smaller dye (r_{33} = 2.7 pm/V). Although this suggests that elongation of the dye enhances stability, the authors have used different loading levels for the two dyes and have not taken into account the effect that the different loading levels may have on the T_g of the films. Recall that in section IV.B it was shown that T_g is intimately connected with the poled-order relaxation. In addition to substrate-specific interactions such as hydrogen bonding, further stabilization of poled order in guest–host systems can be accomplished by physical aging of the polymers to reduce the average void size[153] and by choosing polymers without significant sub-T_g relaxations.[186]

Although thermal history, dopant size, specific polymer relaxation mechanisms, and guest–host interactions are certainly important for the poled order in guest–host nonlinear optical polymers, it has recently been shown that if the chromophore is relatively large, the primary factor influencing the relaxation rate is the T_g of the doped system[59,141,143] as discussed in section IV.B. In order to exploit this relationship between T_g and relaxation rate, guest–host systems have been formulated using high T_g (>200 °C) thermoplastic polyimide hosts.[59,79,141,187] Many fully cured polyimides with high T_g's are insoluble and must be processed as polyamic acid precursors and subsequently cured at high temperatures. One such system is DR1 3 doped into the polyamic acid LQ-2200 (Hitachi).[79,187] The cured polyimide is isotropic and shows very little optical loss at 830 nm (<1 dB/cm). Dielectric measurements have
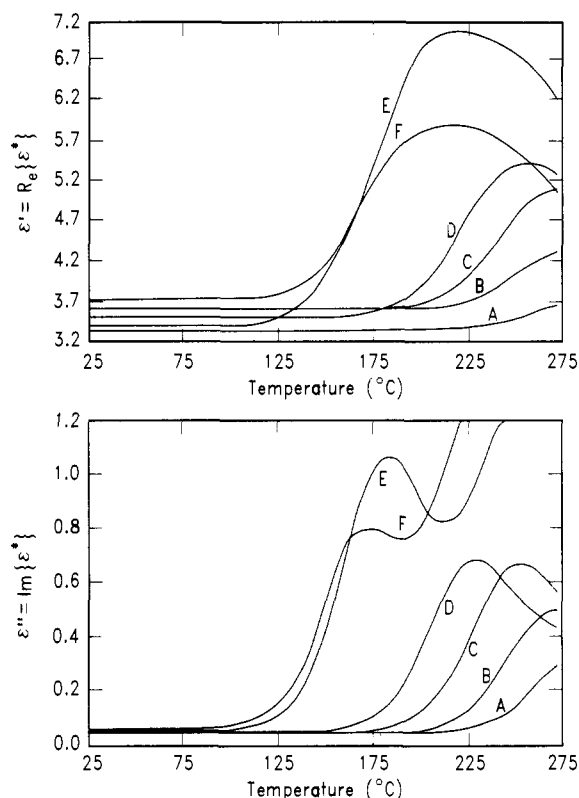

Figure 23. The real (top) and imaginary (bottom) parts of the complex dielectric constant ϵ^* measured at 100 kHz for various concentrations of DR1 3 in the polyimide LQ-2200 (from ref 187). For the curves A–F, the weight per cent of DR1 used was 5, 10, 20, 30, 40, and 50, respectively. The dielectric relaxation data illustrate plasticization upon addition of the chromophore. The sample E does not follow the trend shown by the other samples and this has been attributed to a thickness difference.

shown that the undoped polyimide fully cured at 370 °C has its thermoplastic glass to rubber transition near 260 °C. A WLF fit (see eq 60) to the temperature-dependent dielectric data results in an effective or "fictive" glass transition temperature T_0 = 219 °C. However, the thermal stability of DR1 in the host limits the temperature at which the doped films can be cured at 220 °C. A series of dielectric measurements on films with varying chromophore doping levels showing that DR1 monotonically decreases the T_0, so that it is as low as 133 °C for a 50 wt % film. This is shown in Figure 23. Clearly, plasticization by the chromophore guest is a serious problem which may limit the use of high T_g polymer hosts. For an 11 wt % loaded DR1/LQ-2200 film, the poling was carried out at 190 °C and an r_{13} = 1.5 pm/V at 830 nm was found. Upon ramping the temperature from room temperature at a rate of 3 °C/min, no loss in electrooptic coefficient was observed until 150 °C was reached.

A second thermoplastic polyamic acid, Ultradel 4212 or 3112 (Amoco), has also been investigated.[79] It too shows low optical loss at 830 nm without the chromophore. The chromophore in this case was the laser dye DCM [4-(dicyanomethylene)-2-methyl-6-[p-(dimethylamino)styryl]-4H-pyran], at a 20 wt % loading level. This chromophore has a thermal stability 20–30 °C higher than that of DR1, and the $\mu\beta$ value for DCM measured by electric field induced second harmonic generation (EFISH) is 1.6 times that of DR1.[79] The thermal stability of DCM again limits the curing

temperature for the polyamic acid to ~220 °C. An electrooptic modulator was fabricated using the DCM/Ultradel guest–host system as the nonlinear active layer. The resulting electrooptic coefficient measured in the modulator was found to be r_{33} = 3.4 pm/V at 830 nm, considerably lower than the expected value based on the molecular hyperpolarizability of the DCM chromophore. In a modulator of this type the nonlinear active polymer film is sandwiched between two inactive polymer buffer layers. The relatively high conductivity of the nonlinear layer (possibly due to incomplete imidization) compared with that of the buffer layers was cited as the source of the lower than anticipated electrooptic coefficient. The increased conductivity of the active layer reduces the magnitude of the poling electric field that can be applied across the active layer.

The isotropic poly(ether imide) Ultem (General Electric) is fully imidized and still soluble in a variety of solvents. It has a T_g = 210 °C[59,141] and excellent optical loss characteristics. Guest–host systems based on Ultem thus do not require high-temperature curing. Ultem has been doped with two 2,4,5-triarylimidazoles, Lophine 1 (L1 6) and 2 (L2 7). The thermal stability

L1
6

L2
7
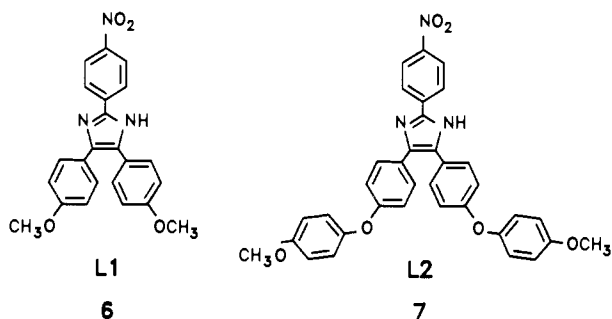
of these two chromophores is outstanding; they do not decompose below 300 °C as indicated by differential scanning calorimetric (DSC) and thermogravimetric analysis (TGA) measurements. The lower molecular weight material L1 6 in Ultem does, however, have a tendency to sublime slowly from the polymer at temperatures above 200 °C.[59,141] The molecular hyperpolarizabilities of these lophine chromophores are moderate (e.g. β_0 = 18 × 10^{-30} esu for L1;[141,188] β_0 is the value of the first hyperpolarizability extrapolated to zero frequency using a two-level model[54]). The solubility of the lophines in Ultem is excellent and loading levels of 30 wt % have been achieved with no evidence of crystallization or phase separation.[59] Addition of the chromophores does, however, plasticize the Ultem, lowering the T_g to 150 °C at a 26 wt % loading level. A 20 wt % L1/Ultem sample has T_g = 170 °C and d_{33} = 12 pm/V measured at 1.06 μm. The temperature dependence of the poled-order decay times of L1 and L2 in a wide variety of polymeric hosts has been measured and is shown in Figure 17.[59]

For those cases in which the polyimide is not thermoplastic, i.e., it either does not have a T_g below its decomposition temperature or the T_g is prohibitively high, polyamic precursors have been used.[57,59,189] This approach was used with the polyamic acid systems described above. The poling field is applied to the film when the polymer is in its preimidized state, and the temperature is gradually increased to initiate imidization. This poling procedure is complicated, as the preimidized films are conductive and during the course

of imidization water or solvent is released.[57,59,189,190] This conductivity and its deleterious effect on the internal poling field has, in general, resulted in low d and r values. Curing of polyamic acids involves two distinct stages: the first is the cyclocondensation involved in imidization, and the second is a densification effect that occurs at temperatures well above 300 °C. Wu et al.[189] were the first to demonstrate that densification of the cured commercial polyimide Pyralin 2611 doped with the NLO chromophore erythrosin at 360 °C dramatically increases the thermal stability of the poled order in the film. This polymer becomes highly anisotropic upon densification. For these films, an initial decay of 35% of the electrooptic signal is observed when the poled film is heated to 300 °C, but there was no further decay after 1 h. At 200 °C, there is an initial decay of 30%, but no further decay after 60 h. The magnitude of the initial electrooptic coefficient measured for this very thermally stable guest–host system is not reported but it is undoubtedly quite low. This is expected since a coplanar poling electrode geometry was used and the erythrosin dye itself is not a particularly good nonlinear chromophore. Wu et al. were unable to pole guest molecules perpendicular to the plane of the substrate[57,189] in this polyimide, which they attribute to the anisotropy of the densified polymer which forms sheets parallel to the substrate.[191] A similar poling during imidization experiment has also been described for the thermally stable chromophore L1 6 in the anisotropic polyimide BPDA-PDA [poly(p-phenylenebiphenyltetracarboximide)].[59] BPDA-PDA is chemically identical to the commercial Pyralin 2611 used by Wu et al. Stähelin et al. were able to pole the chromophore perpendicular to the plane of the film using the corona technique. No significant difference was noted for the decay of poled order between a corona-poled and a coplanar electrode-poled film as measured by second harmonic generation. A d_{33} value of 3 pm/V was obtained for a 20 wt % L1/BPDA-PDA corona-poled film, a value significantly lower than the 11 pm/V obtained for a 20 wt % L1/Ultem film. The poled order for the L1/BPDA-PDA film was shown to be stable for over 15 h at 250 °C, after a significant initial drop occurring within the first few minutes. Increasing the temperature of this sample to 300 °C causes another fast drop in d_{33} within the first several minutes, but only a slight decay occurs over the next hour.

Although the approach described above has led to some exceptionally stable guest–host systems, its utility may be limited, since nonlinear chromophores with the highest molecular hyperpolarizabilities do not seem to have the chemical stability to survive exposure to the temperatures required for complete thermal curing and densification. Wu et al.[190] have suggested that it is possible to ameliorate this problem by using chemical instead of thermal imidization. Infrared studies have suggested that low-temperature chemical imidization of polyamic acids is equivalent to thermal imidization at 250–300 °C. The chromophore DR1 incorporated into a polyamic acid film of PIQ-L100 was poled at 150 °C, cooled, and then chemically imidized by immersing the polymer into a solution of pyridine and acetic anhydride. After this procedure, the electrooptic coefficient of the film was then shown to decrease to 70% of its original value after 1 h at 150 °C. Chemical imidization during poling was not possible due to the
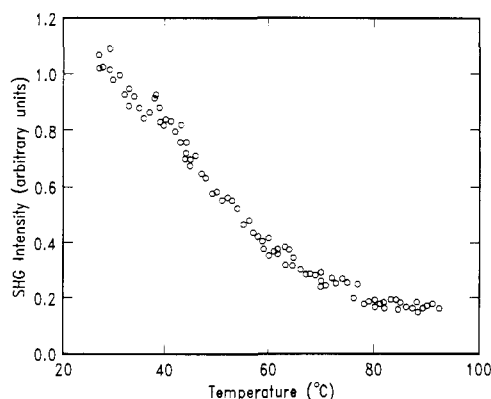
Figure 24. Decay of poled order as the temperature is slowly increased of a film made from DR1 **3** in PMMA which had been poled at room temperature by plasticization of the polymer film with CO_2 (from ref 71).

high electrical conductivity of the imidizing solution and for this reason this process does not seem a practical one for producing well-poled stable polymer films.

In principal, the degree of poling is expected to be somewhat diminished as poling temperatures increase because of thermal randomizing motions associated with the increase in kT. As mentioned in section II.D, this problem has been addressed in a particularly novel way by Barry and Soane.[71] They have purposely plasticized polymers by introducing CO_2 at elevated pressures to allow poling at ambient temperatures. The CO_2 is then easily removed by depressurizing the sample and the T_g of the polymer returns to its original value. Using this technique, they have successfully poled DR1 in both PMMA and a bisphenol A polycarbonate. Unfortunately, they do not compare quantitatively the degree of poling obtained in this manner with that resulting from conventional poling at T_g. As shown in Figure 24, they also observe relaxation of poled order at somewhat lower temperatures than expected from measurements on DR1/PMMA systems that have not been previously plasticized with CO_2. The reduction in thermal stability of the poled order is attributed to large free volume voids left behind by the rapid loss of CO_2. This poling technique can certainly be improved and may become important for successful poling of the very high T_g polymer systems in which the thermal stability of the chromophore is a limiting factor.

Another method allowing room temperature poling has been demonstrated for DR1 in PMMA.[192] This approach has utilized the polarization-sensitive reversible cis–trans photoisomerization that occurs in the azo dye DR1. The trans–cis isomerization is optically pumped with polarized light in the presence of a dc electric field. As the pump beam is removed, the cis isomers will relax back to re-form the trans isomer. The applied electric field causes preferential alignment with the field during this process, resulting in a noncentrosymmetric film with a bulk $\chi^{(2)}$. The electrooptic coefficient r_{33} for films poled in this manner are 3–5 times lower than those obtained for films poled at high temperatures. However, this technique may be useful for accurately creating regions of oriented and nonoriented molecules in films.

The use of chromophores in which charge transfer may occur along two directions has been proposed as a method of slowing the decay of poled order in guest–host polymers.[193] These molecules possess large off-

diagonal components of the molecular hyperpolarizability, such as β_{zyy}. Although the dipole moment of this type of nonlinear chromophore may be reduced when compared to conventional charge-transfer molecules, the order parameter characteristic of the decay of the nonlinearity of a poled two-dimensional charge-transfer molecule is not expected to decay as fast as the order parameter of the dipole moment, leading to the possibility of enhanced stability. As a model for a two-dimensional charge transfer molecule, the chromophore N,N'-bis (p-nitrophenyl)methanediamine (p-NMDA) **8** has been synthesized.[193] β_{zzz} for this molecule is close to zero, whereas it has a large β_{zyy} component.[193] p-NMDA and the more conventional donor–acceptor chromophore MNA **9** have been doped into PMMA and their poled-order decays compared while monitoring the order parameter Φ described in section II.E.
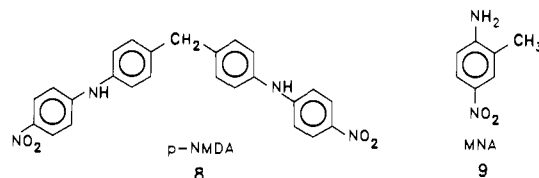
For the MNA/PMMA system, d_{33} decays linearly with the order parameter, decreasing by 37% as the order parameter changes from 0.36 to 0.15. For p-NMDA/PMMA, d_{33} decays more slowly than linearly.

Electric field poling requires high electric fields and may result in the formation of long-lived trapped charges at both the surface and in the bulk of the poled polymers. It would be an advantage to identify systems that would spontaneously order in polymers without poling. Several guest–host systems of this type have been identified and investigated. Watanabe et al.[194] found that PNA **1** incorporated in a poly(oxyethylene) host polymer exhibited a second harmonic signal with the application of electric field strengths of only $\sim 10^{-2}$ mV/cm. They ascribed the SHG signal to a new noncentrosymmetric crystalline phase of PNA formed in the polymer host. Similar results have been obtained without any externally applied poling field for PNA in poly(ϵ-caprolactone)[195] as well as in PMMA and a polycarbonate.[196]

B. Side-Chain Polymers

The initial work on guest–host systems indicated that reasonable values for the nonlinear optical coefficients d and r could be obtained in poled-polymer systems. It was also realized that even larger nonlinear coefficients and improved thermal stability of the poled order could be obtained if the nonlinear chromophore were chemically attached to the polymer backbone. The first systems investigated incorporated the chromophore as part of a side chain attached to the polymer backbone.[180,197,198] These polymers have the advantage that a high nonlinear chromophore concentration can be incorporated into the polymer system without crystallization, phase separation, or the formation of concentration gradients. In addition, the relaxation of poled order might be expected to be substantially slower because motion of the chromophore is hindered by its attachment to the polymer. In most cases, the glass transition of a side-chain polymer is substantially higher than that of a guest–host system containing the same
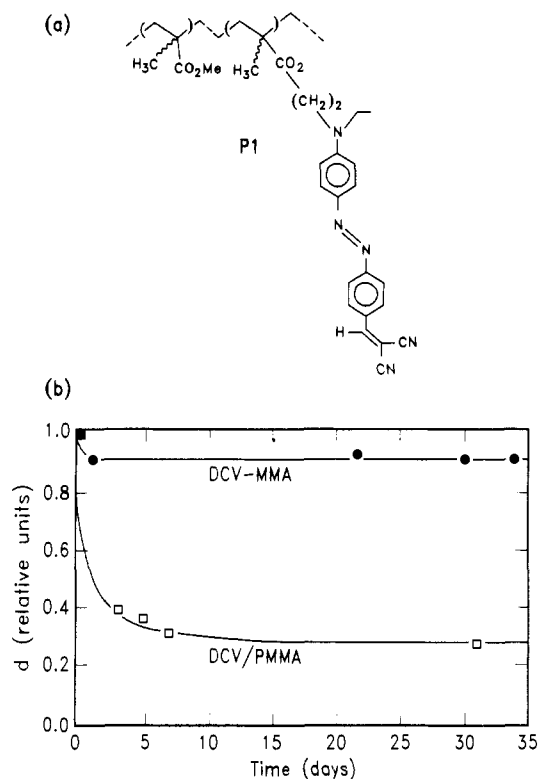
Figure 25. (a) A side-chain polymer made by random copolymerization of methyl methacrylate with a 4-(dicyanovinyl)-4'-(dialkylamino)azobenzene-substituted methacrylate (from ref 182) and (b) comparison of the decay of poled order in a film of the side-chain polymer P1 with that in a film made of PMMA doped with the same chromophore (from ref 181).

Figure 26. Side-chain PMMA-based polymers made using analogs of DR1 3 (from ref 201).

concentration of chromophore molecules. Recall from the previous section that a guest chromophore tends to plasticize the host polymer.

One of the first side-chain systems studied was a random copolymer of methyl methacrylate and a 4-(dicyanovinyl)-4'(dialkylamino)azobenzene-substituted methacrylate (DCV-MMA) P1.[182] The structure of this polymer is shown in Figure 25a. Corona poling of this polymer resulted in a $d_{33} > 50$ pm/V at 1.58 μm, although a somewhat higher value was expected on the basis of the chromophore number density and results on a guest–host system of analogous composition. The smaller than expected nonlinearity was attributed to aggregation of the side-chain chromophores. Although the degree of poling in the guest–host polymer appears to have been better, the poling stability at room temperature was markedly improved for the side-chain polymer.[180] This can be seen in Figure 25b where the normalized SHG decays for both side-chain and guest–host systems involving the same chromophore and polymer backbone are compared. It is not clear from these measurements whether the increased thermal stability of the side-chain system is due to its higher T_g or to hindered rotation of the chromophore itself. The electrooptic coefficient of P1 has been measured at 799 nm and found to be $r_{33} = 18$ pm/V.[199]

Copolymers of DR1 3-substituted methacrylate with methyl methacrylate have also been synthesized.[200] Corona poling of a film of DR1-tethered PMMA P2a at an unspecified substitution level gave $d_{33} = 43$ pm/V at 1.064 μm, and $r_{33} = 18$ pm/V at 633 nm in a sandwich electrode-poled film.[201] These values of d and r are resonantly enhanced. A bis-azo analog of DR1 has also

been covalently attached to PMMA to form polymer P2b, yielding $d_{33} = 69$ pm/V (1.064 μm, corona poled), and $r_{33} = 27$ pm/V (633 nm, electrode poled).[201] Subsequently, the same authors have copolymerized the methacrylate ester of a dicyanovinyl-terminated bis-azo dye with methyl methacrylate P2c.[202] These polymers are shown in Figure 26. With $N = 4 \times 10^{20}$ cm^{-3}, $d_{33} = 150$ pm/V has been measured at 1.7 μm for P2c. This is nearly a factor of 9 better than a DR1-PMMA side-chain polymer P2a with almost the same value of N. The increase in d is due to the larger $\mu\beta$ for the chromophore. This in turn is because the dicyanovinyl substituent is a better electron acceptor than a nitro group.[202,203] The two methyl groups on the central benzene ring of P2c presumably prevent aggregation and thus improve the poling efficiency for this system. The decay of $\chi^{(2)}_{333}$ has been measured at 80 °C over 150 days and shows only a 30% decrease, most of which occurs within the first 30 days.

PNA 1 has been attached to a variety of polymer backbones as a side chain. For example, a highly functionalized polymer has been obtained by attaching a PNA moiety to a polyethylene backbone (PPNA).[44] Every other carbon atom on the polymer backbone has a PNA group attached. The polymer has a $T_g = 125$ °C and when corona poled yields $d_{33} > 30$ pm/V at 1.06 μm. Dielectric relaxation measurements over the frequency range 100 Hz to 100 kHz revealed no transitions in the range from 20 °C to T_g. The order parameter of this polymer after poling was measured using absorbance and birefringence techniques.[72] This type of measurement has been described in section II.E. Polystyrene has also been functionalized with PNA.[204] The polystyrene polymer exhibited a similar d_{33} to the above polymer, with slightly better orientational stability at room temperature despite its lower T_g (103 °C). Ye et al.[197] have functionalized polystyrene with a variety of chromophores, but the lower degree of functionalization (4–12%) resulted in lower d values.

Möhlmann et al. have synthesized an amorphous side chain polymer with a substituent similar to DANS 4 as a pendant side group.[188] This polymer has a relatively high T_g (140 °C) and a large electrooptic coefficient (r_{33} = 28 pm/V at 1.3 μm).[205] Dynamic dielectric relaxation measurements from 0.001 Hz to 5 kHz have been carried out on this polymer[206] in the temperature region T_g – 20 °C to T_g + 40 °C. Over this range, the temperature dependence is described well by the WLF equation. The authors point out that the distribution of relaxation times in these amorphous polymers limits the efficiency of the poling process, since a certain fraction of the chromophores are in constrained environments and will pole extremely slowly. Physical aging experiments have also been performed for this polymer.[207] Samples annealed overnight with the poling electric field on are observed to undergo a single exponential decay in poled order, whereas those which have not been annealed show a fast initial relaxation, consistent with a biexponential functional form for the decay. Although annealing resulted in a 15% increase in the electrooptic coefficient, the rate of decay of r in both the annealed and the unannealed samples was comparable after a few hours. Very fast room temperature poling is observed for this polymer as well as for another polymer with a DANS-like chromophore attached as a sidegroup and a T_g = 175 °C. The fast poling was rationalized by proposing that the side chains can easily undergo small movements in response to the field, as if they were "rattling around in a cage." The electrooptic coefficient of the polymer with T_g = 175 °C is 2–3 times smaller than that of the T_g = 140 °C polymer. From the level of functionalization of the two systems the r values might be expected to be similar. That they are not is presumed to be an indication of more hindered rotation and therefore less efficient poling in the higher T_g polymer.

Very high, resonantly enhanced $\chi^{(2)}$ values have been reported for a polyester polymer with Disperse Red 19 side groups.[208] The dye concentration in this polymer is 68%. A strong photoinduced index change is observed and attributed to trans–cis photoisomerization of the azo groups. Polyurethane derivatives incorporating the Disperse Red 19 chromophore are discussed further in section VI.D.

Ye et al.[209] have designed a side-chain polymer having a strong hydrogen-bonded network by partially functionalizing poly(p-hydroxystyrene) with the tosylate of N-(4-nitrophenyl)-L-prolinol at levels up to 48%. Although the T_g of the parent polymer is 155 °C, that of the functionalized polymer is only slightly above 100 °C, and poling is carried out 20 degrees below T_g. The 25% functionalized polymer after annealing shows a relaxation time constant of ~200 days at 25 °C. The d_{33} value for the 48% functionalized polymer is 7.5 pm/V at 1.064 nm.

Several poly(styrene-co-acrylic acid ester) side-chain copolymers have been synthesized by attaching hydroxy-functionalized azobenzene, benzylidene aniline, and coumarin chromophores to a preformed copolymer by esterification,[91] resulting in materials with T_g's ranging from 80–93 °C and d_{33} values as high as 40 pm/V at 1.06 μm. The poling stabilities of these side chain polymers are superior to those of several dye-doped PMMA films at room temperature.

Recently, a number of coumarin-containing methacrylate side-chain polymers have been prepared.[91,210,211] The topology of these polymers is described as "combshaped". The optimum poling temperature has been determined to be 40 °C above T_g, a characteristic which is attributed to the absence of flexible spacers between the polymer chain and the bulky coumarin chromophore.[211] It has also been suggested that there may be hydrogen bonding associated with the amide groups.[210] A d_{33} of 13 pm/V at 1.06 μm has been measured and physical aging is shown to enhance the stability of poled order.

Side-chain copolymers with a methacrylate backbone and sulfonyl-substituted alkoxy stilbenes as the NLO entity have been synthesized.[99] For these polymers, the functionalization level of the chromophores is limited due to crystallization of the polymer side chains. However, for one polymer at a 41% functionalization level, apparent enhancement of the d_{33} value occurs, possibly due to collective interactions. Severe plasticization by water absorption causes rapid decay of poled order.

A very high T_g side-chain acrylate polymer containing the well-known chromophore MNA 9 has been synthesized.[212] The polymer poly(N-MNA acrylamide) has a T_g = 205 °C (DSC) and a λ_{max} = 304 nm. Films were corona poled well above T_g at 225 °C for 30 min, maintained at 170 °C for 1 h, and then cooled to 40 °C. At 1.064 μm, d_{33} = 3 pm/V was measured. No decay in d_{33} was observed at room temperature over a period of 6 months. Relaxation of poled order in this polymer has not yet been reported at elevated temperatures.
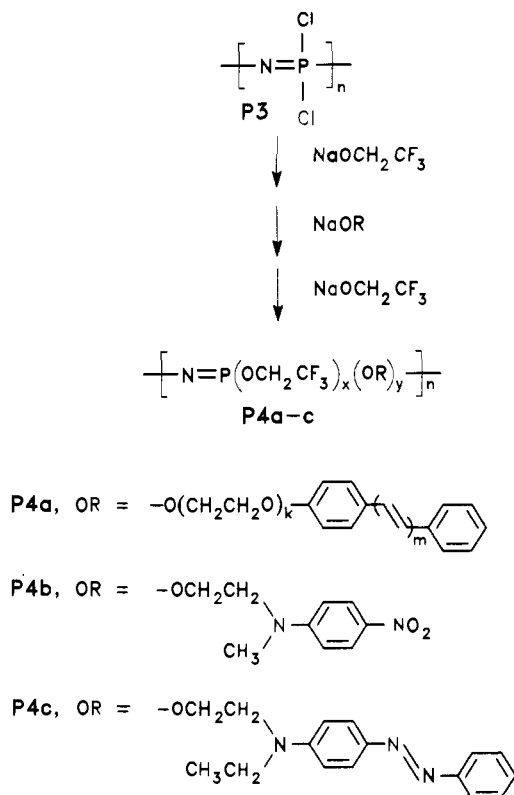
A highly functionalized side-chain polymer based on the high T_g thermoplastic poly(2,6-dimethyl-1,4-phenylene oxide) (PPO) has been synthesized.[213,214] The chromophore substituent N-(4-nitrophenyl)-S-prolinoxy was used, and functionalization levels of 1.63 chromophore units per PPO repeat unit have been achieved. T_g for this polymer is reported to be 173 °C.[214] Despite the relatively low molecular hyperpolarizability of the PNA-like chromophore, d_{33} = 27 pm/V has been measured at 1.064 μm for films corona poled at 180–190 °C. Some poling is observed to occur far below T_g, which is evidence of rotation of the phenylene backbone at low temperatures. Temporal decay of the nonlinearity was monitored at room temperature and a 20–25% loss was observed after 50 days, with most of the loss occurring within the first few days.

Recently a series of side-chain nonlinear chromophores have been incorporated into a polyphosphazene backbone.[215] Polyphosphazenes have the general formula $(NPR_2)_n$, where the group R in the present case represents the nonlinear chromophore. The functionalization sequence of a polyphosphazene **P3** to form the polymers **P4a–c** is shown in Scheme 1. A variety of side-chain systems of this type have been synthesized with d_{33} values ranging form 4.1–34 pm/V at 1.06 μm. The T_g's of these systems were unfortunately low, ranging from –60 to 58 °C.

C. Main-Chain Polymers

Poled-order relaxation should be further restricted if the chromophore were to be chemically incorporated into the polymer backbone itself. The significant difference between this main-chain approach and the

Scheme 1

$$\left[N=P\right]_n$$

P3

with Cl substituents

↓ NaOCH$_2$CF$_3$

↓ NaOR

↓ NaOCH$_2$CF$_3$

$$\left[N=P(OCH_2CF_3)_x(OR)_y\right]_n$$

P4a–c

P4a, OR = $-O(CH_2CH_2O)_k$ —⟨⟩— ⟨⟩$_m$ ⟨⟩

P4b, OR = $-OCH_2CH_2$\
N—⟨⟩—NO$_2$\
CH$_3$

P4c, OR = $-OCH_2CH_2$\
N—⟨⟩—N=N—⟨⟩\
CH$_3$CH$_2$

side-chain one is that large segmental motions of the polymer backbone are required for poling and for relaxation of the former. Although poling may thus be more difficult with a main-chain system, sub-T_g relaxation of poled order is also expected to be significantly inhibited. In addition, a main-chain polymer may show improved tensile and mechanical properties relative to a side-chain polymer.[216]

The earliest studied main-chain polymers consisted of chromophores with their dipole moments oriented "head-to-tail" along the polymer chain.[217-220] It was originally suggested that this head-to-tail arrangement of the molecular dipoles might result in a coherent enhancement of the second-order nonlinear optical properties.[5,216] This can be easily visualized by considering an extended one-dimensional polymer chain in which all chromophores are arranged head-to-tail along the backbone. The dipole moment of the polymer chain considered as a single molecule is $\mu_{total} = N\mu$ where N is the number of chromophore units and μ is the dipole moment of each unit. Similarly, the polymer hyperpolarizability is $\beta_{total} = N\beta$. The susceptibility from eq 40 is then

$$\chi^{(2)} \propto \frac{N^2\mu\beta}{V(N)} \qquad (66)$$

where $V(N)$ is the specific volume of the N-unit chromophore and is itself a function of N. This value is considerably greater than expected for a system of N independent chromophores ($N\mu\beta/V(N)$). Of course as μ increases, the assumption that $\mu\beta < kT$ yielding eq 40 breaks down and the effect of further increasing the dipole moment saturates. Enhancements of this type may have been observed in ethylene chloride solutions of the rigid-rod polymer poly(γ-benzyl-L-glutamate).[101] The enhancement factor will be reduced if the polymer is not strictly linear or if the polymer

chain does not reach an equilibrium orientation in the external poling field. The latter is particularly important for long chains where chain entanglement can restrict the mobility.

Several different homopolymers containing dipolar repeat units all pointing in the same direction along the polymer chain have been synthesized.[217-219,221] Unfortunately, these polymers are, for the most part, insoluble. To overcome this solubility problem a series of smaller oligomers of head-to-tail dipolar chromophores has been prepared.[222] The oligomers exhibited significant dipole moment additivity both in solution and in polymer films. The electrooptic coefficient of the tetramer is estimated to be enhanced by a factor of 1.6 over a film made of analogous monomers with the same chromophore concentration.

Recently, a series of 4-methoxy-4'-carbomethoxy-α-amino-α'-cyanostilbenes have been prepared by condensation polymerization.[216] The resulting homopolymers had relatively high T_g's, ranging from 168 to 187 °C. EFISH measurements at 1.9 μm on dilute solutions of the polymers gave $\mu\beta$ values ranging from 61×10^{-48} to 79×10^{-48} D esu. No enhancement of the nonlinear optical properties was observed due to cooperative interactions. One main-chain polymer has been synthesized which appears to exhibit an enhancement in $\mu\beta$ by a factor of 20 in the solution EFISH measurements, apparently due to cooperative effects.[5] This is an AB copolymer of α-cyano-m-methoxy-p-(ω-oxypropoxy)cinnamate with ω-hydroxydodecanoate. However, no enhancement of $\mu\beta$ in thin films of this polymer was observed, possibly because chain entanglements inhibit alignment.[216]

A series of experiments designed to compare, for the same chromophore, the mechanism of decay of poled order in "head-to-tail" main-chain polymers with that mechanism in side-chain polymers has been reported.[97] The thermally stimulated discharge current (TSD) technique used has been described in section IV.B and typical results are shown in Figure 16. The loss of polar order in the side-chain polymers is associated with local reorientation, while that in the main-chain polymers results from large, global end–end polymer motions together with local reorientation of the chromophore around its long dipolar axis. Annealing and aging of the polymers noticeably increased the stability of poled order for both types of polymers. In addition, dielectric relaxation measurements have been carried out on the same set of side- and main-chain polymers and compared with those of a guest–host system containing the same chromophore.[138] The dielectric relaxation measurements were made in the region above the glass transition and show that time–temperature superposition (associated with WLF type behavior discussed in section IV.B) is obeyed for both the side- and main-chain polymers indicating that the distribution of relaxation times is not a strong function of temperature. However, time–temperature superposition does not appear to hold for the guest–host system, indicating that the distribution of relaxation times is temperature dependent in these systems. The dielectric relaxation measurements did not reveal any large-scale dipolar correlation which would result in enhanced alignment of the chromophores. The synthesis of another head-to-tail, main-chain polymer poly[(4-N-ethylene-N-ethylamino)-α-cyanocinnamate] has recently been re-
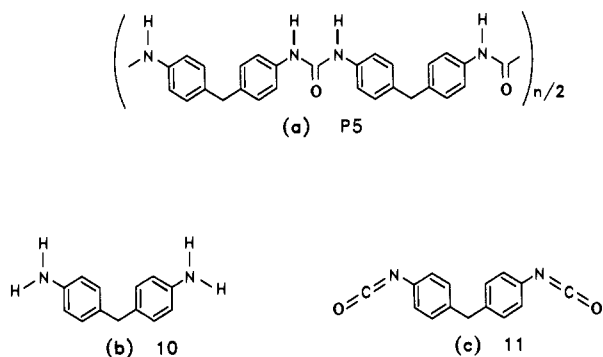
Figure 27. (a) Thin films of polyurea **P5** can be formed by vapor codeposition polymerization of the aromatic diamine **10** (shown in b) and the aromatic diisocyanate **11** (shown in c) (from ref 224).

ported.[223] The T_g for this polymer is 103 °C with a d_{33} = 7 pm/V at 1.06 μm.

A novel film formation technique (i.e. vapor deposition polymerization) has been used to make polyurea films and second-harmonic generation has been observed.[224] This technique can produce films of precisely controlled thicknesses, critical for phase matching. Films of polyurea **P5** were formed by codeposition of the aromatic diamine **10** and the aromatic diisocyanate **11** as shown in Figure 27. Films of thickness 1.3 μm were obtained by this technique, which were corona poled at 180 °C. $\chi^{(2)}_{333}$ = 3.3 pm/V at 1.06 μm was measured and the poled order was stable indefinitely at room temperature after an initial decay of a few percent in the first week.

Highly processable aromatic polyureas having relatively high nonlinear optical coefficients and which are largely transparent to blue light have been synthesized.[225] Polymers were made both with and without pendant p-nitroaniline chromophores, with the corresponding λ_{max} values of 378 and 253 nm and cutoff wavelengths of 460 and 307 nm, respectively. The polymer films were poled at 130 °C and d_{33} values of 8.3 and 5 pm/V at 1.06 μm were obtained for the two polymers, respectively.

Main-chain polymers in which the dipole moment of the NLO group is perpendicular to the polymer chain have also been synthesized. Polymers of this type might be expected to be easier to pole than the "head-to-tail" main-chain polymers, since smaller segments of the polymer backbone must be moved to enable orientation of the chromophore. This class is exemplified by a series of NLO-active chromophores incorporated into linear epoxy polymers.[92,123] The polymers bisphenol A-4-amino-4'-nitrotolan (BisA-ANT **P6**), bisphenol A-4-nitroaniline (BisA-NA **P7**), and bisphenol A-N,N-dimethyl-4-nitro-1,2-phenylenediamine (BisA-DMN-PDA **P8**) have been synthesized and their structures are shown in Figure 28. Dielectric relaxation measurements on BisA-NA **P7** and BisA-DMNPDA **P8** have demonstrated that molecular motions related to the glass transition are the principle mechanism of loss of polar order even at temperatures well below T_g.[226] Furthermore, poling of both polymers was shown to cause the respective T_g's to decrease.[92] It has been proposed that longer, rodlike chromophores such as the tolan units (see compound **2**) in BisA-ANT **P6** will be less susceptible to reorientation following poling because the rotation of such segments requires a greater

volume and therefore more global, cooperative motions of the polymer backbone. Rodlike molecules have much longer rotational relaxation times than more spherical molecules even in the melt.[227] It has also been suggested that thermotropic interactions may favor parallel alignment of chromophores.[228] Poling of BisA-ANT resulted in a d_{33} = 90 pm/V, whereas d_{33} for BisA-NA is ~30 pm/V (both at 1.06 μm). The decay of the birefringence of BisA-NAT was monitored at 100 °C (see Figure 15) and was shown to be consistent with the decay of d_{33}. The decay of poled order at room temperature was much improved over that in BisA-NA and BisA-DMNPDA, a feature attributed to the bulkier chromophores.

In contrast to BisA-NA and BisA-DMNPDA, dielectric relaxation measurements indicate that poling decreases the mobility of the NLO group in Bis-ANT, which may be a manifestation of favorable thermotropic interactions between chromophores in this polymer. Electrooptic measurements on BisA-ANT have shown that $r_{33}/r_{13} > 3$, which is interpreted using a model that includes restricted mobility of the chromophore segment (see section II.E).[95] Subsequently, a variety of tolan chromophores have been incorporated into epoxy-based polymers.[229] Some of these polymers turned out to have liquid crystalline properties due to the high density of tolan groups, but the polymer **P9** is amorphous with a T_g = 180 °C and $d_{33} > 30$ pm/V at 1.06 μm.

P9
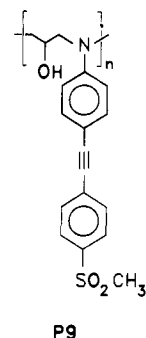
A series of three main-chain nonlinear polymers based on a polyurethane backbone have been synthesized.[230] The chromophore for all polymers is the same azo dye and the polyurethane backbone has been modified, resulting in polymers with varying degrees of stiffness in the backbone. T_g of the most flexible polymer is 74 °C, and that of the most rigid polymer is 116 °C. $\chi^{(2)}$ values ranging from 9 to 12 pm/V have been obtained. The rate of poled-order decay has been compared for the three polymers 20 °C below the poling onset temperatures. Different rates of depoling were observed, with the largest rate occurring for the most rigid polymer with the highest T_g. The authors conclude that relaxation of poled order in these main-chain systems is not merely a function of T_g, but depends in a complicated manner both on the specific interactions in the polymers and on the monomer structure.

A recent approach to main-chain nonlinear optical polymers has been to synthesize syndioregic polymers or "accordion polymers" in which the chromopores are connected with U-shaped bridging groups designed to allow folding of the chromophores to produce roughly parallel dipole alignment.[231-233] This configuration is shown in Figure 29a. An example of such a polymer

BISA–ANT
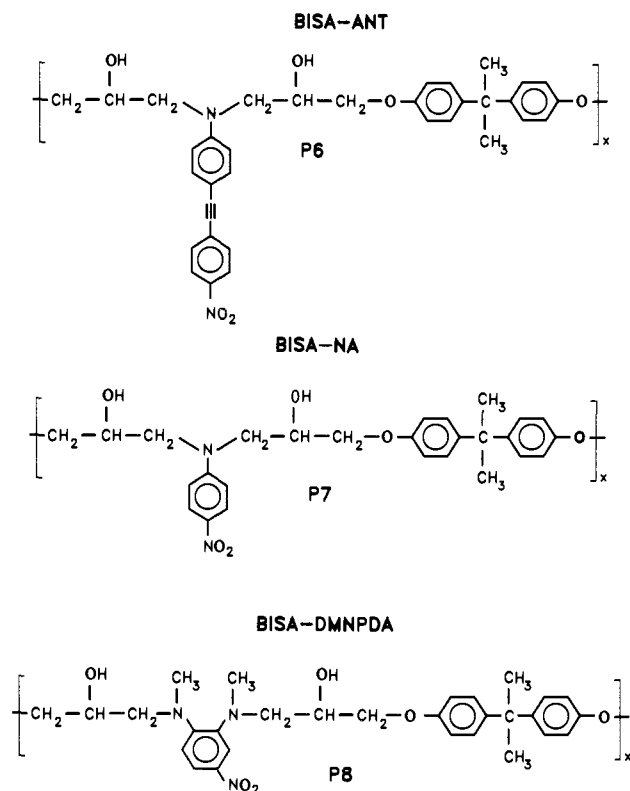

BISA–NA

BISA–DMNPDA

Figure 28. Structures of main-chain linear epoxy polymers.

P10 with a T_g of 208 °C is shown in Figure 29b. This polymer shows no second harmonic generation before poling, but after poling at 215 °C, it exhibits a $\chi^{(2)} = 7$ pm/V.[234] The poled order is reported to be stable at room temperature; however, the stability at elevated temperatures has not been reported.

Yet another approach to main-chain polymers has been to design a polymer in which the alignment of one dipolar segment will require the alignment of adjacent segments because of the geometric constraints of the connecting group. A series of diethynyldiphenylsilicon homopolymers substituted with NLO chromophores has been synthesized for this purpose.[235] The tetrahedral bonding on the Si atom in the connecting group is expected to force the alignment of adjacent segments in a collective manner. However, no enhancement in nonlinear optical properties due to this cooperative phenomenon was observed and an $r_{33} < 1$ pm/V was measured. The relaxation time constant was only 190 h at room temperature.

Although several classes of main-chain polymers have been synthesized, only one has demonstrated enhancement of nonlinear optical properties due to cooperative dipolar interactions in solution, and none have exhibited such an effect in thin films. Thermally stimulated discharge current measurements and dielectric relaxation measurements have indicated that both poling and relaxation in head-to-tail main-chain polymers occurs near the glass transition. The reported nonlinear optical coefficients of the poled main-chain polymers have been significantly lower than those achieved for side-chain polymers. So few temperature-dependent measurements of the relaxation of poled order have been carried out that it is difficult to evaluate whether the expected improved poled-order thermal stability of the main-chain polymers will be experimentally realized. Clearly, the experimental data on this class of nonlinear polymers is preliminary and polymers with

(a)

(b)

P10
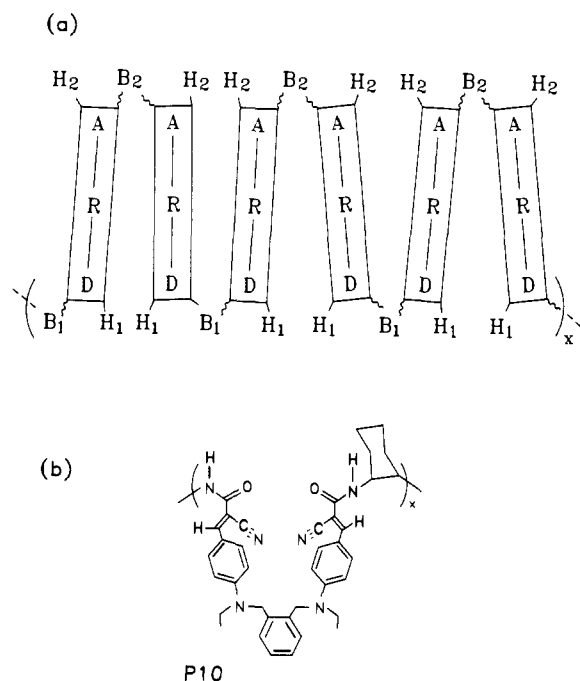
Figure 29. (a) A representation of a syndioregic or "accordion" main-chain polymer in which the chromophores are connected with U-shaped bridging groups (from ref 232) and (b) an example of a syndioregic polymer with $T_g = 208$ °C (from ref 233).

higher nonlinearity must be developed and the issues concerning the poling efficiency and stability must be resolved before their utility can be assessed.

D. Cross-Linked Systems

1. Thermally Cross-Linked Systems—Thermosets

Rotational relaxation processes which limit the lifetime of poled-polymer devices may be suppressed by increasing the glass transition temperature of the system as discussed above, and/or by enhancing the extent of interaction between polymer chains. The latter can be accomplished via the formation of interchain chemical bonds or cross-linking, resulting in the partial immobilization of segments of the polymer chain. The effectiveness in decreasing polymer mobility depends on the number, nature, and sites of cross-linking. Since the poling process used to destroy the natural macroscopic centrosymmetry in most polar systems requires dipole mobility, most of the cross-linking must occur during or after the poling process is completed.

The demand for thermal and orientational stability in polymeric NLO devices has spurred investigators to study thermal and photochemical methods for cross-linking poled-polymer systems. It should be noted, however, that there is often a price to be paid for restricting polymer mobility by cross-linking in terms of polymer insolubility, light scattering, shrinkage, adhesion problems, embrittlement, mechanical stress, etc. These fabrication difficulties are exacerbated for demanding optical applications such as waveguiding in both active and passive configurations.

High-temperature polymeric materials may be roughly classified into two categories, thermoplastics and thermosets. Thermoplastic materials may be heat treated or re-formed many times without changes in the polymer characteristics or properties. Thermosets on the other hand, cannot be reprocessed and are

Scheme 2

Host—Guest Epoxy Curing

Chromophores

DANS

4

DO1

12
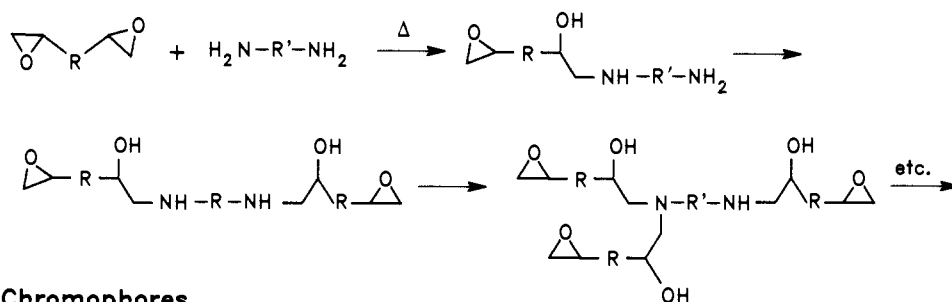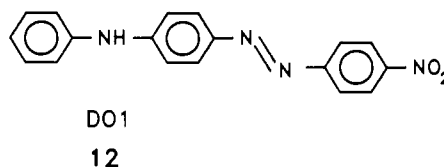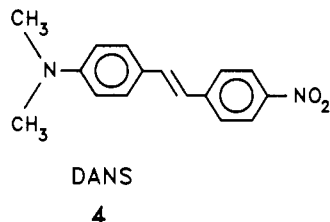
transformed upon heating so that they no longer retain the physical and mechanical properties of the original polymer. These changes are usually produced by cross linking between the individual polymer chains so that polymer mobility is decreased and viscous flow is inhibited. Such chemical changes in the polymer are usually manifested by a decrease in solubility in common solvents and a reduction in polymer-chain mobility. These effects are dependent on the nature, position, and number of chain cross-linking sites.

One of the oldest and most intensively investigated classes of thermosetting materials are the epoxy resins.[236–238] Because of extensive industrial applications, available epoxy resins are myriad. Two component epoxies are composed of a polyfunctional epoxy monomer or oligomer and an initiator or hardener. The initiators themselves are often polyfunctional organic molecules such as amines, anhydrides, acids, etc. Mixing the components causes polymerization by ring opening of the reactive epoxy functionality. Final curing or hardening of the prepolymers is usually accomplished by heating to produce an insoluble and densified network. Since a primary amine can in principle open two epoxide rings, monoamines can produce linear polymers from bis-epoxy precursors. In this polymerization the primary amino group has a functionality of two. Polyamines with higher functionality can therefore result in the linking of polymer chains (cross-linking) leading to thermosetting materials. Because of the commercial importance of epoxy polymers, it is not surprising that the first attempts to produce cross-linked NLO polymers to improve thermal stability of poled polymers involved materials of this type.

Epoxy resins for poled-polymer applications may be roughly classified according to the type of bonding between the components: (i) guest–host systems where the polymer cross-links involve only the epoxy material and an external initiator other than the NLO moiety, (ii) systems where the chromophore is tethered to the polymer backbone, but is not involved in the actual cross-linking, (iii) incorporation of the NLO functionality into the epoxy polymer backbone independent of

the cross-linking sites, (iv) the use of difunctional epoxides and NLO diamines where the amine substituent is not only incorporated into the growing chain but is also involved in cross-linking the chains, and (v) materials formed from polyfunctional epoxides and di- or polyamino functionalized NLO initiators where many polymer chains can be linked together because of the polyfunctional nature of the reagents.

Marks and co-workers[239,240] have reported improved thermal stabilities in the cross-linked epoxy guest–host system shown in Scheme 2. A commercial thermosetting epoxy, EPO-TEK 301-2 (diglycidyl ether of bisphenol A and a polyfunctional aliphatic amine hardening reagent), was intimately mixed with either of the NLO chromophores DANS 4 or DO1 12 in a solvent and introduced into a cell composed of two transparent, conducting ITO (indium–tin oxide) electrodes. Some cross-linking was induced by heating briefly to 80 °C before the poling field was applied. Partial polymerization and increase in fluid viscosity is necessary to avoid dielectric breakdown upon application of the strong poling electric field. Poling was conducted at elevated temperatures while the epoxy resin cured and vitrified and was maintained until the sample had cooled to room temperature. NLO measurements on poled samples at room temperature yielded d_{33} values ranging from 0.04–0.4 pm/V (1.06 μm). The temporal stability of these systems was considerably improved over non-cross-linked guest–host systems. The decay of the second harmonic signal was fit to the biexponential function shown below, rather than the stretched exponential form of eq 58

$$d_{33} = Ae^{-t/\tau_1} + Be^{-t/\tau_2} \qquad (67)$$

The two relaxation times are designated as τ_1 and τ_2. The decay was observed to be dependent on the nature of the NLO chromophore. For example, for films comparably cured, the sample containing DANS 4 decayed to ~60% of the original signal after ~350 h at room temperature while that containing DO1 12 reached the same level only after 700 h. The longer decay time for the DO1 12 was attributed to the larger size and volume requirements of the chromophore (see

Scheme 3. Tethered Guest-Host Epoxy Curing

(a)

P11 —NaH→ P12 + NPPTos **13**

NPP–PHS **P13** —14 or 15→ Crosslinked Polymer

Δ, poling

(b)

P12 + BNPPTos **16** → BNPP–PHS **P14**

—CF$_3$CO$_2$H→ HNPP–PHS **P15**
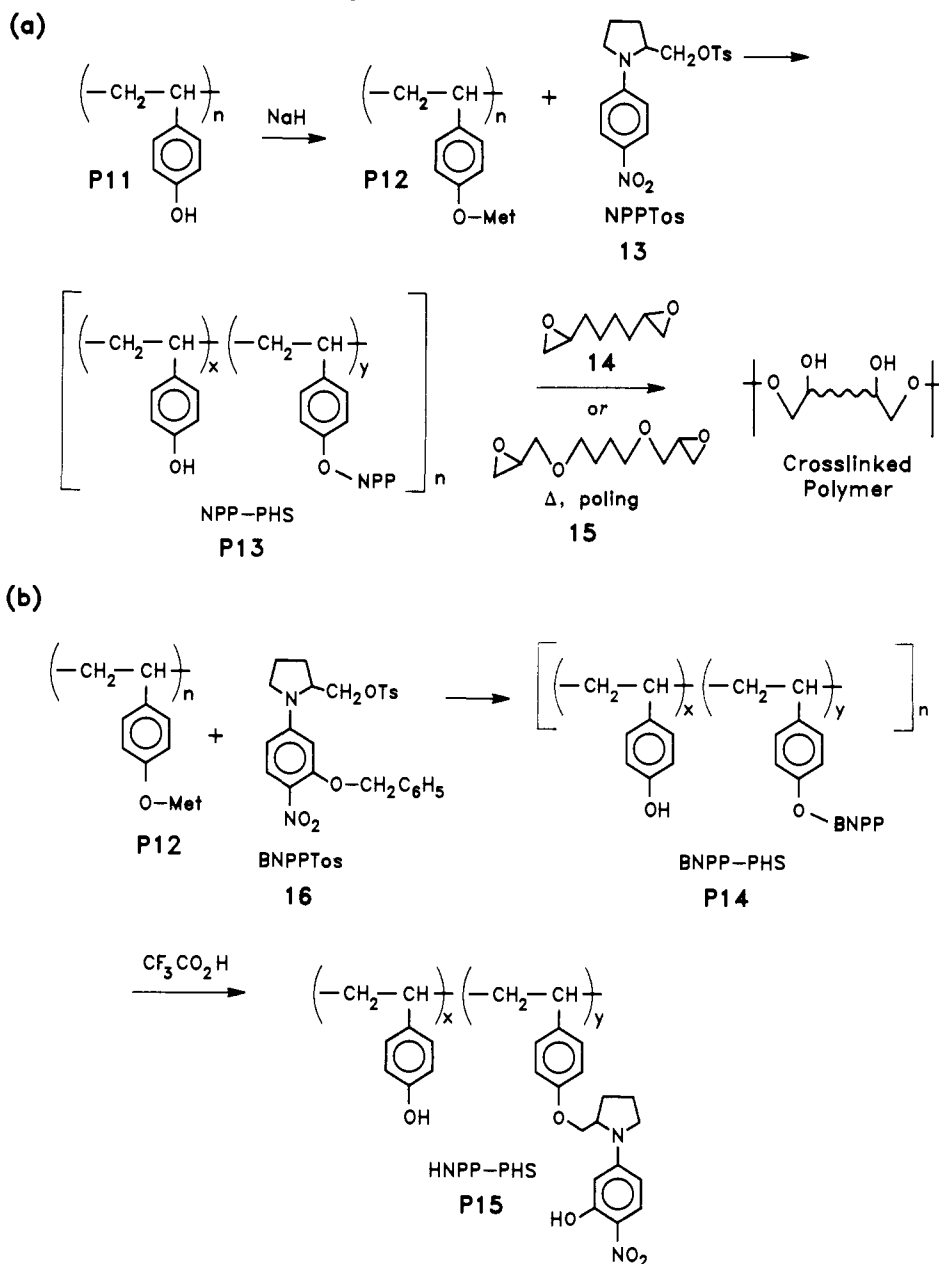
earlier discussions in section IV.B). The decay characteristics of the guest–host cross-linked systems depended to some extent on the time the sample was held at the curing temperature in a manner consistent with the progress of polymer vitrification and subsequent decrease in the available free volume.[214] For example, epoxy films containing DO1 which have been simultaneously poled and cured at 150 °C show only negligible decay in poled order at room temperature after 20 days.[214] This study demonstrates nicely that improved temporal stability can be obtained by partial immobilization of the guest in a cross-linked polymer host. The drawbacks of such a system are low chromophore densities dictated by solubility and phase separation, potential plasticization effects of the guest on the host polymer and limited ability to immobilize a guest not chemically bonded to the cross-linked matrix.

As a logical extension of the guest–cross-linked host studies reported above, Marks and co-workers[241a] studied the effect of epoxy cross-linking in a reactively functionalized polymer where the NLO chromophore is tethered as a polymer side chain, but is not actually

involved in the cross-linking process. Such a system is shown below in Scheme 3. Poly(p-hydroxystyrene) **P11** is partially functionalized using the tosylate derivative of N-(4-nitrophenyl)-(s)-prolinol **13**. Films of the NLO polymer **P13** were cast from solutions containing varying quantities of either 1,2:7,8-diepoxyoctane (14) or 1,4-butanediol diglycidyl diether (15) as potential cross-linking reagents. In this case, the active initiators are the phenolic hydroxy groups of the polymer. Cast films were partially cured at 100 °C prior to poling and corona poled at 180 °C for 1 h. Studies of the nonlinearity at room temperature yielded d_{33} values (1.064 μm) ranging from 0.6–2.9 pm/V. The d values varied both with the nature and the stoichiometry of the cross linker, with the 1,2:7,8-diepoxyoctane (14) at a molar ratio diepoxide/OH = 0.5 producing the most highly nonlinear poled films. As observed earlier, the decay in the second harmonic signal could be analyzed using a biexponential fit. The cross-linked materials were approximately three times more stable than materials which were heated and poled without a cross linker present. For films poled and cured under optimal

conditions, decay in the generated second-harmonic signal of only ~10% was observed after 350 h at room temperature. This should be compared with a signal decay of 25–30% at 350 h for the cross-linked guest–host system described earlier. In each system, the thermal stability tracks the extent of polymer vitrification, as expected. It is clear that attachment of the NLO chromophore to the polymer backbone improves the stability even though the chromophore itself is not directly involved in the cross-linking process. Once again, corona poling appears to result in larger d values than electrode poling. The values measured exceeded those achieved in the earlier guest–host cross-linked systems.

In related work, Marks and co-workers[241b] have studied the effects of the cross-linking site on the temporal stability of a polymer-tethered NLO system. The system studied is shown in Scheme 3b which differs from that in Scheme 3a only by the presence of an additional reactive substituent in position 3 of the aromatic ring of the chromophore. Both polymers (BNPP-PHS **P14** and HNPP-PHS **P15**) could be cross-linked using 1,2:7,8-diepoxyoctane (**14**). In the former, the cross-links between chains involve only the p-hydroxystyrene substituents while those in the latter presumably involve the NLO chromophore as well. In each case, the cross-linking reaction increases the T_g of the polymers by ~10 °C. As expected, the temporal stability of the poled and cross-linked polymers is substantially greater than for the un-cross-linked materials. Surprisingly, however, the thermal stability of cross-linked HNPP-PHS **P15**, where the chromophore is actually involved in the cross-linking, is only slightly greater than cross-linked BNPP-PHS **P14** where only the poly(p-hydroxystyrene) **P11** moieties are involved in the cross-linking reaction. For the un-cross-linked polymers, hydrogen bonding involving the NLO chromophore appears to have little effect on the thermal stability of the system.

In epoxy-based systems, higher chromophore densities and improved thermal stabilities would be expected when amino-containing NLO chromophores are used to initiate the ring opening and subsequently the amino nitrogen becomes incorporated in the epoxy polymer backbone. The first such cross-linked epoxy system was reported by Eich et al.[68] and is described in Scheme 4a. Using the diamine NPDA **17** and bisphenol A diglycidyl ether BPADGE **18**, soluble prepolymers bisA-NPDA **P16** with $T_g \approx 40$ °C were prepared and coated. The film was further vitrified by curing at 140 °C while poling. The T_g of the system slowly rises to the thermal cure temperature, but full curing requires from 12 to 16 h. It is necessary to maintain the corona poling during the entire high-temperature curing cycle (precuring at 100 °C for some hours is necessary before applying the corona) until the sample is returned to room temperature. By using corona poling and slow thermal ramping, fields in excess of 1 MV/cm are possible without dielectric breakdown. Maker fringe experiments were used to determine the nonlinearities of the cured epoxy films ($d_{33} = 13.5$ pm/V, $d_{31} = 3$ pm/V, 1.064 μm). The d values obtained compare favorably with those of LiNbO$_3$ ($d_{33} = 30$ pm/V, $d_{31} = 6$ pm/V[105]). The thermal stability of the poled and cross-linked films was quite good, showing no signal decay at room temperature after 500 h. More remark-

Scheme 4. NLO Incorporated Epoxies
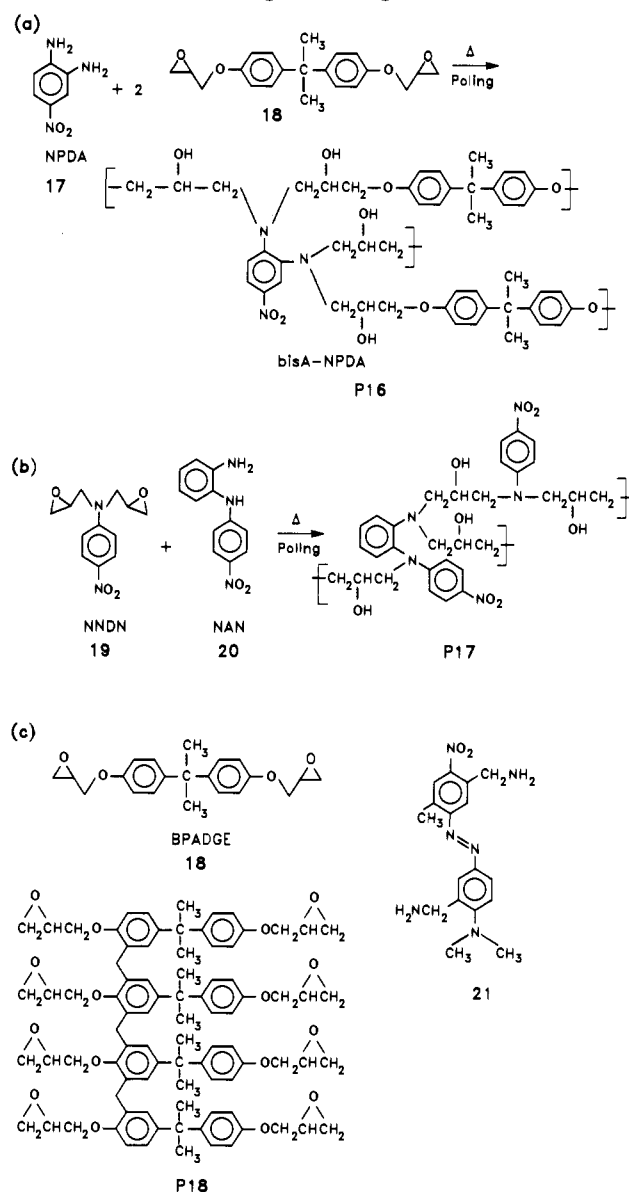
ably, no signal decay was observed when the polymer film was held at 85 °C for 40 min. Chromophore poling occurs as the applied temperature approaches that of the final cure and the polar orientation is stabilized by continuous cross-linking.

A useful variant of this technique was described by Jungbauer et al.[84] and is shown in Scheme 4b. Use of a bis-epoxide also containing a bonded NLO chromophore (NNDN **19**) allows a significant increase in the NLO chromophore density (63 wt %) to be achieved. (The weight fraction of NLO-active groups in the previous example was only 29% since the epoxide serves as a diluent.) Soluble prepolymers **P17** ($T_g \approx 5$ °C) were obtained by melting the reagents and heating the mixture briefly to 130 °C. The prepolymers were coated from diglyme and ultimately cured at 120 °C in a corona field for 16 h. Maker fringe studies on these samples yielded values for d_{33} and d_{31} of 50 and 16 pm/V at 1.06 μm, respectively. The higher d values presumably reflect the increased weight percent of the active chromophores in these samples. No decay in the second harmonic signal was observed at room temperature. Even at 80 °C, after a small initial loss (~10–15%) occurring within the first 15 min, no further decay in

Scheme 5. Flexible Main-Chain NLO Polyurethanes
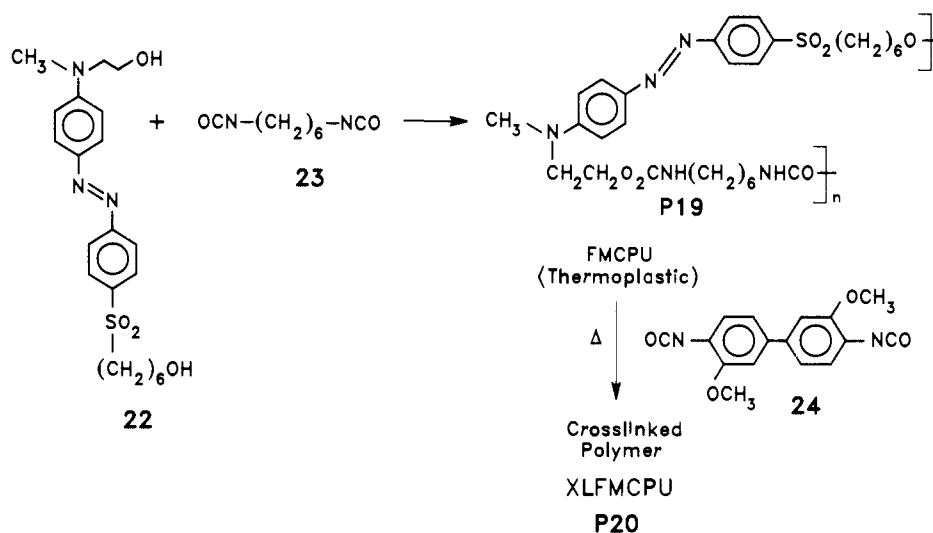
the signal was observed over 50 h. The measured electrooptic coefficient (r_{33} = 6.5 pm/V, 532 nm, 5 kHz), behaved similarly and no further loss in the sample birefringence was observed over a period of 50 days at 80 °C. Hence, it appears that this polymeric network system maintains the polar order at elevated temperatures and relaxation of the "singly connected" chromophores is greatly impeded.

Very recently another epoxy-NLO diamine system has been described by Marks and co-workers[242] (Scheme 4c). The initiating amino substituents in the chromophore 21 were insulated from the aromatic ring both to increase the basicity and to avoid possible deleterious effects on the nonlinearity caused by electronic coupling of the amino groups to the aromatic π system. Although the intrinsic nonlinearity of this chromophore was expected to exceed that of the substituted p-aminonitrobenzenes studied previously, the dilution by the epoxy component limits the maximum chromophore density. For this study both bisphenol A diglycidyl diether (BPADGE 18) and a commercial oligomeric polyepoxide reagent (Epi-Rez SU 8) P18 were examined. Solutions of the reagents were spin cast and precured to 100 °C for 3 h prior to corona poling. The final curing and poling were conducted at 130 °C for 2 h. The cured polymer from 18 had a T_g of 121 °C, while no transition could be detected by DSC analysis in the material prepared from P18. Progress in the polymerization and vitrification was followed by IR analysis. Nonlinear optical measurements yielded values of d_{33} of 6.5 and 14.3 pm/V (1.064 μm) for the polymers prepared from 18 and P18, respectively. These values are still less than expected on the basis of the solution $\mu\beta$ values of the chromophores and the calculated number densities. The authors suggest that partial chromophore immobilization during the precure or possibly steric twisting of the conjugating substituents during curing may be responsible. A significant improvement in the thermal stability was observed for the system prepared from P18 relative to that from 18 ($\sim$20% signal loss at room temperature after 1000 h versus a 50% loss in a comparable time). At 85 °C, the loss in the second-harmonic signal from the polymer prepared from P18 was $\sim$60% after 1000 h with most of this occurring within the first 50 h.

Besides epoxy resins, other NLO-containing thermosetting polymers have been described recently and

some show large nonlinearities and impressive thermal stabilities in the poled state. These include polyurethanes,[243-245] polyamides,[246,247] and a polyimide derivative.[248] In each case, the thermal stability of the induced polar order was considerably improved by the cross-linking.

As discussed in section VI.C, many main-chain polymers with chromophores incorporated in a head-to-tail configuration have been designed in an effort to produce a large and additive dipole moment for each polymer chain in its extended form.[219,249] In general, this effect has not been realized, presumably due to the difficulty in reorienting long molecular chains in viscous polymer media. In fact, due to the random coil nature of most high polymers, it may prove easier to orient randomly organized dipolar segments of a main-chain polymer, as long as these portions are connected by soft flexible segments of sufficient length to permit somewhat independent reorientation. Dalton and co-workers[243] have prepared such a random main-chain polyurethane shown in Scheme 5 where the dipolar segments are connected by flexible spacers. The bishydroxy-functionalized monomer 22 was polymerized with the flexible diisocyanate, 1,6-diisocyanato-hexane (23), to produce the polyurethane P19. The similar reactivities of the two types of hydroxy functionality assure a random orientation of the dipolar segments, each of which is separated by a flexible spacer to facilitate electric field poling. Weight average molecular weights in excess of 7000 Da are achieved by normal solution condensation polymerization techniques. Un-cross-linked polymer films P19 produced by spin casting from solution were corona poled at 115 °C. A second-harmonic coefficient d_{33} of 40 pm/V (1.064 μm) was measured. Examination of the visible absorption spectrum of the NLO polymer suggests that this value is significantly resonance enhanced. An order parameter of >0.2 was calculated by comparison of the absorption spectra for the poled and unpoled samples. Cross-linking concurrent with poling can be achieved by incorporation of the bifunctional isocyanate 4,4′-diisocyanato-3,3′-methoxybiphenyl (24) and heating the film to 120 °C. The cross-linking of polyurethanes by isocyanates is a known reaction proceeding via the formation of allophonate linkages[250] involving the NH main-chain bonds. Cross-linking in this poled-polymer system is inferred by comparison of the temporal

**Scheme 6. Semiflexible NLO Polyurethanes**
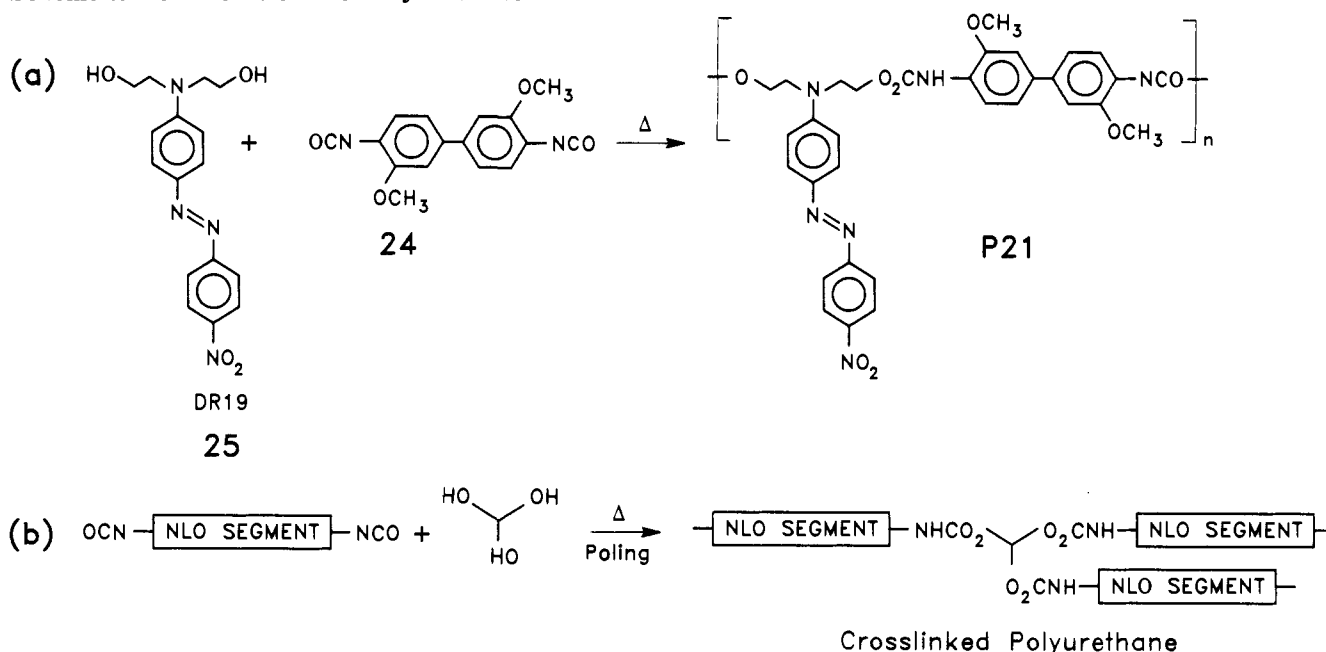
stability with that of the un-cross-linked material. While the SHG coefficient of the cross-linked material **P20** showed essentially no decay after more than 1200 h at room temperature, that of the un-cross-linked material **P19** decayed completely in less than 100 h. No measurements were reported earlier than 0.5 h after poling, so it is not known whether there is a fast decay component in the cross-linked material **P20**. The optical characteristics of the polyurethane films were not discussed.

Encouraging results have also been reported recently for polyurethane derivatives where the amino donor substituent of the NLO chromophore is incorporated into the polymer backbone.[244,245] The preparation of such a polymer is described in Scheme 6a. The highly nonlinear chromophore (DR19 **25**) is polymerized with the rigid bifunctional isocyanate, 4,4'-diisocyanato-3,3'-dimethoxybiphenyl (**24**), to produce the desired polyurethane derivative **P21**. The stoichiometry was controlled so as to produce deliberately a polyurethane with reactive isocyanate end groups. The concentration of the end groups was determined by FTIR and a precise amount of a trifunctional cross-linking reagent was added to the purified polymer solutions, as shown in Scheme 6b. In this case, the preferred cross-linking reagent was triethanolamine. Polymer films prepared by spin coating were poled in a corona discharge while the temperature was ramped from 160 to 200 °C. The poling was maintained for 1 h at elevated temperatures. DSC analysis of both of the cross-linked and un-cross-linked polymers showed no thermal transitions below 270 °C. For the cross-linked system, TGA analysis indicated an onset of weight loss around 300 °C. The un-cross-linked material **P21** was somewhat less stable. Interestingly, the thermal stability of the cross-linked polymer seems to exceed that of the chromophore DR19 **25** itself when measured as a neat sample. The polymer that had been treated with triethanolamine was insoluble in common organic solvents, supporting the suggestion that significant cross-linking occurs under the reaction conditions. A high, strongly resonance enhanced d_{33} value of 120 pm/V (1.064 μm, corrected for chromophore absorption at 532 nm), was measured

for the cross-linked sample. The electrooptic coefficient (r_{13}) was determined to be 13 pm/V (633 nm). This value is also resonance enhanced and falls to 5 pm/V when measured at 800 nm. The order parameter in the poled and cross-linked sample was calculated to be 0.29 from absorption measurements. The thermal stability of the polar order was quite remarkable and no decay in the signal was observed over 3000 h at room temperature. Even at 90 °C, 70% of the original second-harmonic signal was observed after 3000 h. As expected, the chromophore mobility is low in the cross-linked samples and attempts to pole after thermal cross linking produced low-order parameters and marginal nonlinearities. The photostability of the cross-linked material is also reported to be greatly improved relative to similar chromophores in other thermoplastic polymers. These results are encouraging and suggest the possible utility of cross-linked NLO polyurethanes in semiconductor device applications.

Bifunctional NLO chromophores containing differentiated and reactive functionality at both ends of the molecule have been prepared with the idea that polymerization and subsequent cross-linking should result in maximum immobilization of the poled chromophore due to attachment of both ends to polymer chains.[251-253] The first such system was described by Dalton and co-workers,[251] who reported the preparation of the bifunctional chromophore **41**. Condensation polymerization with terephthaloyl chloride **42** yielded the functionalized polymer **P30**. In principle, the pendant methacrylate functionality in **P30** could be either thermally or photochemically cross-linked. Alternatively, the methacrylate moiety in **41** could first be polymerized by free-radical techniques leaving the pendant hydroxyethyl functionality for subsequent cross-linking. The latter has been accomplished in situ, while poling the methacrylate macromonomer, by heating (160–180 °C) with 3,3'-dimethoxy-4,4'-biphenylene diisocyanate. The second-harmonic coefficient d_{33} in the cross-linked material was stable, after an initial rapid loss of nonlinearity, for more than 2000 h at room temperature and for 100 h at 90 °C, clearly demonstrating the efficacy of double-ended polymerizable and

Scheme 7. NLO Polyamide Thermosets
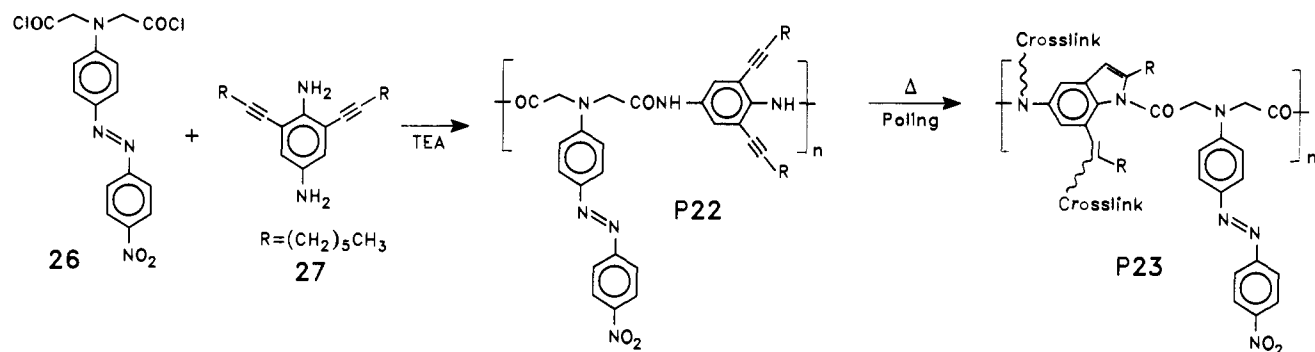
Scheme 8. NLO Polyetherimide Thermosets
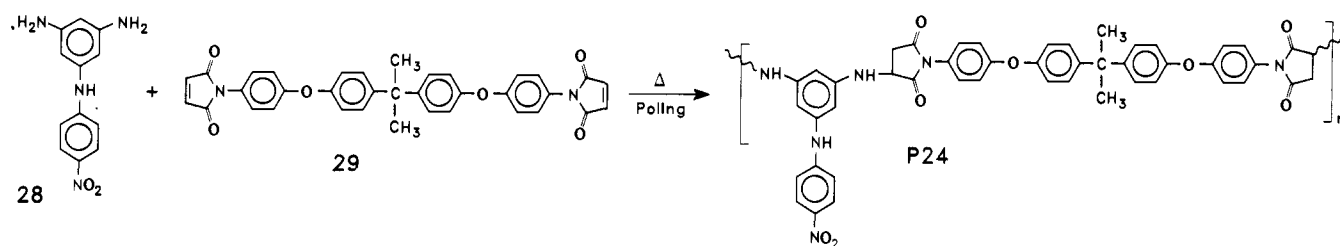
cross-linking functionality for stabilization of poled order. Likewise, Betterton et al.[252] have reported that norbornenyl 4-carboxylates with tethered methacrylate containing NLO functionality can be selectively polymerized using ring-opening metathesis polymerization (ROHP) techniques to produce macromonomers containing pendant methacrylate groups. No NLO or cross-linking studies on these materials were described in this preliminary report.
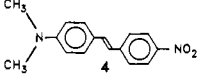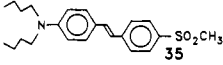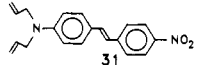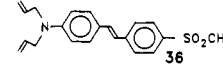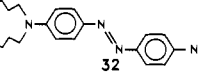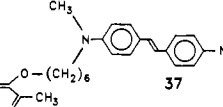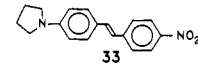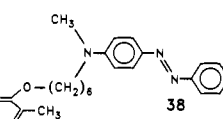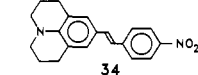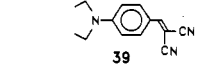
Most recently, the incorporation of bifunctional NLO chromophoric systems into polymers has been discussed by Francis et al.[253] In this case, a bifunctional NLO chromophore was first reacted with the polyfunctional isocyanate tris(hexamethylene isocyanate) isocyanurate to produce a urethane derivative by condensation of the pendant amino substituents of the chromophore. This prepolymer was converted to a network polymer while poling through subsequent reaction at higher temperatures of the predominately unreacted hydroxy functionality present in the chromophore. Unfortunately, some thermal degradation of the chromophore apparently occurs during processing. Even so, films with r_{33} = 3–4 pm/V at 1.3 μm were obtained. Although the nonlinearity of the film decayed by ~40% after 150 days at 100 °C, most of this loss was attributed to chromophore decomposition rather than decay in the polar order.

Recently Yu and co-workers[246,247] have reported the thermal and nonlinear properties of aromatic polyamides containing a bonded azo NLO chromophore 26 in the main chain. The synthetic sequence is shown in Scheme 7. The molecular weight of the soluble polymer P22 produced by standard condensation procedures ranged from 2000 to 10000 Da. The pendant acetylenic functionality provides the capacity for thermosetting upon thermal curing. The presence of two such groups per molecule assures the availability of reactive functionality for cross-linking even if intramolecular cyclization is efficient. Thermal analysis of the polymer P22 (DSC) suggests that the onset of reaction of the acetylene functionality begins around 180 °C and is essentially complete before polymer decomposition

begins around 270 °C. Poling of the polymer film P22 was conducted at 180–190 °C using a corona discharge. This is a temperature region where thermal cross-linking occurs simultaneously. A d_{33} value of 20 pm/V was measured at 1.064 μm. The thermal stability of the poled polymer was improved with the high-temperature processing, and P23 shows a decay of the second-harmonic signal of only 4% after 1000 h at 25 °C. The stability is maintained to some extent even at 125 °C, where a signal decay of 45% was observed after 50 h. The authors suggest that the polymer mobility manifested at elevated temperatures may result from the presence of the long hydrocarbon-like acetylenic tails, a feature amenable to synthetic modification. A possible caveat is that the polymer solubility which facilitates processing may also be a function of the presence of the hydrocarbon-like substituents.

Polyimide derivatives constitute an extremely important class of high-temperature polymers with many industrial applications.[254–256] They have been discussed as hosts in conventional guest–host systems in section VI.A. Marks and co-workers[248] have recently reported a very interesting study of a polyimide-type polymer containing a chemically bound NLO chromophore P24. This material was produced by the addition polymerization of the functionalized triamine 28 to the terminally functionalized bis-maleimide 29 as shown in Scheme 8. Films of the monomers were cast from solution and partially polymerized by heating in vacuo to produce prepolymers capable of supporting an applied electric poling field. Curing was continued by heating to temperatures as high as 240 °C, while corona poling. The glass transition temperatures of the cured samples of P24 tracked the curing temperature as expected. Glass transition temperatures as high as 236 °C were reported for fully cured samples. d_{33} values in the range of 4.6–5.5 pm/V were measured at 1.064 μm for the cured polymer films P24, which are consistent with a nitroaniline type chromophore and a calculated chromophore number density of $N \approx 7 \times 10^{20}$ cm^{-3}. The thermal stability of the poled samples was very impressive. Losses in the second-harmonic signal at 85

Table 5. NLO Chromophores Incorporated in Photopolymerized Polyacrylates

| NLO Chromophores	wt %[a] in host	NLO Chromophores	wt %[a] in host
(structure **4**)	1	(structure **35**)	4
(structure **31**)	23	(structure **36**)	14
(structure **32**)	5	(structure **37**)	5
(structure **33**)	1	(structure **38**)	7
(structure **34**)	9	(structure **39**)	3

[a] Solubility in the photosensitive cross-linking reagent, tris-(β-acrylatoethyl)-1,2,5-tribenzoate.

°C were low (10–15%) over 24 h and little change beyond this was observed over the next month. It is interesting that the temporal stability of the signal seemed little affected by the final cure temperature over the range from 150–240 °C, even though the glass transition temperature closely tracks the final curing temperature. Systems of this type look very promising for device applications provided the poled nonlinearity can be improved and that they can be processed into high-quality optical films.

2. Photochemical Cross-Linking

As discussed, the stability of the polar order in a NLO poled polymer film can often be markedly improved by cross-linking induced during the poling process. Until now, the cross-linking processes that we have discussed have been either thermal and/or reagent induced. These often require extended heating and poling at elevated temperatures, a procedure which is both inconvenient and sometimes leads to degradation of the NLO chromophore. More recently, it has been shown that vitrification in unsaturated systems can be photochemically induced during the poling process. In certain cases, photochemical cross-linking can greatly reduce the time that a sample is exposed to the potentially destructive conditions present during long corona poling at elevated temperatures.

The use of polyfunctional acrylates and methacrylates for photochemical cross-linking have been studied in detail by Robello and co-workers.[257] The first materials of this type were guest–host systems where appropriate NLO chromophores were simply incorporated by mixing and partially immobilized by polymerization of a polyfunctional matrix forming acrylate, such as 30. A number of chromophores studied in this process are shown in Table 5. The chromophores were either
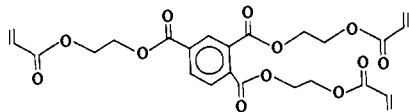
(structure **30**)

dissolved directly in a network-forming host such as 30 whenever soluble or alternatively a low-boiling solvent was utilized. Both transverse and longitudinal electrode-poling techniques were employed depending on the physical characteristics of the resist system. Polymerization was initiated using a variety of photochemical electron transfer sensitizer–activator combinations known to be effective for the vitrification of polyfunctional acrylates. Second-harmonic generation was observed in the photopolymerized guest–host systems poled during the curing process. The efficacy of such systems was often limited by the low solubility (Table 5) of the chromophores in the matrix-forming triacrylate 30. In addition to the problem of low chromophore densities leading to low macroscopic nonlinearities, another drawback of the incorporated guest–host systems is the possibility of chromophore loss during processing. Model thermal polymerization reactions using standard pendant acrylate-containing chromophores with acrylate or methacrylate comonomers (Table 5, 37 and 38) show that they are chemically incorporated suggesting similar behavior for copolymerization with polyfunctional matrix-forming acrylates. The model studies indicate this to be the case for NLO acrylates such as 37 and 38 but not for those systems containing allyl-substituted amino substituents such as 31 and 36, which are not readily copolymerized.

Finally, it was discovered that NLO chromophores containing more than one acrylate or methacrylate group (Table 6) can be photochemically homopolymerized to produce a rigid matrix. Unfortunately, the strong visible absorption of the NLO moieties causes a drastic decrease in the rate of polymerization. Even so, the monomer 40d could be polymerized without a sensitizer to produce hard films. Although the cross-linking was inefficient and reproducibility was a problem, a number of high optical quality films of 40d were prepared and a respectable $\chi^{(2)}$ value (1.4 pm/V) measured for the poled, cross-linked film. The second-harmonic signal was stable over a number of days at room temperature, but decayed over a period of months due to chromophore relaxation suggesting that the glass

Table 6. Photopolymerized NLO Diacrylates
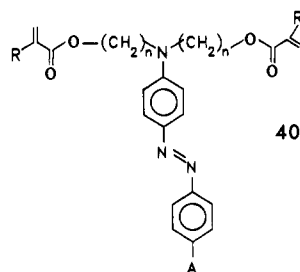
A	n	R
a: NO$_2$	2	CH$_3$
b: NO$_2$	6	CH$_3$
c: NO$_2$	6	H
d: SO$_2$CH$_3$	6	CH$_3$

transition temperature of the matrix was still quite low, perhaps only 20–40 °C greater than the poling temperature. Although the concept of simultaneous poling and photopolymerization of polyfunctional acrylates was demonstrated, the disappointing thermal stability of the polar order suggests the need for more vigorous polymerization conditions, perhaps the use of higher reaction temperatures. The severe shrinkage problems encountered in all acrylate-type addition polymerizations, particularly in polyacrylate matrices **30**, also suggests that the exacting waveguide fabrication necessary for device applications may be difficult with these systems.

An interesting variant of the polyfunctional acrylate photo-cross-linking concept is provided by the work of Hayashi et al.,[258] shown in Scheme 9. These workers showed that irradiation of the azido-containing polymethacrylate **P25** led to decomposition of the azide group and cross-linking occurs. Irradiation while corona poling at 60–70 °C led to a polymer with a d_{33} value of 3.6 pm/V (1.064 μm). The nonlinearity of the cross-linked and poled polymer was ~10 times that of the poled, but unirradiated starting polymer and the T_g increased by 24 °C as well. Since the irradiation of **P25** apparently leads to the reactive nitrene (**P26**), the authors suggest that the cross-linking involves carbon–hydrogen insertion and/or azo formation. In either case, the nonlinearity of the transformed chromophore would be expected to exceed that of the original azidobenzoate, a hypothesis supported by the increased nonlinearity of the cross-linked polymer film. Although photochemical reactions certainly occur during the irradiation, the large solvent swelling ratios of the irradiated film suggests that it is only lightly cross-linked and the immobilization is inadequate to seriously restrict side-chain motion. Consistently, decay in the measured second-harmonic signal at room temperature approached ~50% after only 100 h at room temperature.

A final example of a potentially photo-cross-linkable acrylate containing NLO polymer is provided by Dalton and co-workers,[251] who have reported the synthesis of the nonlinear chromophore **41** with differentiated functionality at each end of the monomer (Scheme 10). Free-radical polymerization of the methacrylate functionality produces a poly(methacrylate) polymer with two potentially chemically reactive hydroxyethyl side chains capable of subsequent condensation polymerization. Alternatively, initial condensation polymerization with appropriate bifunctional reagents such as terephthaloyl chloride or diisocyanates produces a

polymer with pendant methacrylate-containing side chains that could subsequently be thermally or photo-cross-linked to produce orientational stability (**P30**). The macromonomer **P30** prepared by the condensation of **41** with terephthaloyl chloride **42** is soluble in common organic solvents. $\chi^{(2)}$ values of 60 pm/V have been measured for corona-poled but un-cross-linked samples of **P30**. Unfortunately, no photo-cross-linking studies on poled samples of **P30** have been reported (thermal cross-linking is observed), although the large microscopic nonlinearity and the potential for further immobilization upon photo-cross-linking are intriguing. Presumably the short wavelength initiation of the macromonomer would be complicated by competitive light absorption by the NLO moiety itself.[257]

Acrylate and methacrylate derivatives are certainly not the only photosensitive functionality capable of cross-linking polymer chains. In fact, a very large number of photoreactive polymers are known to the photoimaging industry.[259] Some of the oldest and most thoroughly investigated examples involve the photodimerization of side- and main-chain polymeric cinnamate derivatives. A particularly well-studied example is that of poly(vinyl cinnamate) (PVCM, **P32**) shown in Scheme 11. Irradiation causes cross-linking, proposed to occur via 2 + 2 cycloaddition of the reactive functionality, and various photosensitizers have been employed to extend the effective spectral range. A number of promising schemes for the production of thermally stable NLO polymers based on this type of photochemistry have been reported recently. These have been utilized for guest–host arrays, side-chain tethers, and main-chain unsaturation.

The simplest scheme involving photosensitive-substituted cinnamate polymers is one of guest–host incorporation, where photochemical cross-linking produces a vitrified host that hinders the mobility of incorporated guests. Such a concept was discussed earlier for the thermally cross-linked epoxy resins. Accordingly, Matsuda et al.[260] have dissolved a variety of NLO chromophores (e.g., p-nitroaniline (PNA **1**), 2-amino-7-nitrofluorene (ANF), and DR1 **3** in solutions of poly(vinyl cinnamate) (PVCN, **P32**; $T_g \approx 73$ °C) or poly(4-vinylphenyl cinnamate) (PVPC, $T_g \approx 128$ °C) and prepared films by spin coating. Although films containing up to 15 wt % of the chromophores in PVCN could be prepared, photobleaching of the PNA and ANF containing chromophores during irradiation was severe. DR1 was also photodecomposed, but less so and was employed in further experiments. The T_g of the 15 wt % system was low initially (≈32 °C) but a glass transition was undetectable by DSC analysis after photo-cross-linking. A 10 wt % sample was poled and irradiated until ~80% of the pendant unsaturation was converted. Over the period of irradiation, a loss of ~35% in the absorbance of the nonlinear chromophore was observed in the irradiated but unpoled sample. Use of a UV cutoff filter reduced the absorption loss for the chromophore to less than 10%. Maker fringe measurements (1.064 μm) yielded a resonance enhanced d_{33} value of 28 pm/V for those samples which were poled and cross-linked simultaneously at 100 °C if the poling field was maintained briefly at 140 °C after irradiation. For these samples, the second harmonic signal decay over three months at 25 °C was ~70%, a considerable improvement over guest–host arrays in low T_g poled

Scheme 9. Photo-Cross-Linking in Linear Polymethacrylates
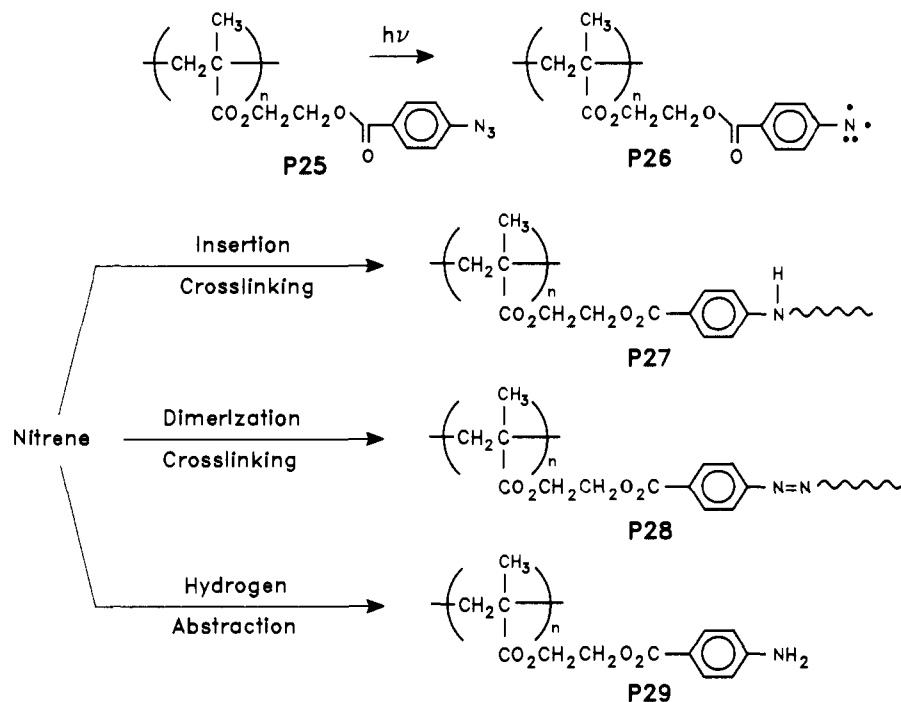
Scheme 10. Photopolymerizable Acrylates Tethered to Condensation Polymers
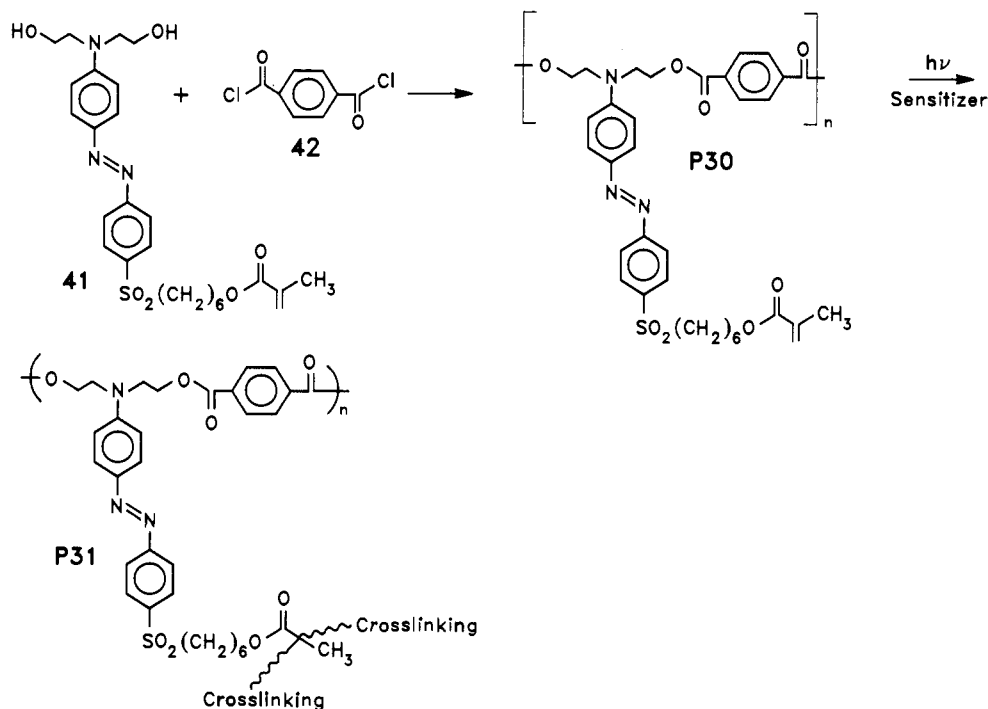

but un-cross-linked systems. The thermal stability of this photo-cross-linked system appears somewhat lower than the thermally cross-linked guest–host epoxies described earlier. Use of visible light for cross-linking only improved the measured d_{33} value by $\sim 15\%$, but had little effect on the temporal stability of the sample. Once again, cross-linking reactions, this time initiated photochemically, have been demonstrated to substantially increase temporal stability, but in this guest–host array there are problems with homogeneity at high chromophore loading levels, plasticization by the guest, and photodecomposition of the NLO chromophore.

Tripathy and co-workers[261–265] have also described a guest–host photo-cross-linking system composed of the polymer PVCN **P32**, this time doped with the NLO chromophore **43** (Scheme 11). The potentially reactive bifunctionality of the NLO chromophore assures restricted chromophore mobility, if the cross-linking reaction can be driven to completion. In this guest–host assembly, chromophore loading levels of up to 20 wt % can apparently be achieved without detectable phase separation. Films are spin coated from organic solvents and dried at 60 °C under vacuum to remove the casting solvent. As expected for a guest–host assembly, the T_g of the dried polymer film is relatively low (80–84 °C) and depends on the chromophore loading level. In this case, the plasticization effect of the chromophore is astonishingly small, as the T_g of the

Scheme 11. Photo-Cross-Linking Hosts and Guests

R=H, COCH=CHPh, COCH=CH-CH=CH-Ph
43a   43b   43c
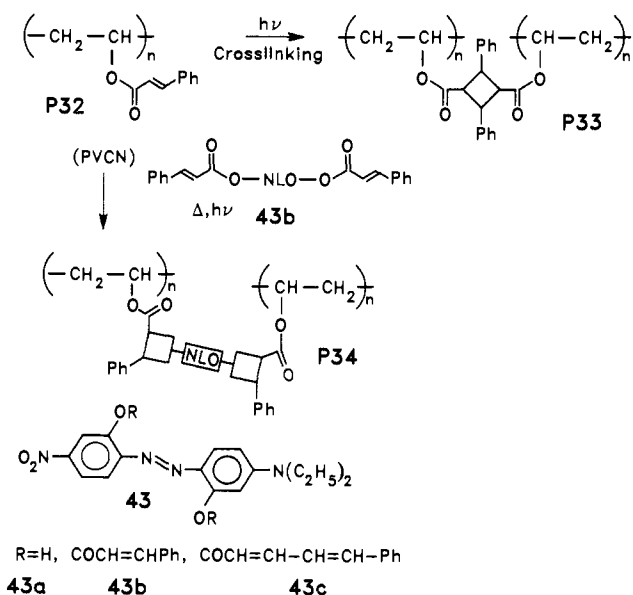
pure polymer is 88 °C. Spectroscopic studies indicate that this system is easily corona poled at 70 °C and cross-linking is initiated by a few minutes of intense deep UV irradiation (254 nm) while poling. From spectral absorption studies, an order parameter of 0.24 was calculated for the material containing 20 wt % of the chromophore. The use of β-styrylacrylate groups (43c) in place of cinnamates permits cross-linking at longer irradiation wavelengths (366 nm). Irradiation at 254 nm causes only minor increases in the T_g of the system at moderate absorbed doses, although some cross-linking certainly occurs as evidenced by the changes in the solubility characteristics of the films. At higher doses, a glass transition is not detectable by classical DSC thermal analysis techniques. The results of this photochemical cross-linking are, however, manifested by changes in the specific heat capacities measured at the original T_g. This quantity falls monotonically with absorbed dose, reaching zero upon formation of a vitrified intractable matrix, a state which is achieved after relatively short irradiation times (3–12 min) for the guest–host systems studied. The efficiency of the photo-cross-linking is remarkable considering the relatively high chromophore levels present that contribute significantly to the optical absorbance at 254 nm. Not surprisingly, measurements on the poled, cross-linked films **P34** show respectable nonlinearities (d_{33} = 11.5–21.5 pm/V, at 1.54 μm). As expected, the nonlinearities increase with the loading level of the chromophore and the higher values reported above correspond to a loading level of 20 wt %. Absorption measurements suggest substantial poled-order stability for the cross-linked system and the optical absorbance at the λ_{max} remains unchanged for many months at room temperature, unlike the poled but un-cross-linked films. The thermal stability of the poled polymer films is significantly improved upon photo-cross-linking as predicted by the absorption measurements. No significant decay in the second harmonic signal at 65 °C was observed over several hours. Comparable studies on the poled but un-cross-linked polymers resulted in ~25% decay in the second harmonic signal over the same time period. Similar results were observed at temperatures as high as 85 °C. Surprisingly, no decomposition of the azo chro-

mophore was reported for *short* irradiation periods, although some decomposition occurs for longer irradiations.

In an effort to overcome the problems characteristic of many guest–host systems, i.e., limited solubility of the highly polar guest in the polymer host and loss of some chromophore upon processing, Müller and co-workers[266] have prepared terpolymers containing both the cinnamoyl cross-linking functionality and the NLO chromophore incorporated as side-chain tethers (Scheme 12). The substituents are appended by reaction of appropriate hydroxy-terminated functionalities with a 50/50 copolymer of methyl methacrylate and methacryloyl chloride (**P35**). The composition of the resulting terpolymer **P36** is controlled by the stoichiometry of the reagents. A terpolymer containing ~19 mol % of the azo chromophore 44 and 14 mol % of cinnamoyl groups 45 was prepared in this fashion and forms good optical quality films. This polymer also contains cyclic anhydride units apparently formed spontaneously under the coupling reaction conditions employed. The polymer could be poled near its glass transition temperature (~125 °C) and photo-cross-linked by simultaneous deep UV radiation. The progress of the cross-linking reaction, which plateaus at ~50% conversion, was followed by IR spectroscopy. The photoreaction is apparently much slower with the NLO chromophore present and requires irradiation for hundreds of minutes at 125 °C to reach maximum cross-linking. The long irradiation times also lead to some degradation of the chromophore. Fortunately, the films become insoluble after shorter irradiation periods where little of the chromophore is decomposed. Preliminary NLO measurements showed an r_{eff} = 7 pm/V (1.15 μm) in a poled and cross-linked sample. (r_{eff} is defined as a combination of r_{ij}'s similar to the definition of d_{eff} in eq 43.) No long-term thermal stability studies of the nonlinearity have been reported, although it seems likely that this will also be significantly improved in the cross-linked system. The decomposition of the chromophore that occurs with extended irradiation is unfortunate, since the higher cross-linking densities achievable at longer irradiation periods should substantially improve the thermal stability of the poled film.

There have been several recent reports of photo-cross-linkable polymeric systems containing either the nonlinear chromophore or the photoreactive moiety incorporated into the polymer main chain. The former is illustrated by the work of the group of Tripathy et al.[267,268] on nonlinear epoxies containing pendant cinnamoyl groups (Scheme 13). The linear epoxy polymers **P37** and **P38** are prepared by the thermal ring-opening polymerization of bisphenol A diglycidyl diether (18) initiated by p-nitroaniline (1). The pendant hydroxy functionality created in the ring opening polymerization is esterified with either cinnamoyl chloride or β-styrylacryloyl chloride to produce a photosensitive resin (**P38a,b**). In the linear polymers, the concentration of the NLO moiety is diluted by the inactive epoxy moiety. Higher concentrations of the NLO chromophore can be prepared from bis-epoxides such as 46 where both the epoxy reagent and the polymerization initiator contain NLO chromophores. In this case, the thermal polymerization is terminated to produce a prepolymer before insolubility occurs and the pendant hydroxy

Scheme 12. Photo-Cross-Linking Host–Tethered NLO Chromophore

Scheme 13. Photo-Cross-Linked NLO Epoxy Resins

a.

P38a R = C$_6$H$_5$CH=CH–
P38b R = C$_6$H$_5$CH=CH–CH=CH–

b.

P39a R = C$_6$H$_5$CH=CH–
P39b R = C$_6$H$_5$CH=CH–CH=CH–

groups are esterified as before with either cinnamoyl chloride or β-styrylacryloyl chloride. Both the linear (P38a,b) and branched polymers (39a,b) are reported to be soluble in common organic solvents. The T_g values for the four polymers studied ranged from 78 to 88 °C. The polymers were spin coated from solution and corona poled within 5 degrees of the measured polymer glass transition temperatures. Cross-linking was initiated by concurrent irradiation for 10 min or less at either 254 or 366 nm depending on the pendant cross-linker. The d_{33} values of the un-cross-linked polymers were

3.2, 5.0, 7.0, and 8.8 pm/V for the polymers 38a,b and 39a,b respectively. The respective r_{33} values were 2.4, 4.8, 2.9, and 5.0 pm/V. The d_{33} values were measured at 1.064 μm and the r_{33} values at 633 nm and both are probably resonance enhanced. As expected, the non-linearity of the branched systems is significantly larger due to the higher NLO chromophore density in the polymer. Preliminary thermal stability studies on the linear but photothermally cross-linked polymer P38a also show substantial improvements relative to the un-cross-linked system. While the former showed no decay in the second harmonic signal over 25 h at room temperature, that of the un-cross-linked material decayed by ~50% relative to the initial values over the same period. Thermal stability measurements at elevated temperatures were not described. Similarly, no stability studies were reported for the more nonlinear branched polymer.

Finally, the preparation of a number of linear polymers (P40–P42) containing photoreactive functionality in the main chain of a linear polymer and NLO active groups as pendant substituents has been reported.[269] The polymers are all prepared from the same reactively functionalized NLO chromophore DR19 25 as shown below in Scheme 14. The glass transition temperatures of the polymers before cross-linking vary from 92 to 122 °C. As expected, polymer P40 containing a flexible aliphatic spacer had the lowest T_g. Each of the polymers is cross-linked upon exposure to a mercury light source as determined by solvent solubility studies. Unfortunately, concurrent with the cross-linking, significant spectral bleaching of the chromophore also occurs upon irradiation, possibly due in part to trans-cis isomerization of the azo chromophore. Only a portion of the original absorbance could be recovered upon thermal annealing of the irradiated samples. Nonlinear optical measurements on the poled-polymer films at 1.064 μm yielded d_{33} values ranging from 5–13 pm/V, values that are strongly resonance enhanced. Studies on the temporal stability of the induced polar order in the un-cross-linked systems showed that polymer P40 with the flexible spacer was the least stable and a 60% decay in the second harmonic signal was observed after ~200 h at room temperature. Under similar conditions, the decay in signal for the other polymers was only 10–20%. The thermal stability of the nonlinearity of the cross-linked polymers was not described, suggesting that chromophore bleaching during the photo-cross linking is a serious problem. Perhaps reduced irradiation times or a filtered long

Scheme 14. Main-Chain Cross-Linking NLO Condensation Polymers

wavelength source would result in acceptable nonlinearities where the thermal stabilities are improved by partial cross-linking, although the cross-linking efficiency for the main-chain photoreactive chromophores is apparently less than for those systems with pendant functionality.

In summary, it appears that NLO polymers containing photoreactive functionality both pendant and main chain incorporated can be successfully poled and photochemically cross-linked. For the most reactive systems, photochemical cross-linking occurs without significant destruction of the NLO chromophore. In a number of cases, the photoinduced vitrification leads to significant improvements in poled-order stability at room temperature and slightly above. These preliminary results suggest that by judicious selection of photoreactive chromophores, perhaps coupled with the employment of appropriate photosensitizers and the use of higher T_g polymers and elevated reaction temperatures, improved stability of the NLO properties at temperatures above 100 °C may be attainable. Photochemical cross-linking potentially offers certain processing advantages, such as photopatterning while poling, providing that the irradiation does not adversely affect the properties of the film (e.g., excessive shrinkage and loss of dimensional stability, photobleaching of NLO chromophores, embrittlement, etc.).

E. Other Systems

1. Sol–Gel Glasses

Inorganic glasses composed of oxides of boron, aluminum, silicon, titanium, zirconium, vanadium, etc.

Scheme 15. Sol–Gel Process
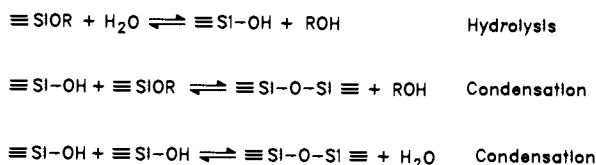
are rigid, amorphous, three-dimensional structures often with excellent optical clarity.[270,271] As such, they should represent excellent host materials for the incorporation of various organic NLO chromophores. Unfortunately, the processing temperatures of most preformed inorganic glasses exceed the decomposition temperatures of common organic NLO chromophores.

Fortunately, clear inorganic and modified inorganic-organic glasses can often be prepared in situ by low-temperature polymerization of appropriate monomers in a sol–gel process.[272-274] This technique, shown simplistically in Scheme 15 for a silicon-containing glass, uses hydrolytically labile derivatives where the metal is substituted with halogen, acetate, nitrate, or alkoxy substituents (preferably the latter). Initial hydrolysis produces reactive, hydroxy-substituted monomers that subsequently produce linear and cross-linked oligomers and polymers by a variety of condensation reactions depicted in Scheme 15. The initial monomers and oligomers are often soluble in the reaction media and can be processed into film form. Further condensation produces a gel structure that ultimately densifies at longer reaction times and/or at elevated temperatures. The final product is a rigid and often optically clear glass matrix. The optical and mechanical properties of the matrix depend variously on the monomer

Sol–Gel Incorporated NLO Chromophores
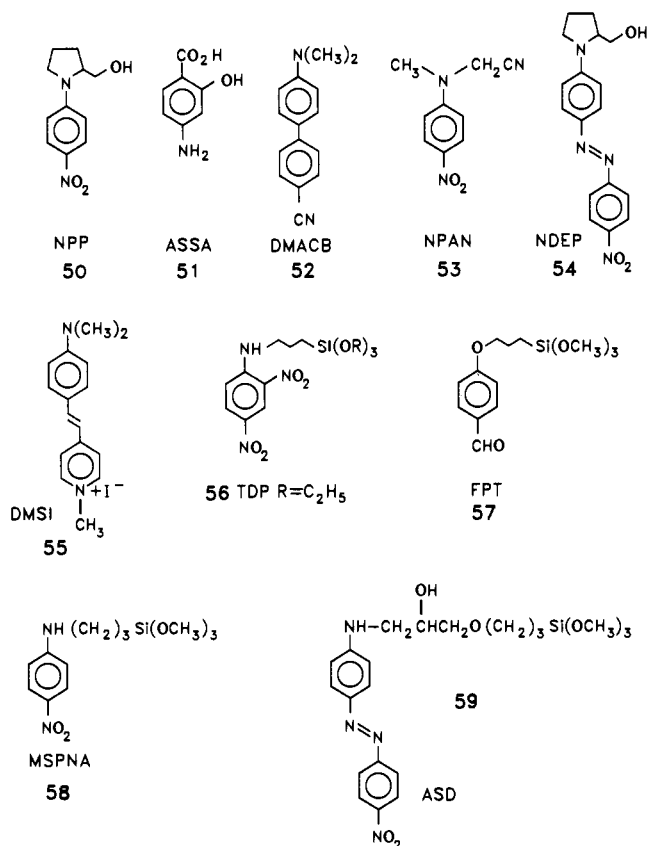
Figure 30. Examples of chromophores which have been incorporated into inorganic glasses using the sol–gel method.

structure, solvent, reagent stoichiometry, reaction conditions, etc. Catalysts are usually added to facilitate hydrolysis prior to condensation polymerization and cross-linking.[275,276] For this purpose, acids are often employed, although ionic residues are troublesome, particularly for electric field poling applications, and may also react with many common NLO chromophores which often contain basic electron donor groups. It has been reported that bases such as ammonia,[277] methylamine,[277] p-(dimethylamino)pyridine (DMAP),[278] etc. are also effective catalysts for the sol–gel process. The sol–gel polymerization process proceeds via a complex series of equilibrium reactions. The glasses produced by subsequent densification are often brittle and prone to cracking due to volume contraction and the expulsion of volatile condensation products. This problem is exacerbated when the films are generated on substrates. A wide variety of solvents and additives including surfactants have been employed in an effort to minimize this problem. Haruvy and Webber[277] have recently studied the sol–gel process in some detail as a function of monomer structure, solvent, temperature, reagent stoichiometry, etc. and have developed a relatively simple procedure for the preparation of crack-free, optically clear films containing a variety of organic chromophores without additives or surfactants. The spectral properties (both absorption and emission) of the glass-incorporated chromophores were typical of the monomeric species.

A number of NLO chromophores (e.g., PNA **1**, MNA **9**, DR1 **3**, DO3 **5**, and others shown in Figure 30) have been incorporated into a variety of inorganic glasses

via the sol–gel technique. These materials may be classified either as network modifying (**1, 3, 5, 9, 50–55**) or network incorporated (**56–59**), depending on the functionality. The former is functionally equivalent to a polymer guest–host system, while the latter more closely resembles a side-chain-tethered (albeit in a cross-linked matrix) polymer system. The guest–host systems often suffer from lower achievable chromophore densities and phase separation at high concentrations leading to poor quality optical films. Even so, guest–host systems have been considered for NLO applications with some success (vide infra).

In an early study of guest–host SiO_2 films produced by the sol–gel process, Nakamura et al.[279] demonstrated that the ionic chromophore 4'-(dimethylamino)-N-methyl-4-stilbazolium iodide (**55**) could be incorporated into optically clear SiO_2 films. The spectral characteristics of these films suggested that the structure of the chromophore in the matrix film depended on processing conditions such as temperature, solvent, and pH. $\chi^{(3)}$ of (4–5) × 10^{-14} esu were measured for films by third-harmonic generation containing this chromophore. No poling experiments were reported, presumably due to the ionic nature of the chromophore.

The use of sol–gel NLO systems for second-order applications requires electric field poling to destroy the isotropic molecular symmetry of the chromophore ensemble. The molecular environment at various stages in the sol–gel process has been studied by Zyss and co-workers[278] using EFISH techniques. This procedure, normally used to determine the quadratic molecular polarizabilities of NLO chromophores in isotropic solution, has also been applied to chromophore–sol-gel systems at various stages in the curing process. As a pulsed dc electric field ($\sim 1~\mu s$) is employed to orient the chromophores, the nonlinearity, as measured by second-harmonic generation, is a sensitive probe of the chromophore mobility and poling environment. Zyss et al. have determined the hyperpolarizabilities β of a variety of common NLO chromophores in a silicon-zirconium oxide composite sol–gel system using the EFISH technique. Early in the sol–gel process, the values of the molecular hyperpolarizabilities of incorporated chromophores were quite similar to those measured in solution. This is true even at the gel point t_{gel}, where the samples no longer exhibit macroscopic flow characteristics. At this stage, the mobility of the chromophores permits rapid reorientation and the poling environment is still predominately liquidlike. Beyond the gel point, the SHG macroscopic susceptibility decreases only slightly and remains $\sim 80\%$ of the initial value even far beyond $t > 30{-}40 t_{gel}$. Further curing, however, particularly at elevated temperatures, severely restricts the mobility of the guest molecule.

The onset of the decrease in the SHG macroscopic susceptibility when the chromophore is actually chemically incorporated into the polymerizing media (e.g., **56**) occurs much earlier than for guest–host systems, thus providing a more sensitive probe of the microscopic environment in the sol–gel process. Bound NLO chromophores are also less sensitive to the phase-separation problems that often plague guest–host systems. $\chi^{(2)}$ measurements on thermally cured and poled films containing the bound chromophore **56** showed a value of 0.02 pm/V measured at 1.06 μm 1 month after poling, indicating significant stabilization

of the induced polar order. Initial values of $\chi^{(2)}$ in this system ranged from 0.7–3.2 pm/V.

Prasad and co-workers[280] have studied the NLO properties of SiO_2–TiO_2 composite glass films, prepared by the sol–gel technique, containing up to 15 wt % of the nonlinear guest chromophore **50**. Either corona or electrode poling was used, although the former appeared more efficient. For electrode poling, the second-order macroscopic hyperpolarizability varied linearly with the poling field for electric fields less than 2 MV/cm, as predicted by theory. Using corona poling, a $\chi^{(2)}$ value of 11 pm/V at 1.06 μm was measured for the dried film immediately after poling, although the nonlinearity decayed rapidly over a few hours. In an electrooptic modulation experiment using the heat-treated films, a value of $\chi^{(2)}_{333}(-\omega;\omega,0) = 2$ pm/V was measured at 632.8 nm and a modulation frequency of 1.59 kHz (100 V peak-to-peak). In a related study, Zyss and co-workers[281] have reported a $\chi^{(2)}$ value of ~0.16 pm/V for this chromophore poled in a composite silica–zirconia sol–gel glass, although their chromophore concentration was limited to 4 wt % due to phase-separation problems. Significant improvements in thermal stability were obtained by heating the film with the poling field on to accelerate the densification of the matrix. Under these conditions, ~80% of the initial second harmonic intensity was maintained after 3 h at room temperature.

Nonlinear dyes have also been incorporated into polyceram hosts prepared by sol–gel processes. For example, both MNA **9** and PNA **1** have been incorporated into polycerams prepared by the hydrolysis of the comonomers tetraethoxysilane and (trimethyoxysilyl)propyl-substituted poly(ethylene imine).[282] The cured films prepared by spin casting showed second harmonic generation *without* poling, showing that the environment of the NLO chromophores was noncentrosymmetric in the films. In the case of MNA, the second-harmonic signal increased with MNA concentration. Optical birefringence studies showed that NLO chromophores were noncrystalline in the films and suggested that the polar order was induced by the presence of the matrix incorporated poly(ethylene imine). It is possible, of course, that microcrystalline domains were formed which were too small for detection by optical techniques, although the authors suggest that the materials form optically transparent, X-ray amorphous films. It should also be noted that films containing PNA also produce a second-harmonic signal even though PNA tends normally to crystallize in a centrosymmetric form. Films containing MNA heated to 150 °C (above the melting point of MNA) also still showed significant SHG upon cooling in spite of chromophore losses due to volatilization.

Nonlinear chromophores have also been incorporated into glass–organic polymer composites prepared by sol–gel techniques. Gel-derived SiO_2 glass–PMMA composites containing the NLO chromophore MNA[283] produced by polymerization of methyl methacrylate–MNA in a porous glass have been prepared and electrooptical dc Kerr measurements performed. In another related guest–host study, composite SiO_2–TiO_2 films prepared by sol–gel techniques containing a variety of poly(p-phenylene vinylene) polymers have been doped with PNA.[284] Corona poling at 120 °C led to orientation of the NLO chromophore and a d_{33} value of 11 pm/V at 1.06 μm was measured at room temper-

ature. Similarly, electrooptic modulation studies yielded a value of $\chi^{(2)}(-\omega;\omega,0) = 2$ pm/V at 1.6 kHz. No studies of the temporal stability of the polar order were reported. The presence of the organic polymer in the composite was necessary to prevent the loss of the PNA due to sublimation during the sol–gel processing.

Although most guest–host studies on glasses produced by the sol–gel technique have been on SiO_2, TiO_2, SiO_2–TiO_2, or SiO_2–ZrO_2 composites, Kobayashi et al.[285] have reported the preparation of optically transparent Al_2O_3 glasses doped with the NLO chromophore MNA. Since these glasses were prepared from aqueous solution, a surfactant, cetyltrimethylammonium bromide (CTAB), was employed. The films were corona poled and heated slowly to 110 °C. Higher temperatures produced MNA crystallites readily detected by X-ray analysis. The authors suggest that very small microcrystals of MNA are present even in the films poled and cured at 110 °C although the optical characteristics were acceptable. The stability of the poled order in the cured alumina films exceeds that of many guest–host organic polymer systems and 80% of the original second harmonic intensity remains after 5 days at room temperature. The effect of residual surfactant on the polar order stability in unknown.

Some of the processing problems associated with in situ sol–gel processing can be reduced by employing already partially polymerized, soluble prepolymer precursors known as spin-on-glasses (SOG). Jeng et al.[89] have studied a guest–host system composed of the NLO chromophore DR1 **3** doped into a commercial prepolymer Accuglas 204 (A204) available from Allied Signal. The prepolymer composition is shown:

$$[(SiO)_a(C_6H_5)_b(OC_2H_5)_c(OH)_d]_n$$

$$a \geq 1 \quad b{-}d \leq 0.5 \quad n = 5{-}100$$
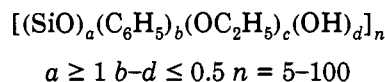
This material vitrifies upon heating by condensation losing the elements of volatile alcohol and water. The sample films doped with DR1 were spin coated and corona poled at 80 °C before heating to 220 °C in the poling field to accelerate the vitrification. A substantial quantity of dye is lost during the processing due to sublimation. This problem is endemic to many guest–host systems. Values for $d_{33} = 1.54$ pm/V (1.064 μm) and the electrooptic coefficient $r_{33} = 0.7$ pm/V (633 nm) have been measured for the thermally cured systems. Both values are significantly resonance enhanced. Significant improvements in the stability of the polar order are achieved during the densification process. For example, the authors report only a 4.7% decrease in the second-harmonic intensity at 100 °C after 1 h. Presumably the stability could be further increased with increasing processing temperatures, currently limited by the sublimation and decomposition of the NLO chromophore.

Sublimation of the chromophore during processing can be eliminated by tethering the chromophore to a matrix forming monomer. For sol–gel-type processes this involves the use of a matrix incorporated nonlinear chromophore. Jeng et al.[286] have reported the incorporation of such an NLO chromophore **59** into the Accuglas 204 spin-on-glass discussed above. Such matrix-incorporated systems also alleviate the phase separation problems often encountered in guest–host systems, particularly at high chromophore loading levels. Clear films containing the chromophore were

poled and vitrified at 200 °C. Again the temperature maximum is dictated by the thermal stability of the azo chromophore. A modest d_{33} value of 5.28 pm/V was measured for the poled and cured system at 1.064 μm. The thermal stability of the matrix incorporated system is greater than the DR1 3 guest–host ensemble, although the initial nonlinearity of the former is lower (5.28 vs 11.43 pm/V). After 40 h at 100 °C the matrix incorporated material shows a decay in the d_{33} value of 45% while the value for the guest–host system is 67%. The authors conclude that the use of matrix incorporated hosts in glass matrices offers substantial advantages.

Other matrix-incorporated monomers have been employed in sol–gel polymerizations.[278,281,282,287,288] For example, Plawsky and co-workers[287] have prepared films containing the nonlinear chromophores **56** and **57** by copolymerization with tetraethoxysilane and tetramethoxysilane. The thermal properties of the cured but unpoled films largely reflect those of the nonlinear chromophores. In this regard, **56** is somewhat more stable than **57**. The films were cured and corona poled at 120 °C. They were homogeneous on a molecular scale and showed respectable nonlinearities (TDP **56**-based films, d_{33} = 9.1–11.7 pm/V; FPT **57**-based films d_{33} = 0.8–1.3 pm/V at 1.06 μm). The thermal stability of the poled order was not reported, although spectral absorption studies suggested little reorientation of the nonlinear chromophore after 168 h at room temperature. Similarly, Claude et al.[288] have incorporated the chromophore N-[(3-(trimethoxysilyl)propyl]-4'-nitroaniline (**58**) into a sol–gel matrix prepared by the hydrolysis of trimethoxysilane in dimethylacetamide. The films were heated slowly as high as 220 °C while corona poling. Measurements of the nonlinearity in the processed films at 1.064 μm yielded d_{33} = 13 pm/V. The NLO–sol–gel film was thermally stable after processing to around 300 °C as measured by TGA, indicating that the NLO chromophore had been incorporated into the three-dimensional matrix. No measurements of the temporal stability in the oriented films were reported.

Optically clear composite films containing nanoclusters of SiO$_2$ and TiO$_2$ in a polyimide host have been prepared by curing polyamic acid precursors in the presence of orthosilicate and orthotitanate esters.[289] This technique has recently been applied to the preparation of nonlinear chromophore-containing polyimide–ceramic composites. Tripathy et al.[290] have found that such systems can be prepared by curing polyamic acid prepolymers in the presence of functionalized trimethoxysilanes (see Scheme 16). A polymer solution composed of the polyamic acid **P43** (Skybond 705, Monsanto Chemical Co.) and the NLO chromophore **59** was coated on a substrate and dried. Corona poling was conducted while curing the film slowly from 80 to 220 °C. Over this range, dehydration of the polyamic acid to the polyimide occurs concurrently with glass formation from the silicon-containing chromophore to create a semi-interpenetrating modified polyimide–silica network. The poled and cured film had a d_{33} value of 13.7 pm/V. The orientational stability of this system was impressive. A 27% reduction in the second harmonic signal was observed after 168 h at 120 °C, with most of the loss occurring early in the measurement. At room temperature, no signal loss was observed over the same period. Since the

Scheme 16. NLO Polyimide–Glass Composites (PIGC)
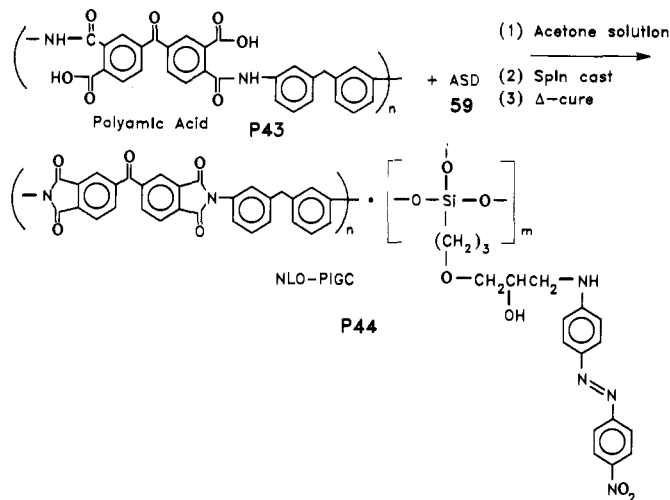
densification of the composite film is surely incomplete upon curing to 220 °C, improvements would be expected at higher curing temperatures. In this system, the maximum curing temperature is again limited by the thermal stability of the nonlinear chromophore ($\approx$240 °C).

2. Organic Glasses

A number of second-order nonlinear chromophores form molecular glasses when cooled appropriately. It has been demonstrated that thin glassy films of these low molecular weight organic molecules can be poled.[44] This approach has a potential advantage over a conventional guest–host polymer system because of the inherently high chromophore density. In effect the chromophore plays the roles of both guest and host. The organic compounds (S)-2-N-α-(methylbenzylamino)-5-nitropyridine (MBANP) and 2-N-(cyclooctylamino)-5-nitropyridine (COANP) form glasses relatively easily, have large ground state dipole moments and relatively large molecular hyperpolarizabilities. The T_g's of these glasses are low, however, 0 and –10 °C, respectively. Films of these glasses were poled between transparent electrodes and poling and relaxation dynamics measured in the region near T_g. Complete relaxation of poled order was observed to occur rapidly above T_g and with increasing rate as the melting temperature T_m of the glasses was approached. Upon cooling the glasses to 10 °C below T_g the poled order was observed to be stable for 17 h. A maximum d_{33} = 2 pm/V was obtained for the MBANP glass, whereas d_{33} = 7.5 pm/V was achieved for COANP at 1.06 μm.

VII. Future Directions

This review has discussed second-order nonlinear polymers and glasses in two contexts, as materials in which to study slow orientational relaxations processes and as practical systems for frequency doubling and electrooptic devices. In both areas much interesting work remains to be done.

In order to study orientational relaxation in poled polymers, it is important to make certain that the observed poled-order decay is in fact due to thermally induced reorientation and not to changes in the internal electric field distribution as a result of the motion of trapped charges left in the highly insulating polymer after poling. Surface charge can at least partially be

removed by wiping the surface of the polymer after poling is completed with the consequent loss of early time decay information; however, there still may be charges imbedded in the material. Perhaps other methods of removing the trapped charges can be identified that will provide access to the entire time range after the removal of the poling electric field.

It is surprising that no clear evidence for chromophore–chromophore cooperative effects has been found in polymers where the chromophore density may exceed 30 wt %. An interesting study would be to compare the results from photobleaching recovery experiments[117,118] with poled-order relaxation results. The photobleaching experiments are done at very low concentrations. Differences in the experimental results might be due to cooperative effects or to the fact that the photobleaching decay measures the decay of $\langle P_2 \rangle$, whereas the poled-order decay measures $\langle P_1 \rangle$.

The observation that the poled-order relaxation time for a large number of guest–host systems obeys eqs 61 and 62 remains unexplained. Further experiments need to address why T_g is the dominant parameter determining the relaxation time, why the nature of the chromophore or the polymer host does not play a more dominant role, and in particular, how universal the relationship expressed by these equations is.

The use of second-order nonlinear polymers in devices still awaits solutions to a number of key problems. For frequency-doubling applications, absorption of the second harmonic at about 400 nm remains a critical problem. Given the connection between chromophores with large β's and short wavelength absorption, the solution to this problem may require moving away from the traditional donor–acceptor-type chromophores to other, as yet unidentified, molecules. Another approach would be to investigate the origins of the absorption line broadening in donor–acceptor chromophores in the polymer environment. Armed with this information, one might attempt to design chromophores with narrower absorption bands.

Poled-polymer systems have been identified with large enough r coefficients to be practical in electrooptic devices. What is needed now is to identify systems that simultaneously possess high nonlinearity and an array of other properties necessary in a practical device. Key among these is thermal stability, both long term (5 years at ~ 80 °C) and short term (minutes at > 250 °C). Equations 61 and 62 are helpful in this regard and can be used to estimate the polymer T_g required for thermal stability. For example, if one wants a device that will lose no more than 10% of its initial nonlinearity after processing for 10 min at 250 °C, one requires a polymer with a T_g of ~ 300 °C. This is also the range of T_g required for long-term operational stability at 85 °C. Focus should shift away from identification of poled polymer systems with large r coefficients, regardless of glass transition temperature, to simultaneous optimization of poled-order stability and electrooptic coefficient—a much more difficult task.

It is clear that much progress has been made in the 10 years since the first identification of second-order poled-polymer systems. Work on understanding the mechanisms responsible for orientational relaxation and on identification of systems with large d and r coefficients has been impressive. However, it is also clear that more work remains to be done.

References

(1) Meredith, G.; VanDusen, J.; Williams, D. *Macromolecules* **1982**, *15*, 1385.
(2) Garito, A.; Singer, K. *Laser Focus* **1982**, *80*, 59.
(3) Williams, D. *Angew. Chem., Int. Ed. Engl.* **1984**, *23*, 690.
(4) Garito, A.; Teng, C.; Wong, K.; Zammani'Khamiri, O. *Mol. Cryst. Liq. Cryst.* **1984**, *106*, 219.
(5) Willand, C.; Williams, D. *Ber. Bunsen-Ges. Phys. Chem.* **1987**, *91*, 1304.
(6) Pantelis, P.; Hill, J.; Oliver, S.; Davies, G. *Br. Telecom. Technol. J.* **1988**, *6*, 1.
(7) Meijer, E.; Nijhuis, S.; Havinga, E. *Philips J. Res.* **1988**, *43*, 506.
(8) Broussoux, D.; Chastaing, E.; Esselin, S.; Barny, P. L.; Robin, P.; Bourbin, Y.; Pocholle, J.; Raffy, J. *Rev. Tech. Thomson-CSF* **1989**, *20–21*, 151.
(9) Eich, M.; Bjorklund, G.; Yoon, D. *Poly. Adv. Tech.* **1990**, *1*, 189.
(10) Williams, D. In *Materials for Nonlinear Optics—Chemical Perspectives*; Marder, S. R., Sohn, J. E., Stucky, G. D., Eds.; American Chemical Society: Washington, 1991; Chapter 2, p 31.
(11) Staring, E. *Recl. Trav. Chim. Pays-Bas* **1991**, *110*, 492.
(12) Zyss, J. *J. Mol. Electron.* **1985**, *1*, 25.
(13) Ulrich, D. *Mol. Cryst. Liq. Cryst.* **1988**, *160*, 1.
(14) Boyd, G. *J. Opt. Soc. Am. B* **1989**, *6*, 685.
(15) Groh, W.; Lupo, D.; Sixl, H. *Adv. Mater.* **1989**, *11*, 366.
(16) Ulrich, D. *Mol. Cryst. Liq. Cryst.* **1990**, *189*, 3.
(17) Möhlmann, G. *Synth. Met.* **1990**, *37*, 207.
(18) Chemla, D.; Zyss, J. *Nonlinear Optical Properties of Organic Materials and Crystals*; Academic Press: Orlando, FL, 1987; Vols. 1 and 2.
(19) Prasad, P.; Williams, D. *Nonlinear Optical Effects in Molecules and Polymers*; John Wiley and Sons: New York, 1991.
(20) Oudar, J.; Chemla, D.; Batifol, E. *J. Chem. Phys.* **1977**, *67*, 1626.
(21) Singer, K.; Sohn, J.; Lalama, S. *Appl. Phys. Lett.* **1986**, *49*, 248.
(22) Zyss, J.; Chemla, D. In *Nonlinear Optical Properties of Organic Materials and Crystals*; Chemla, D., Zyss, J., Eds.; Academic Press: Orlando, FL, 1987; Vol. 1, pp 23–191.
(23) Craig, D. *Adv. Chem. Phys.* **1964**, *8*, 27.
(24) Kaminow, I. *An Introduction to Electrooptic Devices*; Academic Press: New York, 1974; p 56.
(25) Orr, B.; Ward, J. *Mol. Phys.* **1971**, *20*, 513.
(26) Willetts, A.; Rice, J.; Burland, D.; Shelton, D. *J. Chem. Phys.* **1992**, *97*, 7590.
(27) Singer, K.; Kuzyk, M.; Sohn, J. *J. Opt. Soc. Am. B* **1987**, *4*, 968.
(28) Maki, J.; Malcuit, M.; Sipe, J.; Boyd, R. *Phys. Rev. Lett.* **1991**, *67*, 972.
(29) Chen, Z.; Sheng, P. *Phys. Rev. B* **1991**, *43*, 5735.
(30) Zyss, J.; Chemla, D. In *Nonlinear Optical Properties of Organic Materials and Crystals*; Chemla, D., Zyss, J., Eds.; Academic Press: Orlando, FL, 1987; Vol. 1, p 97.
(31) Brown, W., Jr. In *Encyclopedia of Physics*; Flügge, S., Ed.; Springer-Verlag: Berlin, 1956; Vol. XVII, pp 47–62.
(32) Böttcher, C. *Theory of Electric Polarization*; Elsevier: Amsterdam, 1973; Vol. I, pp 208 ff.
(33) Chikazumi, S. *Physics of Magnetism*; John Wiley and Sons: New York, 1964; p 19.
(34) Hurst, M.; Munn, R. *J. Mol. Electron.* **1986**, *2*, 139.
(35) Munn, R. *Int. J. Quant. Chem.* **1992**, *43*, 159.
(36) Osborn, J. *Phys. Rev.* **1945**, *67*, 351.
(37) Stoner, E. *Philos. Mag.* **1945**, *36*, 803.
(38) Kielich, S. *IEEE J. Quantum Electron.* **1969**, *QE-5*, 562.
(39) Dick, B. *Chem. Phys.* **1985**, *96*, 199.
(40) Grange, J. L.; Kuzyk, M.; Singer, K. *Mol. Cryst. Liq. Cryst.* **1987**, *150b*, 567.
(41) Onsager, L. *J. Am. Chem. Soc.* **1936**, *58*, 1456.
(42) Levine, B.; Bethea, C. *Appl. Phys. Lett.* **1974**, *24*, 445.
(43) Singer, K.; Garito, A. *J. Chem. Phys.* **1981**, *75*, 3572.
(44) Eich, M.; Looser, H.; Yoon, D.; Twieg, R.; Bjorklund, G.; Baumert, J. *J. Opt. Soc. Am. B* **1989**, *6*, 1590.
(45) Paley, M.; Harris, J.; Looser, H.; Baumert, J.; Bjorklund, G.; Jundt, D.; Twieg, R. *J. Org. Chem.* **1989**, *54*, 3774.
(46) Bosshard, C.; Knöpfle, G.; Prêtre, P.; Günter, P. *J. Appl. Phys.* **1992**, *71*, 1594.
(47) Stähelin, M.; Burland, D.; Rice, J. *Chem. Phys. Lett.* **1992**, *191*, 245.
(48) Prasad, P.; Williams, D. *Nonlinear Optical Effects in Molecules and Polymers*; John Wiley and Sons: New York, 1991; pp 93–94.
(49) Kleinman, D. *Phys. Rev.* **1962**, *126*, 1977.

(50) Yariv, A. *Introduction to Optical Electronics*; Holt, Rinehardt, Winston: New York, 1976; Chapter 9.
(51) Kaminow, I. *An Introduction to Electrooptic Devices*; Academic Press: New York, 1974; p 67.
(52) Skinner, I.; Garth, S. *Am. J. Phys.* **1990**, *58*, 177.
(53) Sigelle, M.; Hierle, R. *J. Appl. Phys.* **1981**, *52*, 4199.
(54) Oudar, J.; Chemla, D.; Batifol, E. *J. Chem. Phys.* **1977**, *66*, 2664.
(55) Teng, C.; Garito, A. *Phys. Rev.* **1983**, *28*, 6766.
(56) Clays, K.; Schildkraut, J. *J. Opt. Soc. Am. B* **1992**, *8*, 2274.
(57) Wu, J.; Valley, J.; Ermer, S.; Binkley, E.; Kenney, J.; Lipscomb, G.; Lytel, R. *Appl. Phys. Lett.* **1991**, *58*, 225.
(58) Yitzchaik, S.; Berkovic, G.; Krongauz, V. *J. Appl. Phys.* **1991**, *70*, 3949.
(59) Stähelin, M.; Walsh, C.; Burland, D.; Miller, R.; Twieg, R.; Volksen, W. *J. Appl. Phys.* **1993**, *73*, 8471.
(60) Suzuki, A.; Matsuoka, Y.; Ikushima, A. *Jpn. J. Appl. Phys.* **1991**, *30*, L1493.
(61) Ling, H.; Holland, W.; Gordon, H. *J. Appl. Phys.* **1991**, *70*, 6669.
(62) Mortazavi, M.; Knoesen, A.; Kowel, S.; Higgins, B.; Dienes, A. *J. Opt. Soc. Am. B* **1989**, *6*, 733.
(63) Hampsch, H.; Torkelson, J.; Bethke, S.; Grubb, S. *J. Appl. Phys.* **1990**, *67*, 1037.
(64) Knoesen, A.; Molau, N.; Yankelevich, D.; Mortazavi, M.; Dienes, A. *Int. J. Nonlinear Opt. Phys.* **1992**, *1*, 73.
(65) Shaffert, R. *Electrophotography*; John Wiley and Sons: New York, 1975.
(66) Sessler, G. In *Electrets*; Sessler, G. M., Ed.; Springer-Verlag: Berlin, 1987; p 13.
(67) Hill, J.; Pantelis, P.; Dunn, P.; Davies, G. *SPIE* **1989**, *1147*, 165.
(68) Eich, M.; Bjorklund, G. C.; Yoon, D. Y. *Polym. Adv. Technol.* **1990**, *1*, 189.
(69) Shahin, M. *Photogr. Sci. Eng.* **1971**, *15*, 322.
(70) Gallo, C. *IEEE Trans. Ind. Appl.* **1975**, *IA-11*, 739.
(71) Barry, S.; Soane, D. *Appl. Phys. Lett.* **1991**, *58*, 1134.
(72) Page, R.; Jurich, M.; Reck, B.; Sen, A.; Twieg, R.; Swalen, J.; Bjorklund, G.; Willson, C. *J. Opt. Soc. Am. B* **1990**, *7*, 1239.
(73) Havinga, E.; van Pelt, P. *Ber. Bunsen-Ges. Phys. Chem.* **1979**, *83*, 816.
(74) Jen, S.; Clark, N.; Pershan, P.; Priestley, E. *J. Chem. Phys.* **1977**, *66*, 4635.
(75) Wu, J. *J. Opt. Soc. Am. B* **1991**, *8*, 142.
(76) Chandrasekhar, S. *Liquid Crystals*; Cambridge University Press: Cambridge, 1977; pp 44 ff.
(77) Böttcher, C. *Theory of Electric Polarization*; Elsevier: Amsterdam, 1973; Vol. I, pp 161–165.
(78) Yamaoka, K.; Charney, E. *J. Am. Chem. Soc.* **1972**, *94*, 8983.
(79) Ermer, S.; Valley, J.; Lytel, R.; Lipscomb, G.; Van Eck, T.; Girton, D. *Appl. Phys. Lett.* **1992**, *61*, 2272.
(80) Mohajerani, E.; Gilbert, A.; Mitchell, G. *J. Phys. D: Appl. Phys.* **1992**, *25*, 1304.
(81) Hu, S.; Carlisle, G.; Martinez, D. *J. Mater. Sci. Lett.* **1992**, *11*, 794.
(82) Wijekoon, W.; Zhang, Y.; Karna, S.; Prasad, P.; Griffin, A.; Bhatti, A. *J. Opt. Soc. Am. B* **1992**, *9*, 1832.
(83) Levine, B.; Bethea, C. *J. Chem. Phys.* **1975**, *63*, 2666.
(84) Jungbauer, D.; Reck, B.; Twieg, R.; Yoon, D.; Willson, C.; Swalen, J. *Appl. Phys. Lett.* **1990**, *56*, 2610.
(85) Amano, M.; Kaino, T.; Yamamoto, F.; Takeuchi, Y. *Mol. Cryst. Liq. Cryst.* **1990**, *182A*, 81.
(86) Meyrueix, R.; Lecomte, J.; Tapolsky, G. *Nonlinear Opt.* **1991**, *1*, 201.
(87) Eldering, C.; Knoesen, A.; Kowel, S. *J. Appl. Phys.* **1991**, *69*, 3676.
(88) Boyd, G.; Francis, C.; Trend, J.; Ender, D. *J. Opt. Soc. Am. B* **1991**, *8*, 887.
(89) Jeng, R. J.; Chen, Y. M.; Jain, A. K.; Tripathy, S. K.; Kumar, J. *Opt. Commun.* **1992**, *89*, 212.
(90) Yitzchaik, S.; Berkovic, G.; Krongauz, V. *Macromolecules* **1990**, *23*, 3541.
(91) Hayden, L.; Sauter, G.; Ore, F.; Pasillas, P.; Hoover, J.; Lindsay, G.; Henry, R. *J. Appl. Phys.* **1990**, *68*, 456.
(92) Teraoka, I.; Jungbauer, D.; Reck, B.; Yoon, D.; Twieg, R.; Willson, C. *J. Appl. Phys.* **1991**, *69*, 2568.
(93) Dumont, M.; Levy, Y.; Morichere, D. In *Organic Molecules for Nonlinear Optics and Photonics*; Messier, J., Ed.; Kluwer Pub.: 1991; p 194; p 461.
(94) Kuzyk, M.; Singer, K.; Zahn, H.; King, L. *J. Opt. Soc. Am. B* **1989**, *6*, 742.
(95) Herminghaus, S.; Smith, B.; Swalen, J. *J. Opt. Soc. Am. B* **1991**, *11*, 2311.
(96) Cheng, L.; Tam, W.; Stevenson, S.; Meredith, G.; Rikken, G.; Marder, S. *J. Phys. Chem.* **1991**, *95*, 10631.
(97) Köhler, W.; Robello, D.; Dao, P.; Willand, C.; Williams, D. *J. Chem. Phys.* **1990**, *93*, 9157.
(98) Ye, C.; Minami, N.; Marks, T.; Yang, J.; Wong, G. *Macromolecules* **1988**, *21*, 2899.
(99) Rikken, G.; Seppen, C.; Nijhuis, S.; Meijer, E. *Appl. Phys. Lett.* **1991**, *58*, 435.
(100) Teng, C.; Man, H. *Appl. Phys. Lett.* **1990**, *56*, 1734.
(101) Levine, B.; Bethea, C. *J. Chem. Phys.* **1976**, *65*, 1989.
(102) Kurtz, S. In *Quantum Electronics: A Treatise*; Rabin, H., Tang, C. L., Eds.; Academic Press: New York, 1975; Vol. I, pp 209–281.
(103) Jerphagnon, J.; Kurtz, S. *J. Appl. Phys.* **1970**, *41*, 1667.

(104) Jerphagnon, J.; Kurtz, S. *Phys. Rev. B* **1970**, *1*, 1739.
(105) Choy, M.; Byer, R. *Phys. Rev. B* **1976**, *14*, 1693.
(106) Eckardt, R.; Masuda, H.; Fan, Y.; Byer, R. *IEEE J. Quant. Elect.* **1990**, *26*, 922.
(107) Roberts, D. *IEEE J. Quant. Elect.* **1992**, *28*, 2057.
(108) Oudar, J. *J. Chem. Phys.* **1977**, *67*, 446.
(109) Yariv, A. *Introduction to Optical Electronics*; Holt, Rinehardt, Winston: New York, 1976; p 361.
(110) Kuzyk, M.; Sohn, J.; Dirk, C. *J. Opt. Soc. Am. B* **1990**, *7*, 842.
(111) Uchiki, H.; Kobayashi, T. *J. Appl. Phys.* **1988**, *64*, 2625.
(112) Morichere, D.; Dentan, V.; Kajzar, F.; Robin, P.; Levy, Y.; Dumont, M. *Optics Commun.* **1989**, *74*, 69.
(113) Hyde, P.; Evert, T.; Ediger, M. *J. Chem. Phys.* **1990**, *93*, 2274.
(114) Hyde, P.; Ediger, M. *J. Chem. Phys.* **1990**, *92*, 1036.
(115) Hyde, P.; Evert, T.; Cicerone, M.; Ediger, M. *J. Non-Cryst. Solids* **1991**, *131*, 42.
(116) Nozaki, R.; Mashimo, S. *J. Chem. Phys.* **1987**, *87*, 2271.
(117) Jones, P.; Jones, W.; Williams, G. *J. Chem. Soc., Faraday Trans.* **1990**, *86*, 1013.
(118) Cicerone, M.; Ediger, M. *J. Chem. Phys.* **1992**, *97*, 2156.
(119) Doi, M.; Edwards, S. *The Theory of Polymer Dynamics*; Oxford University Press: Oxford, 1986; pp 46 ff.
(120) Meyrueix, R.; Mignani, G. *SPIE Proc.* **1989**, *1127*, 160.
(121) Doi, M.; Edwards, S. *The Theory of Polymer Dynamics*; Oxford University Press: Oxford, 1986; p 291.
(122) Wang, C.; Pecora, R. *J. Chem. Phys.* **1980**, *72*, 5333.
(123) Jungbauer, D.; Teraoka, I.; Yoon, D.; Reck, B.; Swalen, J.; Twieg, R.; Willson, C. *J. Appl. Phys.* **1991**, *69*, 8011.
(124) Böttcher, C.; Bordewijk, P. *Theory of Electric Polarization*; Elsevier: Amsterdam, 1978; Vol. II, pp 45 ff.
(125) Blumen, A.; Klafter, J.; Zumofen, G. In *Optical Spectroscopy of Glasses*; Zschokke, I., Ed.; D. Reidel: New York, 1986; Chapter 2, p 199.
(126) Lindsey, C.; Patterson, G. *J. Chem. Phys.* **1980**, *73*, 3348.
(127) Chung, S.; Stevens, J. *Am. J. Phys.* **1991**, *59*, 1024.
(128) Singer, K.; King, L. *J. Appl. Phys.* **1991**, *70*, 3251.
(129) Dhinojwala, A.; Wong, G.; Torkelson, J. *Macromolecules* **1992**, *25*, 7395.
(130) Abramowitz, M.; Stegun, I. *Handbook of Mathematical Functions with Formulas, Graphs, and Mathematical Tables*; Dover: New York, 1965.
(131) Chow, T. *Adv. Polym. Sci.* **1992**, *103*, 152.
(132) Williams, G.; Cook, M.; Hains, P. *J. Chem. Soc., Faraday Trans. 2* **1972**, *2*, 1045.
(133) Jonscher, A. *Phys. Status Solidi* **1977**, *6*, 585.
(134) Hampsch, H.; Yang, J.; Wong, G.; Torkelson, J. *Macromolecules* **1990**, *23*, 3640.
(135) Lindsay, G.; Henry, R.; Hoover, J.; Knoesen, A.; Mortazavi, M. *Macromolecules* **1992**, *25*, 4888.
(136) Hedvig, P. *Dielectric Spectroscopy of Polymers*; John Wiley and Sons: New York, 1977.
(137) Lei, D.; Runt, J.; Safari, A.; Newnham, R. *Macromolecules* **1987**, *20*, 1797.
(138) Köhler, W.; Robello, D.; Willand, C.; Williams, D. *Macromolecules* **1991**, *24*, 4589.
(139) Ferry, J. *Viscoelastic Properties of Polymers*; New York, 1961; p 201.
(140) Grest, G.; Cohen, M. *Adv. Chem. Phys.* **1981**, *48*, 455.
(141) Stähelin, M.; Burland, D.; Ebert, M.; Miller, R.; Smith, B.; Twieg, R.; Volksen, W.; Walsh, C. *Appl. Phys. Lett.* **1992**, *61*, 1626.
(142) Rusch, K. C. *J. Macromol. Sci.-Phys. B* **1968**, *2*, 179.
(143) Walsh, C.; Burland, D.; Lee, V.; Miller, R.; Smith, B.; Twieg, R.; Volksen, W. *Macromolecules* **1993**, *26*, 3720.
(144) Cohen, M.; Turnbull, D. *J. Chem. Phys.* **1959**, *31*, 1164.
(145) Turnbull, D.; Cohen, M. *J. Chem. Phys.* **1961**, *34*, 120.
(146) Cohen, M.; Grest, G. *Phys. Rev. B* **1979**, *20*, 1077.
(147) Victor, J.; Torkelson, J. *Macromolecules* **1987**, *20*, 2241.
(148) Royal, J.; Victor, J.; Torkelson, J. *Macromolecules* **1992**, *25*, 729.
(149) Royal, J.; Torkelson, J. *Macromolecules* **1992**, *25*, 4792.
(150) Deng, Q.; Jean, Y. *Macromolecules* **1993**, *26*, 30.
(151) Rusch, K. C.; Beck, R. H. *J. Macromol. Sci. B* **1969**, *3*, 365.
(152) Man, H.; Yoon, H. *Adv. Mater.* **1992**, *4*, 159.
(153) Hampsch, H.; Yang, J.; Wong, G.; Torkelson, J. *Macromolecules* **1990**, *23*, 3648.
(154) Lee, S.; Kidoguchi, A.; Watanabe, T.; Yamamoto, H.; Hosomi, T.; Miyata, S. *Polym. J.* **1991**, *23*, 1209.
(155) Haase, M.; Qui, J.; DePuydt, J.; Cheng, H. *Appl. Phys. Lett.* **1991**, *59*, 1272.
(156) Lenth, W.; Macfarlane, R. *Opt. Photonics News* **1992**, *3*, 8.
(157) Burland, D.; Miller, R.; Reiser, O.; Twieg, R.; Walsh, C. *J. Appl. Phys.* **1992**, *71*, 410.
(158) Suhara, T.; Nishihara, H. *IEEE J. Quant. Elect.* **1990**, *26*, 1265.
(159) Khanarian, G.; Norwood, R.; Haas, D.; Feuer, B.; Karim, D. *Appl. Phys. Lett.* **1990**, *57*, 977.
(160) Norwood, R.; Khanarian, G. *Electron. Lett.* **1990**, *26*, 2105.
(161) Cahill, P.; Singer, K.; King, L. *Opt. Lett.* **1989**, *14*, 1137.
(162) Cahill, P.; Tallant, D.; Kowalczyk, T.; Singer, K. *Proc. SPIE* **1991**, *1560*, 130.
(163) Sugihara, O.; Kai, S.; Uwatoko, K.; Kinoshita, T.; Sasaki, K. *J. Appl. Phys.* **1990**, *68*, 4990.
(164) Risk, W. *Appl. Phys. Lett.* **1991**, *58*, 19.

(257) Robello, D. R.; Willand, C. S.; Scozzafava, M.; Ullman, A.; Williams, D. J. In *Materials for Nonlinear Optics. Chemical Perspectives*, ACS Symposium Series 455; Marder, S. R., Sohn, J. E., Stucky, G. D., Eds.; American Chemical Society: Washington, DC, 1991; p 279.

(258) Hayashi, A.; Goto, Y.; Nakayama, M.; Sato, H.; Watanabe, T.; Miyata, S. *Macromolecules* 1992, *25*, 5094.

(259) Reiser, A. *Photoreactive Polymers: The Science and Technology of Resists*; John Wiley and Sons: New York, 1989; Chapter 2.

(260) Matsuda, H.; Okada, S.; Minami, N.; Nakanishi, H.; Kamaimoto, Y.; Hashidate, S.; Nagasaki, Y.; Kato, M. In *Nonlinear Optics: Fundamentals, Materials and Devices*; Miyata, S., Ed.; Elsevier Science Publishers: Holland, 1992; p 195.

(261) Mandal, B. K.; Lee, J. Y.; Zhu, X. F.; Chen, Y. M.; Prakienavincha, E.; Kumar, J.; Tripathy, S. K. *Syn. Met.* 1991, *41–43*, 3143.

(262) Mandal, B. K.; Kumar, J.; Huang, J.; Tripathy, S. *Makromol. Chem. Rapid Commun.* 1991, *12*, 63.

(263) Mandal, B. K.; Chen, Y. M.; Lee, V. Y.; Kumar, J.; Tripathy, S. *Appl. Phys. Lett.* 1991, *58*, 2459.

(264) Chen, Y. M.; Mandal, B. K.; Lee, J. Y.; Miller, P.; Kumar, J.; Tripathy, S. *Mat. Res. Soc. Symp. Proc.* 1991, *214*, 35.

(265) Mandal, B. K.; Tripathy, S. K.; Huang, J.; Kumar, J. U.S. Patent 1992, 5,112,881.

(266) Müller, H.; Müller, I.; Nuyken, O.; Strohriegl, P. *Makromol. Chem. Rapid. Commun.* 1992, *13*, 289.

(267) Mandal, B. K.; Jeng, J.; Kumar, J.; Tripathy, S. K. *Makromol. Chem. Rapid. Commun.* 1991, *12*, 607.

(268) Zhu, X.; Chen, Y. M.; Li, L.; Jeng, R. J.; Mandel, B. K.; Kumar, J.; Tripathy, S. K. *Opt. Commun.* 1992, *88*, 77.

(269) Chen, M.; Luping, Y.; Dalton, L. R.; Shi, Y.; Steier, W. H. *Macromolecules* 1991, *24*, 5421.

(270) Nasu, H.; Osaka, Y. *New Glass* 1988, *2*, 15.

(271) Vogel, E. M. *J. Am. Ceram. Soc.* 1989, *72*, 719.

(272) Klein, L. *Sol–gel Technology for Thin Films, Fibers, Preforms, Electronics and Speciality Shapes*; Noyes Publications: Park Ridge, NJ, 1988.

(273) Mackenzie, J. D.; Ulrich, D. R. *SPIE Proc.* 1990, *2*, 1328.

(274) Brinker, C. J.; Sherrer, G. W. *Sol–Gel Science*; Academic Press: Orlando, 1970.

(275) Hench, L. L. In *Science of Ceramic and Chemical Processing*; Hench, L. L., Ulrich, D. R., Eds.; John Wiley and Sons: New York, 1986.

(276) Corriu, R. J.; LeClercq, D.; Vioux, A.; Pauthe, M.; Phalippou, J. *Ultrastructure Processing of Advanced Ceramics*; Wiley: New York, 1988.

(277) Haruvy, Y.; Webber, S. *Chem. Mater.* 1991, *3*, 501.

(278) Pircetti, G.; Toussaere, E.; Ledoux, I.; Zyss, J. *Polym. Prepr.* 1991, *32*, 61.

(279) Nakamura, M.; Nasu, H.; Kamiya, K. *J. Non-Cryst. Solids* 1991, *135*, 1–7.

(280) Zhang, Y.; Prasad, P. N.; Burzynski, R. *Chem. Mater.* 1992, *4*, 851.

(281) Toussaere, E.; Zyss, J.; Griesmar, P.; Sanchez, C. *Nonlinear Opt.* 1991, *1*, 349.

(282) Boulton, J.; Thompson, J.; Fox, H.; Gorodisher, I.; Teowee, G.; Calvert, P.; Uhlmann, D. *Mat. Res. Soc. Symp. Proc.* 1990, *180*, 987.

(283) Jessie, M.; Carney, R.; Khanarian, G.; Keosian, R. *J. Noncryst. Solids* 1988, *102*, 280.

(284) Zhang, Y.; Cui, Y. P.; Wung, C. J.; Prasad, P. N.; Burzynski, R. *Proc. SPIE* 1991, *1560*, 264.

(285) Kobayashi, Y.; Muto, S.; Matsuzaki, A.; Kurokawa, Y. *Thin Solid Films* 1992, *213*, 126.

(286) Jeng, R. J.; Chem, Y. M.; Jain, A. K.; Kumar, J.; Tripathy, S. K. *Chem. Mater.* 1992, *4*, 972.

(287) Kim, J.; Plawsky, J. L.; LaPeruta, R.; Korenowski, G. M. *Chem. Mater.* 1992, *4*, 249.

(288) Claude, C.; Garetz, B.; Okamota, Y.; Tripathy, S. *Mater. Lett.* 1992, *14*, 336.

(289) Nandi, M.; Conklin, J. A.; Salvati, L.; Sen, A. *Chem. Mater.* 1991, *3*, 201.

(290) Jeng, R. J.; Chen, Y. M.; Jain, A. K.; Kumar, J.; Tripathy, S. K. *Chem. Mater.* 1992, *4*, 1141.